Summer 2010

Comparative investigations of H-transfer in dihydrofolate reductases from different families

Atsushi Yahashiri
University of Iowa

COMPARATIVE INVESTIGATIONS OF H-TRANSFER IN DIHYDROFOLATE REDUCTASES FROM DIFFERENT FAMILIES

by

Atsushi Yahashiri

An Abstract

Of a thesis submitted in partial fulfillment of the
requirements for the Doctor of Philosophy degree
in Chemistry in the Graduate College of
The University of Iowa

July 2010

Thesis Supervisor: Associate Professor Amnon Kohen

ABSTRACT

This thesis presents an effort to understand the C-H-C transfer in enzymatic reactions from the comparison of different variants of enzymes that have unrelated protein sequences and structures, but catalyze the same chemical transformation. I evaluated the kinetic isotope effects (KIEs) and their temperature dependences and interpreted the findings in accordance with Marcus-like models. The enzyme system studied is dihydrofolate reductase (DHFR), which catalyzes the reduction of 7,8-dihydrofolate (H_2F) to 5,6,7,8-tetrahydrofolate (H_4F) using reduced β-nicotinamide adenine dinucleotide 2' phosphate (NADPH) as a reducing agent. H-transfer reactions in typical enzymes from three genetically unrelated families, *E. coli* chromosomal DHFR (cDHFR, *FolA*), plasmid coded R67 DHFR (*FolB*), and pteridine reductase 1 (PTR1, *FolM*) were comparatively investigated. Chapter I provides a brief introduction to the thesis. Chapter II presents optimized procedures for a one-pot, enzymatic microscale synthesis of several NADPH isotopologues used in KIE experiments. Chapter III focuses on the application of novel competitive primary H/D KIE determinations. Chapter IV compares the H-transfer reactions between primitive R67 DHFR and the chromosomal DHFR, and Chapter V describes the investigation of H-transfer reactions at high and low ionic strengths with theoretical and experimental approaches in order to understand the unusual enhancement in H-transfer rate of R67 DHFR with increasing ionic strength. Chapter VI discusses an improved PTR1 purification procedure and comparisons of steady state kinetic parameters using PTR1 and cDHFR with H_2F and dihydrobiopterin (H_2B) substrates. Thus, the investigation of the H-transfer reaction catalyzed by cDHFR

with an unnatural substrate, H_2B is described. Finally, a summary is provided and future directions are discussed in Chapter VII.

Abstract Approved: _____
Thesis Supervisor

_____
Title and Department

_____
Date

COMPARATIVE INVESTIGATIONS OF H-TRANSFER IN DIHYDROFOLATE REDUCTASES FROM DIFFERENT FAMILIES

by

Atsushi Yahashiri

A thesis submitted in partial fulfillment
of the requirements for Doctor of Philosophy degree
in Chemistry in the Graduate College of
The University of Iowa

July 2010

Thesis Supervisor: Associate Professor Amnon Kohen

Graduate College
The University of Iowa
Iowa City, Iowa

CERTIFICATE OF APPROVAL

_____

PH.D. THESIS

_____

This is to certify that the Ph.D. thesis of

Atsushi Yahashiri

has been approved by the Examining Committee
for the thesis requirement for the Doctor of Philosophy
degree in Chemistry at the July 2010 graduation.

Thesis Committee: _____
Amnon Kohen, Thesis Supervisor

_____
Daniel M. Quinn

_____
James B. Gloer

_____
Lei Geng

_____
Shahram Khademi

父へ
To my father
Teruo Yahashiri
January 5, 1935 – June 11, 2007

Strive for excellence and keep your standard high.

Bryce V. Plapp, at his 70th birthday Ceremony

ACKNOWLEDGMENTS

I would like to give my thanks to my research advisor, Dr. Amnon Kohen for his valuable guidance, encouragement, patience, and support in the preparation of this dissertation. His knowledge and dedication have facilitated my academic progress. I express my sincere thanks to Zhen Wang, Daniel Roston, and Arundhuti Sen for their significant and indispensible help, and all members of the Kohen group for their input and support. I would also like to thank all undergraduate students who assisted and supported my research activities; Hyun Jo, Michael J. Toraason, Asad Hashmi, Robert T. Nixon III, and Nikhil Manjunath.

I would like to thank Drs. D.M. Quinn, L. Geng, J.B. Gloer and S. Khademi for their precious suggestions and advice while serving on my committee. I would like to thank Dr. Elizabeth E. Howell for providing R67 DHFR enzyme and suggestions for publication. I thank Dr. Santhana Velupillai of the University of Iowa NMR Central Research Facility for his friendship and assistance in our research. I appreciate Drs. M. A. Arnold, A. J. Haes and B. V. Plapp for providing lab and office spaces. My warm thanks are due to all the supports in the Chemistry Department, especially Drs. C. Margulis, J. Leddy, Ms J. Kruger, M. R. Ivanov, S. Robertson, L. Pierce, Mr. Ying Hua Chung, T. Koon, and A. Lynch. Here I express special thanks to Karen Fox for her encouragement and Oreo truffles that were indispensable for my long night experiments in the Chemistry Building.

I am grateful to Drs. Brandy Barren and Kartik Shanmuganatham for technical advice. I also express my gratitude to my teachers, Drs T. Ito, K. Sugawara, E. M. Fujinari, S. Gronert, P. A. Rubenstein, and M. S. Wold, for helping me to reach this stage

in my life. Also I appreciate the help from Dr. Lois K. Cox, Mr. W. S. McCabe, and Dr. D.E. Wurster.

I would also like to give my thanks to my parents who have taught me the significance of education and the importance of being a caring person. And I really appreciate my sister Yoko and uncle Mr. Masao Morimoto for their encouragements and support. Lastly, I would like to thank Pam Kuen Kuen Yahashiri for her sincere analyses and appropriate advice on my daily events, and for being a precious wife. The possibility of my PhD degree in the United States is due to her help.

ABSTRACT

This thesis presents an effort to understand the C-H-C transfer in enzymatic reactions from the comparison of different variants of enzymes that have unrelated protein sequences and structures, but catalyze the same chemical transformation. I evaluated the kinetic isotope effects (KIEs) and their temperature dependences and interpreted the findings in accordance with Marcus-like models. The enzyme system studied is dihydrofolate reductase (DHFR), which catalyzes the reduction of 7,8-dihydrofolate (H_2F) to 5,6,7,8-tetrahydrofolate (H_4F) using reduced β-nicotinamide adenine dinucleotide 2' phosphate (NADPH) as a reducing agent. H-transfer reactions in typical enzymes from three genetically unrelated families, *E. coli* chromosomal DHFR (cDHFR, *FolA*), plasmid coded R67 DHFR (*FolB*), and pteridine reductase 1 (PTR1, *FolM*) were comparatively investigated. Chapter I provides a brief introduction to the thesis. Chapter II presents optimized procedures for a one-pot, enzymatic microscale synthesis of several NADPH isotopologues used in KIE experiments. Chapter III focuses on the application of novel competitive primary H/D KIE determinations. Chapter IV compares the H-transfer reactions between primitive R67 DHFR and the chromosomal DHFR, and Chapter V describes the investigation of H-transfer reactions at high and low ionic strengths with theoretical and experimental approaches in order to understand the unusual enhancement in H-transfer rate of R67 DHFR with increasing ionic strength. Chapter VI discusses an improved PTR1 purification procedure and comparisons of steady state kinetic parameters using PTR1 and cDHFR with H_2F and dihydrobiopterin (H_2B) substrates. Thus, the investigation of the H-transfer reaction catalyzed by cDHFR

with an unnatural substrate, H_2B is described. Finally, a summary is provided and future directions are discussed in Chapter VII.

TABLE OF CONTENTS

LIST OF TABLES

Table

LIST OF FIGURES

Figure

LIST OF SCHEMES

Scheme

LIST OF EQUATIONS

Equation

LIST OF ABBREVIATIONS

µN	Micronormality
ADH	Alcohol dehydrogenase
AMP	Adenosine 5'-monophosphate
ADP	Adenosine 5'-diphosphate
ATP	Adenosine 5'-triphosphate
*bm*GDH	Glucose dehydrogenase from *Bacillus megaterium*
*c*DHFR	Dihydrofolate reductase from *Escherichia Coli* (same as ecDHFR)
*cu*GDH	NADPH dependent glucose dehydrogenase from *Cryptococcus uniguttulatus*
DHF	Dihydrofolate (same as H_2F, and H_2folate)
DHFR	Dihydrofolate reductase
DHPR	dihydropteridine reductase
DMP	Dimethoprim
*ec*DHFR	Dihydrofolate reductase from *Escherichia coli* (same as *c*DHFR)
EDTA	Ethylenediaminetetraacetic acid
FSA	Flo scintillation Analyzer
G121V	Mutation of Gly-121 to Valine
GDH	Glucose dehydrogenase
H_2B	Dihydrobiopterin
H_4B	Tetrahydrobiopterin
H_2F	Dihydrofolate (same as H_2folate, and DHF)

H_2folate	Dihydrofolate (same as H_2F, and DHF)
H_4F	Tetrahydrofolate
H_4folate	Tetrahydrofolate (same as H_4folate, and THF)
HPLC	High performance liquid chromatography
HPLC-FSA	Flo Scintillation Analysis of elution from High Performance Liquid chromatography
HPLC-LSC	Liquid scintillation counter analysis of elution from high performance liquid chromatography
kDa	Kilodalton
K_m	Michaelis constant
LSC	Liquid scintillation counter
MTX	Methotrexate
PTR1	Pteridine reductase 1
R67DHFR	Dihydrofolate reductase encoded on R67 plasmid
SDS	Sodium dodecyl sulfate
*ta*GDH	Glucose dehydrogenase from *Thermoplasma acidophilum*
*tb*ADH	Alcohol dehydrogenase from *Thermoanaerobium brockii*
THF	Tetrahydrofolate (same as H_4folate, and H_4F)

CHAPTER I

INTRODUCTION

Scope of Research

The broad objective of my dissertation is to seek a better understanding of how enzymes activate specific C-H bonds in enzyme reactions. Our investigation focuses on several intellectual and practical interests including; (i) how enzymes with unrelated sequences and structures catalyze the same chemical reaction, (ii) what are the differences in catalysis between the fine-tuned and robust enzymes, (iii) how enzymes catalyze specific chemical reactions between their substrates, and (vi) what is the role of enzyme dynamics in catalysis? To address these issues we focused on the chemical step of dihydrofolate reductase catalyzed reaction. We evaluated the temperature dependence of the intrinsic kinetic isotope effects, and also compared well-evolved and primitive enzymes that catalyze the same reaction. A phenomenological model was applied to rationalize the temperature effects on kinetic isotope effects in this H-transfer reaction. The effects of enzyme dynamics, active site structure, and H-tunneling on the enzyme catalyzed H-transfer reaction were investigated.

Thesis Overview

This thesis consists of the following chapters: First, chapter II covers the synthetic procedures of radiolabeled nicotinamide adenine compounds. Second, chapter III shows the development of a method to measure competitive H/D kinetic isotope effects and its applications. Third, chapters IV and V report studies of the H-transfer reaction in a

primitive enzyme, the plasmid coded R67 DHFR. Fourth, chapter VI presents an improved purification procedure for pteridine reductase 1 and subsequent steady state kinetic studies of that system, and the study of an H-transfer reaction catalyzed by *E. coli* DHFR using an alternative substrate. Finally, Chapter VII summarizes the dissertation and suggests future directions of study.

Background

Enzyme Catalysis

Enzymes have an essential role in sustaining cellular activities. Acting in organized sequences, enzymes facilitate the rates of numerous chemical reactions, including the decomposition of large molecules, transformations of chemical energy, and syntheses of essential molecules in biological pathways. The rate enhancement (typically from 10^5 up to 10^{22} fold) by enzymes supplies essential chemicals to sustain biological activity under physiological conditions.[1-3] Since Emil Fischer proposed the lock-and-key enzyme model in the late 19th century, various explanations for the catalytic power of enzymes have been proposed.[4, 5] Pauling proposed stabilization of the transition state complex in 1948.[6] Koshland introduced a concept, the "induced fit" model in 1958.[7] Jencks proposed destabilization of the ground state in 1977.[8] Acid/base catalysis, metal-ion related Lewis acid/base catalysis, and hydrogen tunneling effects are also proposed to explain enzyme catalysis.[1, 3, 9, 10] In recent years, many researchers have focused on the contributions of enzyme dynamics to catalysis.[11-14]

Numerous studies have tried to identify the potential factors that contribute to the rate enhancement of enzymes. Years of research in enzymology have determined that

enzymes undergo conformational changes during the turnover process, and reduce the activation energy of specific chemical reactions. For instance, enzymes specifically bind to their own substrates, form transition state complexes, optimize the chemical transformations by forming conformations that stabilize their transition states, and release their products. Contemporary questions in enzymology focus on why and how enzymes effectively and selectively catalyze specific chemical reactions. The questions discussed in this dissertation mainly cover physical phenomena such as how enzyme dynamics, electrostatics, and quantum mechanical hydrogen tunneling contribute to enzyme catalysis, by evaluating the temperature dependency of kinetic isotope effects in H-transfer reactions.

Isotope Effects in Chemical Reactions

Isotope effects in chemical transformations are powerful tools for the mechanistic study of enzymes. Isotope effects are measured by comparing two isotopologues* in the same reaction. Kinetic isotope effects (KIEs) can be obtained by comparing the ratio of the rate of the reaction between two isotopologues, whereas equilibrium isotope effects (EIEs) are calculated by comparing two equilibrium constants. Primary (1˚) isotope effects are on atoms involved in bond cleavage or formation during the reaction while secondary (2˚) isotope effects occur more distant from the reactive center.[15] In this dissertation, I focus on the development of a method for and the subsequent investigation of 1˚ KIEs.

* Isotopologues are molecules that differ only in their isotopic composition.

Kinetic Isotope Effects

Semiclassically, a KIE is defined by the Bigeleisen equation in terms of the transition state theory.[16]

Equation I.1. Kinetic Isotope Effects from Partition Functions

$$KIE = \frac{k_l}{k_h} = \left(\frac{\kappa_l}{\kappa_h}\right) \times ZPE \times MMI \times EXC$$

where k_l and k_h are the rate constants for the light and heavy isotopic substrates, respectively. κ_l and κ_h are the transmission coefficients for light and heavy isotopes, respectively. *ZPE* is the isotope effect on the zero-point energy, *MMI* is the isotope effect on the mass moments of inertia that consist of translational and rotational degrees of freedom, and *EXC* represents the isotope effect on excited states populations. In the cases addressed here, KIE significantly depends on the *ZPE*, and the contributions of the *MMI* and *EXC* are small. Shown in Figure I.1, the zero-point energy of a light isotopologue is higher than the one of a heavy isotopologue. In H transfer reactions, the transferable hydrogen is labeled with one of the three isotopes of hydrogen, *i.e.*, protium (^{1}H, or H), deuterium (^{2}H, or D), or tritium (^{3}H, or T) (Figure I.2), and KIEs can be measured as k_H/k_T (H/T), k_H/k_D (H/D), or k_D/k_T (D/T).

According to the differences in the zero-point energy of three hydrogen isotopes, in 1958 Swain et al. proposed an equation that explains the kinetic relationships between reaction rate constants for the three isotopes of hydrogen.[17] They can be represented as:

Equation I.2 Swain-Schaad Relationship for 1° KIE using H as a Reference

$$\frac{k_H}{k_T} = \left(\frac{k_H}{k_D}\right)^{Exp_{HD}}$$

Equation I.3 Swain-Schaad Relationship for 1° KIE using T as a Reference

$$\frac{k_H}{k_T} = \left(\frac{k_D}{k_T}\right)^{Exp_{DT}}$$

where *k* is the rate constant for each isotope of hydrogen, and *Exp* represents the Swain-Schaad exponent, which is calculated based on differences in the zero-point energy between two hydrogen isotopes. Exp_{HD} and Exp_{DT} are for the relationship for H/T vs. H/D, and H/T vs. D/T, respectively. Each *Exp* is calculated from the following equations:

Equation I.4 Swain-Schaad Exponential using Hydrogen as a Reference

$$Exp_{HD} = \frac{\ln\left(\frac{k_H}{k_T}\right)}{\ln\left(\frac{k_H}{k_D}\right)} = \frac{\frac{1}{\sqrt{\mu_H}} - \frac{1}{\sqrt{\mu_T}}}{\frac{1}{\sqrt{\mu_H}} - \frac{1}{\sqrt{\mu_D}}} = \frac{\frac{1}{\sqrt{m_H}} - \frac{1}{\sqrt{m_T}}}{\frac{1}{\sqrt{m_H}} - \frac{1}{\sqrt{m_D}}}$$

Equation I.5 Swain-Schaad Exponential using Tritium as a Reference

$$Exp_{DT} = \frac{\ln\left(\frac{k_H}{k_T}\right)}{\ln\left(\frac{k_D}{k_T}\right)} = \frac{\frac{1}{\sqrt{\mu_H}} - \frac{1}{\sqrt{\mu_T}}}{\frac{1}{\sqrt{\mu_D}} - \frac{1}{\sqrt{\mu_T}}} = \frac{\frac{1}{\sqrt{m_H}} - \frac{1}{\sqrt{m_T}}}{\frac{1}{\sqrt{m_D}} - \frac{1}{\sqrt{m_T}}}$$

where μ_x is the reduced mass for the hydrogen isotope x bound to carbon. The Exp_{HD} was calculated as a value of 1.44 using atomic masses[18] whereas based on reduced mass it is a value of 1.42. The calculated Exp_{DT} is 3.34 from reduced mass, and 3.26 from atomic mass.[19, 20]

Hydrogen Tunneling in Enzyme Reactions

Quantum mechanical tunneling is the physical phenomenon by which a particle transfers through a reaction energy barrier due to its wave-like properties.[21] Figure I.1 illustrates this phenomenon graphically for a symmetric double well system such as the C-H-C hydrogen transfer. Tunneling is affected by many factors including the distance between the particle donor and acceptor wells (donor-acceptor distance, DAD) and the

reactant-product wells symmetry. A light isotope has a higher probability of tunneling because of its higher zero-point energy and more diffuse wavefunction (Figure I.1).

An Experimental Approach for Analyzing Temperature Dependence of KIEs

A powerful experimental approach to examine the physical nature of the H transfer is the determination of the temperature dependence of KIEs. In accordance with the Arrhenius equation, the rate constant of the reaction is exponentially proportional to E_a and the reciprocal absolute temperature, $\frac{1}{T}$.

Equation I.6 Arrhenius Equation

$$k = Ae^{\frac{-\Delta E_a}{RT}}$$

where *k* represents the rate constant, *A* is the Arrhenius preexponential factor, and E_a is activation energy for the reaction. Using the Arrhenius equation, the relationship between the KIE, $\frac{k_L}{k_H}$, and temperature, T, can be expressed as follows,

Equation I.7 Arrhenius' Equation for KIEs

$$\frac{k_L}{k_H} = \frac{A_L e^{\frac{-\Delta E_{aL}}{RT}}}{A_H e^{\frac{-\Delta E_{aH}}{RT}}} = \frac{A_L}{A_H} e^{\frac{\Delta E_{a(H-L)}}{RT}}$$

where k_x represents the rate constant, A_x is the Arrhenius preexponential factor, and E_{ax} is activation energy for the transfer of isotope x. H and L designate the heavy and the light isotopes, respectively. $\Delta E_{a(H-L)}$ represents the difference in activation energy for the reaction of heavy and light isotopologues.

When we plot ln(KIE) as a function of $\frac{1}{T}$, the plot is often expressed as a linear line. The slope is the difference in activation energies between two isotopes, $\frac{\Delta E_{a(H-L)}}{R}$, and

the y-intercept represents the KIE on the Arrhenius preexponential factor, $\ln \frac{A_L}{A_H}$. The term temperature dependency/ independency of KIEs corresponds to ΔE_a. Below some of the models that have been proposed to explain the experimental results on the temperature dependency of KIEs are presented.

Semiclassical Models

Semiclassical models deal with quantum-mechanical effects at the ground state, but ignore those effects close to the transition state. Based on semiclassical models, a primary H/D KIE for C–H cleavage at 298 K is calculated to be 6.9 based on the stretching frequencies of a C-H bond and a C-D bond.† Similarly, k_H/k_T is predicted to be 18. These models are not able to explain temperature independent KIE values, or small KIEs with steep temperature dependency.[22]

Bell Model

The Bell model was proposed to add a tunneling correction to semiclassical theory.

Equation I.8 Bell Model using Tunnel Effect Correction

$$k = Q_t k_{SC}$$

Equation I.9 Tunnel Effect Correction to the Reaction Velocity

$$Q_t = \frac{1}{kT} e^{\frac{E}{kT}} \int G(W)\, e^{-\frac{W}{kT}} dW$$

† The stretching frequencies of a C-H bond, C-D bond, and C–T bond are ~3000 cm^{-1}, 2200 cm^{-1}, and 1800 cm^{-1}, respectively.

where Q_t is a tunneling correction, and k_{sc} is the semiclassical rate constant. G is the probability that the particle shall cross the barrier (often described as the permeability of the barrier), and is a function of the particle's mass. W represents the energy of the particle, and k is Boltzman's constant. Tunneling occurs below the energy of the transition state, and its effect is predicted to be the most significant for H due to its light mass. This leads both to a 1˚ KIE which exceeds the semiclassically predicted value, and to large isotopic differences in E_a.

Arrhenius plots of ln$k$ and lnKIE versus inverse of temperature are shown in Figure I.3 (a) and (b), respectively. In the high temperature region (Figure I.3, red region), the slope of the Arrhenius plot is exponentially proportional to ΔE_a. This suggests that *the contribution of tunneling to the rate* is minimal at high temperature; therefore, the KIE tends to converge to unity at infinite temperature and ln(A_L/A_H) converges to zero. On the other hand, at very low temperatures tunneling contributions dominate the reaction rates because of the lack of thermal energy (Figure I.3, blue region). As a result, a particle is transferred by ground-state tunneling, where the rates are temperature independent, and KIEs are large and temperature independent, with A_L/A_H larger than unity. In the middle temperature range, the contribution of H tunneling to the rate is significant, but the contribution of tunneling for heavy isotopes is *smaller*, so the KIE on A_L/A_H will be smaller than unity. These non-unity A_L/A_H values have been taken as one of the proofs for tunneling.

In the last four decades, KIEs have been determined for many different enzymes and experimental data on the temperature dependency of KIEs have accumulated (Table I.1). Surprisingly, many of those reports could not be fully rationalized with the simple

Bell model. For instance, KIEs for soybean lipoxygenase greatly exceeded the semiclassical limit and A_L/A_H surpassed unity. Moreover, some of these systems were found to have a nonzero E_a for the H transfer process, even for temperature-independent KIEs.[22] As a one-dimensional rigid potential surface, the Bell tunneling correction models explain temperature-dependent KIEs and large temperature-independent KIEs for systems which showed no energy of activation for the isotopically sensitive step. However, that model fails to explain small "temperature independent" KIEs with significant energies of activation. More contemporary treatments of H-transfer reactions take into account the motion(s) of the heavy atom environment that modulate the potential surface of the reaction, and the multidimensional process of H-tunneling.

Phenomenological Marcus-like Models

In explaining H-transfer reactions in enzyme systems, following the framework of the Marcus theory, many researchers have developed models that describe most of the features of their own experimental results.[23-33] The models have been named in different ways, and they try to explain the contribution of dynamics to H transfer reactions. The terminology used in all of those models is different; however, these proposed models share the common fundamental concept that there exist two requirements for efficient tunneling. One is degeneracy of the reactant and product energy levels and the other is a short average DAD. Given the fact that these models were inspired by Marcus theory for electron transfer, we call them "Marcus like models", as represented in Figure 1.4. The models propose that environmental reorganization assists to form the conformation of the

transition state for tunneling (tunneling ready conformation).[34, 35] The Marcus-like model is mathematically represented as;

Equation I.10 Marcus-Like Model for Hydride Transfer

$$k = Ce^{\frac{-(\Delta G^\circ + \lambda)^2}{4\lambda RT}} \int_{DAD_0}^{DAD_1} e^{F(m)} e^{\frac{-E_{F(m)}}{k_b T}} dDAD$$

where C is a constant often determined by preorganization of enzymes, ΔG° is exoergicity of the reaction, λ is reorganization energy, R is the gas constant and T is the temperature. The first exponential is the Marcus-term which corresponds to the reorganization of the heavy atoms to adjust the relative energy levels of the reactants and the products to generate configurations that would allow for overlap of the donor and acceptor wavefunctions resulting in efficient tunneling. The second exponential is the overlap between the donor and acceptor wavefunctions that gives the tunneling probability. This term is DAD and isotope dependent. The third term is the expression of the DAD fluctuations, namely the conformational space. The probability of having a "particular DAD" is dictated by the energy associated with the configurations. This is temperature as well as isotope sensitive.

According to the Marcus-like model, a system will have temperature independent KIEs if the enzyme's tunneling ready states (TRS) have optimized conformational distribution. In a "perfect enzyme", the enzyme TRS is well-organized and both H and D DAD are ideal for tunneling.

The Model System: Dihydrofolate Reductase

Dihydrofolate reductase (DHFR: EC 1.5.1.3) catalyzes the reduction of 7,8-dihydrofolate (H_2F) to 5,6,7,8-tetrahydrofolate (H_4F) using NADPH as a cofactor.

DHFRs have been studied extensively model systems in many experimental and theoretical studies due to their medical and biological importance in DNA synthesis and cell division. For a few decades, two major families of DHFR have been known: *FolA* (or *DfrA*) DHFRs are typical chromosomally encoded, and *FolB* (or *DfrB*) DHFRs are plasmid encoded enzymes. Recently, following the discovery of organisms lacking *FolA*, alternative DHFRs *FolC*, *FolM*, and *FolP* were reported. All five families of DHFRs are genetically different (Figures I.5 and I.6). They are all able to compensate for the lost DHFR activity in their host cells, and are proposed as alternative DHFRs.[36, 37] Although five different DHFR families are intriguing subjects to study, we focused on *FolA* (cDHFR), *FolB* (R67 DHFR), and *FolM* (PTR1) DHFRs in this dissertation (Figure I.7). These three classified families of DHFRs are compared in Table I.2, and presented below.

<u>*FolA* DHFR</u>

The chromosomally encoded DHFRs share high sequence homology, and they are classified as *FolA* DHFRs. Perhaps the most studied chromosomal DHFR is that from *Escherichia coli* (*c*DHFR). Our lab found that cDHFR has a finely-tuned catalytic system in the H-transfer reaction between H_2F and NADPH.[38] *c*DHFR is a small monomeric enzyme that consists of 4 α-helices and 8 stranded β-sheets with several flexible loops (Figure I.7). Recent dynamic analysis showed that the enzyme is highly mobile and that motions of the enzyme are important for the rate of H-transfer.[3, 39-41]

Previously, temperature independent KIEs were reported for the *c*DHFR catalyzed H-transfer reactions.[38] In accordance with Marcus-like models, this indicates

that at its tunneling ready state, *c*DHFR has ideal DAD as well as a well–reorganized active site for tunneling. As a result, thermal activation of the DAD fluctuation does not affect the KIEs, and KIEs are temperature independent. In order to understand further correlation between rate-promoting motions of the enzyme and the physical nature of H transfer, the temperature dependence of KIEs for three DHFR mutants have been examined.[42-44]

FolB DHFR

The *FolB* or *DfrB* DHFR family is of particular interest as it is unrelated genetically and structurally to either the *FolA* or the *FolM* families. The origin of these *FolB* DHFR genes is not identified, but recent Psi-BLAST searches have only indicated that *FolB* has homology to *src* homology 3 domain, which is a DNA binding protein. These genes were discovered in the R-plasmid‡ that is present in dimethoprim§ resistant bacteria. It has been suggested that the host organisms incorporated this plasmid in order to survive antibiotic treatments.[45]

A typical *FolB* DHFR is R67 DHFR, which has a unique structure (Figure I.7 middle). It is a double funnel-like homotetramer of 78 amino acid residues (per monomer). NMR studies have shown that R67 DHFR has a rigid active site, and the protein backbone motion is minimal.[46] The 222 symmetric homotetramer forms a central large pore as a solvent accessible active site, and this large promiscuous active site pore

‡ R-plasmids have been found in many antibiotic-resistant microorganisms. R represents resistance.

§ Dimethoprim is a potent inhibitor of *FolA* DFHRs.

allows R67 DHFR to utilize several cofactors including α-NADPH, and thio-NADPH. The k_{cat} for R67 DHFR is approximately 10^2 smaller than that of cDHFR although K_m values of R67 DHFR for NADPH and H_2F are similar to *c*DHFR. Presteady-state kinetics, and calorimetry studies revealed that the chemical step, hydride transfer, is the rate limiting step for R67 DHFR.[47, 48] At the transition state, R67 DHFR seems to use an *endo* conformation in which the nicotinamide ring is located over the more bulky side of the pteridine ring, whereas cDHFR prefers an *exo* transition state with minimal overlap of the pteridine and nicotinamide rings (Figure I.7).

FolM DHFR

Giladi et al. experimentally demonstrated that *Fol*M, pteridine reductase 1 (PTR1)-like protein can replace DHFR, and proposed it as an alternative DHFR family.[36] PTR1 was discovered from the protozoan parasites *Leishmania* and *Trypanosoma* species,[37] and it is the only enzyme known to reduce biopterin in *Leishmania*. PTR1 primarily catalyzes the reduction of biopterin and dihydrobiopterin (H_2B) to produce tetrahydrobiopterin (H_4B), but unlike other pteridine reductases, PTR1 also reduces folate and H_2F to produce H_4F. Due to the fact that PTR1 is less sensitive to methotrexate (MTX) than DHFR (IC_{50} = 1.1 μM and 0.005 μM for *L. major* PTR1 and DHFR-TS, respectively), it compromises antibiotic treatments targeting DHFR. Genetically, PTR1s are not related to either *FolA* or *FolB* DHFRs (Figure I.5 and I.6). PTR1 has a relatively large tetrameric structure of 288 amino acids. In accordance with its crystal structure, PTR1 is proposed to utilize the pro*S* H on C4 of NADPH (Type B DHFR) in the reduction of H_2F.

Enzymes	Type of transfer	Temperature dependence	k_H/k_D	A_H/A_D	Ref
aromatic amine dehydrogenase	proton	No	55		[49]
methylamine dehydrogenase	proton	No	16.8	13.3	[50]
trimethylamine dehydrogenase	proton	No	4.6	7.8	[51]
sarcosine oxidase	proton	No	7.3	5.8	[52]
thymidylate synthase	proton	Yes	2.2		[53]
thymidylate synthase	hydride	No	3.7		[54]
pentaerythritol tetranitrate reductase	hydride	No	~4.1	4.1	[55]
dihydrofolate reductase (cDHFR)	hydride	No	3.5	4.0	38
cDHFR, dihydrobiopterin	hydride	Yes	6.1	4.0	[56]
G121V-M42W cDHFR	hydride	Yes	3.5	0.04	[43]
R67 DHFR	hydride	Yes	3.5		34
alcohol dehydrogenase (*Bacillus stearothermophilus)*	hydride	Yes	5.6 (k_H/k_T)	4.3 (A_H/A_T)	[57]
ethanolamine ammonia lyase	H radical		4.4 - 4.7		[58]
glutamate mutase	H radical		2.4		[59]
soybean lipooxygenase (SLO)	H radical	Yes	81	18	[60]
SLO, mutants	H radical	Yes	93 - 112	0.12 - 4	[60]

Table I.1 Enzymatic systems with properties outside the limits predicted by "tunneling correction" models

This table was constructed based on Table 3 in Stojkovic, V.; Kohen, A., Enzymatic H transfers: quantum tunneling and coupled motion from kinetic isotope effect studies. *Isr. J. Chem.* **2009,** 49, 163-173. with permission Israel-LPP Ltd. [22]

	cDHFR	R67 DHFR	PTR1
Subunit	Monomer, 18 kDa	Tetramer, 34kDa	Tetramer, 34kDa
Residues	157	78[61]	288[62]
Active site	1	1	4
Crystal structure	Eight-stranded β sheet with four α helical connecting strands[63]	Double funnel-like 222 symmetric structure, four β barrels [45]	A seven-stranded parallel β-sheet sandwiched between three helices on either side[62]
Volume of active site	1677 [45]	3626[45]	N.D.
Trimethoprim (K_i)	20 pM[45]	150 μM[45]	N.D.
Methotrexate (K_i)	5 nM	N.D.	1.1 μM
k_{cat} (s^{-1})	29 (hydride transfer) 240 (product release)	1.3	0.022
Natural substrate	Dihydrofolate	Dihydrofolate	Biopterin/Dihydrobiopterin
Stereospecificity on 4-H on NADPH	pro*R*	pro*R*	pro*S*
Rate-limiting	Product release	Hydride transfer[34]	N.D.
Substrate specificity	β-NADPH Dihydrofolate	α and β-NADPH Dihydrofolate/PAB-pterin	β-NADPH Folate, Dihydrofolate, biopterins, and dihydrobiopterin

Table I.2 A comparison of cDHFR (FolA), R67 DHFR (FolB), and PTR1 (FolM).

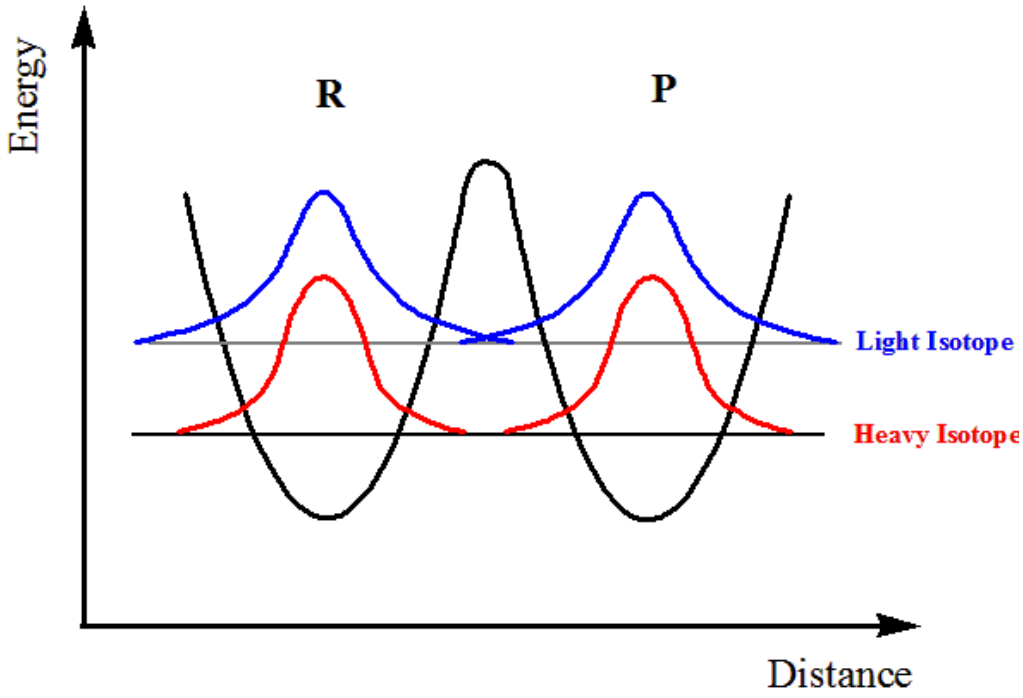

Figure I.1 An example of ground-state tunneling along the reaction coordinate. The blue and red lines represent probability density functions for lighter and heavier isotopes, respectively. Overlap of the probabilities between the reactant and product states indicates the probability for the particle to tunnel.

This figure was reconstructed based on Figure 4 in Kohen, A.; Klinman, J. P., Hydrogen tunneling in biology. *Chem. Biol.* 1999, 6, R191-198.with permission from Elsevier.[64]

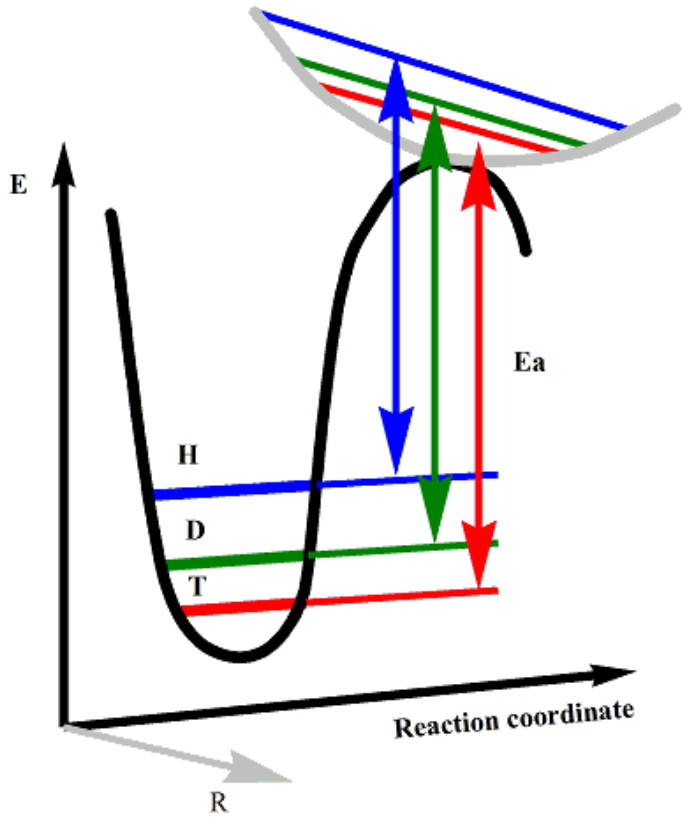

Figure I.2 Energies of activation (E_a) for H (blue), D (green), and T (red) resulting from their different zero-point energies at the ground state (GS) and transition state (TS). The GS-ZPE is constituted by all degrees of freedom, and the TS- zero-point energies is constituted by all degrees of freedom orthogonal to the reaction coordinate (**R**). This type of consideration (quantum mechanical zero-point energies with no tunneling) is referred to as semiclassical.[19]

This figure is reconstructed based on Figure 2 in "Hydrogen Tunneling in Biology" Kohen, A. and Klinman, J.P., Chemistry and Biology 1999, 6, R191-198, with permission from Elsevier.

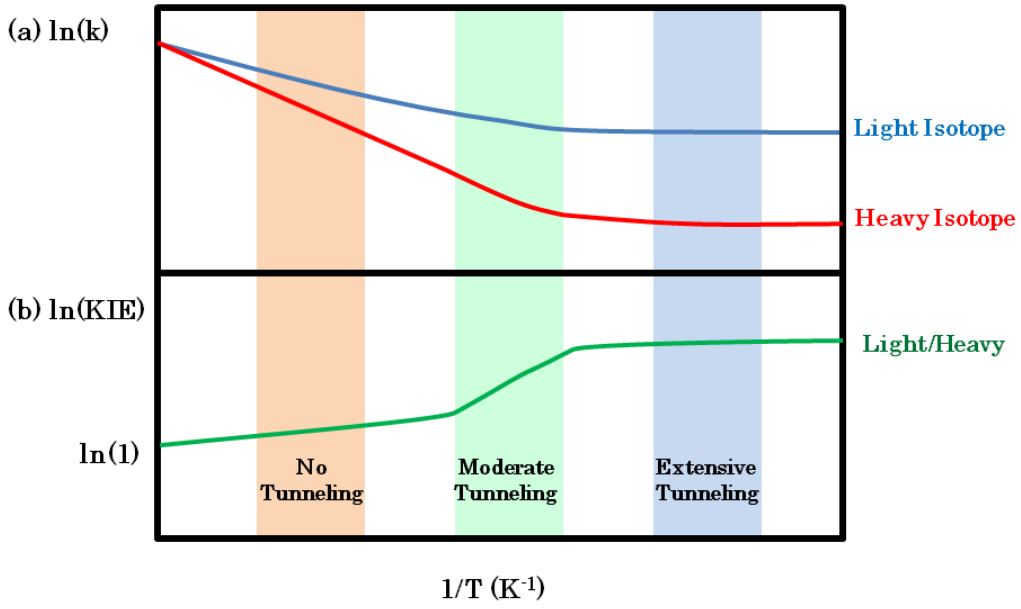

Figure I.3 Arrhenius plot of a hydrogen transfer reaction for TST-models with a tunneling correction. (a) Arrhenius plot of reaction rate constants for light (blue) and heavy (red) isotopes. (b) Arrhenius plot for their KIEs.

This figure is reconstructed based on Figure 3 in "Hydrogen Tunneling in Biology" Kohen, A. and Klinman, J.P., Chemistry and Biology 1999, 6, R191-198, with permission from Elsevier.

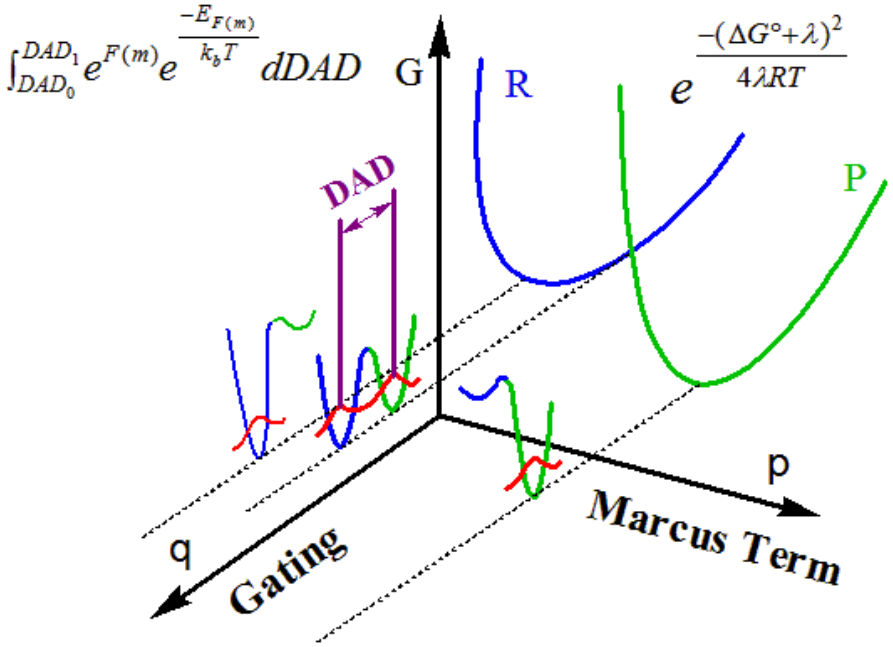

Figure 1.4 Three dimensional illustration of a Marcus-like model. Two orthogonal coordinates are presented: p, the environmental energy parabolas for the reaction state (R: blue) and the product state (P: green), and q, the gating coordinate, along which the red lines represent the hydrogen's probability wavefunction. Thermal fluctuations in the DAD along the q coordinate lead to the temperature dependence of KIE. [34]

This figure is reconstructed based on Figure 3 in Yahashiri, A.; Howell, E. E.; Kohen, A., Tuning of the H-transfer coordinate in primitive versus well-evolved enzymes. *Chemphyschem* **2008,** 9, (7), 980-982., with permission from WILEY-VCH Verlag GmbH & Co.

```
Ecoli_DHFR              ----------------------------------------------------
Ccrescentus_DHFR        ----------------------------------------------------
MTuberculosis_DHFR      ----------------------------------------------------
Mleprae_DHFR            ----------------------------------------------------
Mavium_DHFR             ----------------------------------------------------
Gmetallireducens_DHFR   ----------------------------------------------------
Banthracis_DHFR         ----------------------------------------------------
Bsubtilis_DHFR          ----------------------------------------------------
Spneumoniae_DHFR        ----------------------------------------------------
Saureus_DHFR            ----------------------------------------------------
Cperfringensstr_DHFR    ----------------------------------------------------
DfrB3/DHFRIIc           ----------------------------------------------------
R388DHFR                ----------------------------------------------------
R67DHFR                 ----------------------------------------------------
Ltropica_PTR1           ----------------------MTAPTVPVALVTGAAKRLGSSIAEGLHA 28
Linfantum_PTR1          ----------------------MAAPTVPVALVTGAAKRLGSGIAEGLHA 28
Lmajor_PTR1             ----------------------MTAPTVPVALVTGAAKRLGRSIAEGLHA 28
FolM                    ----------------------MGKTQPLPILITGGGRRIGLALAWHFIN 28
FolP_Hpylori            MIVKRLNPNTLKNALQKIGPEEIAQNHMRQKGVSFVFEIQHLPLSATLIL 50


Ecoli_DHFR              ----------------------------------------------------
Ccrescentus_DHFR        ----------------------------------------------------
MTuberculosis_DHFR      ----------------------------------------------------
Mleprae_DHFR            ----------------------------------------------------
Mavium_DHFR             ----------------------------------------------------
Gmetallireducens_DHFR   ----------------------------------------------------
Banthracis_DHFR         ----------------------------------------------------
Bsubtilis_DHFR          ----------------------------------------------------
Spneumoniae_DHFR        ----------------------------------------------------
Saureus_DHFR            ----------------------------------------------------
Cperfringensstr_DHFR    ----------------------------------------------------
DfrB3/DHFRIIc           ----------------------------------------------------
R388DHFR                ----------------------------------------------------
R67DHFR                 ----------------------------------------------------
Ltropica_PTR1           EGYAVCLHYHRSAAEANTLAATLNARRPNSAITVQADLSNVAKAPVSGAD 78
Linfantum_PTR1          EGYAVCLHYHRSAAEANTLAATLNARRPNSAITVQADLSNVAKAPAGGAD 78
Lmajor_PTR1             EGYAVCLHYHRSAAEANALSATLNARRPNSAITVQADLSNVATAPVSGAD 78
FolM                    QKQPVIVSYRTHYPAIDGLIN-------AGAQCIQADFSTN--------- 62
FolP_Hpylori            KQEAISVGGDFATPRDCILAKEPFYDGVLVVSANQLERLIVKCHSQPFGL 100


Ecoli_DHFR              ----------------MISLIAALAVDRVIGMENAMPWNLPADLAWFKRN 34
Ccrescentus_DHFR        ------------MSMPTLAIVVARAANGVIGRDGDLPWRLKSDLALFKAN 38
MTuberculosis_DHFR      ----------------MVGLIWAQATSGVIGRGGDIPWRLPEDQAHFREI 34
Mleprae_DHFR            --------------MTVVGLIWAQSTTGVIGRDGGMPWRVPEDLTRFKQL 36
Mavium_DHFR             ------------MTRAEVGLVWAQSTSGVIGRGGDIPWSVPEDLTRFKEV 38
Gmetallireducens_DHFR   ---------------MIVTIIAAMAGNRVIGKEGAMPWHLPDDLARFKAI 35
Banthracis_DHFR         ---------------MIVSFMVAMDENRVIGKDNNLPWRLPSELQYVKKT 35
Bsubtilis_DHFR          ----------------MISFIFAMDANRLIGKDNDLPWHLPNDLAYFKKI 34
Spneumoniae_DHFR        --------------MTKKIVAIWAQDEEGVIGKENRLPWHLPAELQHFKET 37
Saureus_DHFR            ----------------MTLSILVAHDLQRVIGFENQLPWHLPNDLKHVKKL 35
Cperfringensstr_DHFR    ----------------MFSIIVAKSINNIIGVNNKMPWNIPSDLKRFKEL 34
DfrB3/DHFRIIc           ----------------------------------------MDQHNNGVSTL 11
R388DHFR                ----------------------------------------MGQSSDEANAP 11
R67DHFR                 ----------------------------------------MERSSNEVSNP 11
Ltropica_PTR1           GSAPVTLFKRCAGLVAACYTHWGRCDVLVNNASSFYPTPLLRSDEDGHEP 128
Linfantum_PTR1          GAAPVTLFKRCADLVAACYTHWGRCDVLVNNASSFYPTPLLRKDEDGHVP 128
Lmajor_PTR1             GSAPVTLFTRCAELVAACYTHWGRCDVLVNNASSFYPTPLLRNDEDGHEP 128
FolM                    ------------DGVMAFADEVLKSTHGLRAILHNASAWMAEKPGAPLAD 100
FolP_Hpylori            KHLAQELKSHLKAKKPNAPQIMAILNLTPDSFYEKSRFDSKKALEEIYQL 150
```

Figure I.5 A Multiple sequence alignment of DHFR enzymes using CLUSTALW 2.0.12

```
Ecoli_DHFR                TLNKPVIMGRHTWESIGR----------PLPGRKNIILSS------QP-G 67
Ccrescentus_DHFR          TLFKPIIMGRKTWDSLPRK---------PLPGRTNIVLSRDQSF--EPEG 77
MTuberculosis_DHFR        TMGHTIVMGRRTWDSLPAKV-------RPLPGRRNVVLSRQADF--MASG 75
Mleprae_DHFR              TMGHPVVMGRRTWDSLPVGV-------RPLPGRRNIVLSRQIDF--MAEG 77
Mavium_DHFR               TMGHTVIMGRRTWESLPAKV-------RPLPGRRNVVVSRRPDF--VAEG 79
Gmetallireducens_DHFR     TMGHPVVMGRKTFESIG----------RPLPGRLNIVLTRQAGY--APSG 73
Banthracis_DHFR           TMGHPLIMGRKNYEAIG----------RPLPGRRNIIVTRNEGY--HVEG 73
Bsubtilis_DHFR            TSGHSIIMGRKTFESIG----------RPLPNRKNIVVTSAPDS--EFQG 72
Spneumoniae_DHFR          TLNHAILMGRVTFDGMGR---------RLLPKRETLILTRNPEE--KIDG 76
Saureus_DHFR              STGHTLVMGRKTFESIG----------KPLPNRRNVVLTSDTSF--NVEG 73
Cperfringensstr_DHFR      TMGKKILMGRKTFESLP----------FVLPGRTHLVLTTKKDFSYNHKD 74
DfrB3/DHFRIIc             VAGQ---FALPSHATFG------------LGDRVR----KKSGAAW---- 38
R388DHFR                  VAGQ---FALPLSATFG------------LGDRVR----KKSGAAW---- 38
R67DHFR                   VAGN---FVFPSNATFG------------MGDRVR----KKSGAAW---- 38
Ltropica_PTR1             CVGDREAMEAAAADLFGSNAIAPYFLIKAFAHRVADTPAEQRGTNYSIVN 178
Linfantum_PTR1            CVGDREAMEAAAADLFGSNAMAPYFLIKAFAHRVADTPAEQRGTNYSIVN 178
Lmajor_PTR1               CVGDREAMETATADLFGSNAIAPYFLIKAFAHRVAGTPAKHRGTNYSIIN 178
FolM                      VLACMMQIHVNTPYLLN-----------HALERLLRGHGHAASDIIHFTD 139
FolP_Hpylori              LEKGITLIDIGAASSRPESEIIDPKTEQDRLKEILLEIKSQKLYQCAKFS 200
                                 :                          .

Ecoli_DHFR                TDDRVTWVKSVDEAIAACGD--VPEIMVIGGGRVYEQFLPKAQKLYLTHI 115
Ccrescentus_DHFR          AVACETWMEAFEIAREQAADDGADEVCVIGGSALFELALPKAKRLYLTEV 127
MTuberculosis_DHFR        AEVVGSLEEALT----------SPETWVIGGGQVYALALPYATRCEVTEV 115
Mleprae_DHFR              AEVFGSLEETISNLET------EPEMWVIGGEQIYRLALPLATRCGVTEV 121
Mavium_DHFR               ARVAGSLEAALAYAGS------DPAPWVIGGAQIYLLALPHATRCEVTEI 123
Gmetallireducens_DHFR     VTVARTLAEALILAGT------AGEVFICGGGEVYREALPLADRIHLTVI 117
Banthracis_DHFR           CEVAHSVEEVFELCKNE-----EE-IFIFGGAQIYDLFLPYVDKLYITKI 117
Bsubtilis_DHFR            CTVVSSLKDVLDICSGP-----EE-CFVIGGAQLYTDLFPYADRLYMTKI 116
Spneumoniae_DHFR          VATFQDVQSVLDWYQDQ-----EKNLYIIGGKQIFQAFEPYLDEVIVTHI 121
Saureus_DHFR              VDVIHSIEDIYQLPG---------HVFIFGGQTLFEEMIDKVDDMYITVI 114
Cperfringensstr_DHFR      IIIYNDLNKLIEEYKDS-----KEEIFVIGGGKIYSELLKYTSKLYITEV 119
DfrB3/DHFRIIc             ------QGQVVGW--Y------------------CTKLTP---------E 53
R388DHFR                  ------QGQVVGW--Y------------------CTKLTP---------E 53
R67DHFR                   ------QGQIVGW--Y------------------CTNLTP---------E 53
Ltropica_PTR1             MVDAMTNQPLLGYTIYTM----AKGALEGLTRSAALELAPLQVRVNGIGP 224
Linfantum_PTR1            MVDAMTSQPLLGYTIYTM----AKGALEGLTRSAALELAPLQIRVNGVGP 224
Lmajor_PTR1               MVDAMTNQPLLGYTIYTM----AKGALEGLTRSAALELAPLQIRVNGVGP 224
FolM                      YVVERGSDKHIAYAAS-------KAALDNMTRSFARKLAP-EVKVNSIAP 181
FolP_Hpylori              IDTYHATTAQMALEHYFSILNDVSGFNSAEMLEVARDYKPTCILMHTQKT 250


Ecoli_DHFR                DAEVEGDTH---FPDYEPDDWESVFSEFHDADAQNSHSYCFEILERR--- 159
Ccrescentus_DHFR          AAEVEGDVR---FPAFDESAWTEVRREAHPAGDGDDHAFVFRVLERR--- 171
MTuberculosis_DHFR        DIGLPREAG-DALAPVLDETWRGETGEWRFSRSG--LRYRLYSYHRS--- 159
Mleprae_DHFR              DTYLLHEDD-DVLAPVLDDTWVGVTGEWLVSCSG--LRYRLHSYHRS--- 165
Mavium_DHFR               EIDLRRDDD-DALAPALDDSWVGETGEWLASRSG--LRYRFHSYRRDPRS 170
Gmetallireducens_DHFR     HRAYGGDTTFPELPADFEETCR-EHGEGKPPHSF--ITFERRRGSTP--- 161
Banthracis_DHFR           HHAFEGDTFFP-EMDMTN--WKEVFVEKGLTDEKNPYTYYYHVYEKQQ-- 162
Bsubtilis_DHFR            HHEFEGDRHFP-EFDESN--WKLVSSEQGTKDEKNPYDYEFLMYEKKNSS 163
Spneumoniae_DHFR          HARVEGDTYFPEELDLSL--FETVSSKFYAKDEKNPYDFTIQYRKRKEV- 168
Saureus_DHFR              EGKFRGDTFFP-PYTFED--WEVASSVEGKLDEKNTIPHTFLHLIRKK-- 159
Cperfringensstr_DHFR      LKEYKGDTYFP---KVDYSKWIKTYESSIYEENDN--KFKFFNYKKI--- 161
DfrB3/DHFRIIc             GYAVESESHP--------GSVQIYP----VAALERVA------------- 78
R388DHFR                  GYAVESESHP--------GSVQIYP----VAALERVA------------- 78
R67DHFR                   GYAVESEAHP--------GSVQIYP----VAALERIN------------- 78
Ltropica_PTR1             GLSVLADDMPPAVREDYRSKVPLYQRDSSAAEVSDVVIFLCSSKAKYITG 274
Linfantum_PTR1            GLSVLADDMPPAVREDYRSKVPLYQRDSSAAEVSDVVIFLCSSKAKYVTG 274
Lmajor_PTR1               GLSVLVDDMPPAVWEGHRSKVPLYQRDSSAAEVSDVVIFLCSSKAKYITG 274
FolM                      SLILFNEHDDA---EYRQQALNKSLMKTAPGEKEVIDLVDYLLTSCFVTG 228
FolP_Hpylori              PKDMQENVFYHNLFDEMDRFFKEKLEVLEKYALQDVILDIGFGFAKLKEH 300
                                :
```

Figure I.5-continued

```
Ecoli_DHFR              --------------------------------------------------
Ccrescentus_DHFR        --------------------------------------------------
MTuberculosis_DHFR      --------------------------------------------------
Mleprae_DHFR            --------------------------------------------------
Mavium_DHFR             SVRGCSPSRPS---------------------------------------- 181
Gmetallireducens_DHFR   --------------------------------------------------
Banthracis_DHFR         --------------------------------------------------
Bsubtilis_DHFR          KAGGF---------------------------------------------- 168
Spneumoniae_DHFR        --------------------------------------------------
Saureus_DHFR            --------------------------------------------------
Cperfringensstr_DHFR    --------------------------------------------------
DfrB3/DHFRIIc           --------------------------------------------------
R388DHFR                --------------------------------------------------
R67DHFR                 --------------------------------------------------
Ltropica_PTR1           TCVKVDGGYSLTRA------------------------------------ 288
Linfantum_PTR1          TCVKVDGGYSLTRA------------------------------------ 288
Lmajor_PTR1             TCVKVDGGYSLTRA------------------------------------ 288
FolM                    RSFPLDGGRHLR-------------------------------------- 240
FolP_Hpylori            NLALIKHLSHFLKFKKPLLVGASRKNTIGLITGREVQDRLAGTLSLHLMA 350


Ecoli_DHFR              ------------------------------
Ccrescentus_DHFR        ------------------------------
MTuberculosis_DHFR      ------------------------------
Mleprae_DHFR            ------------------------------
Mavium_DHFR             ------------------------------
Gmetallireducens_DHFR   ------------------------------
Banthracis_DHFR         ------------------------------
Bsubtilis_DHFR          ------------------------------
Spneumoniae_DHFR        ------------------------------
Saureus_DHFR            ------------------------------
Cperfringensstr_DHFR    ------------------------------
DfrB3/DHFRIIc           ------------------------------
R388DHFR                ------------------------------
R67DHFR                 ------------------------------
Ltropica_PTR1           ------------------------------
Linfantum_PTR1          ------------------------------
Lmajor_PTR1             ------------------------------
FolM                    ------------------------------
FolP_Hpylori            LQNGASILRVHDIDEHIDLIKVFKSLEETD 380
```

Figure I.5-continued

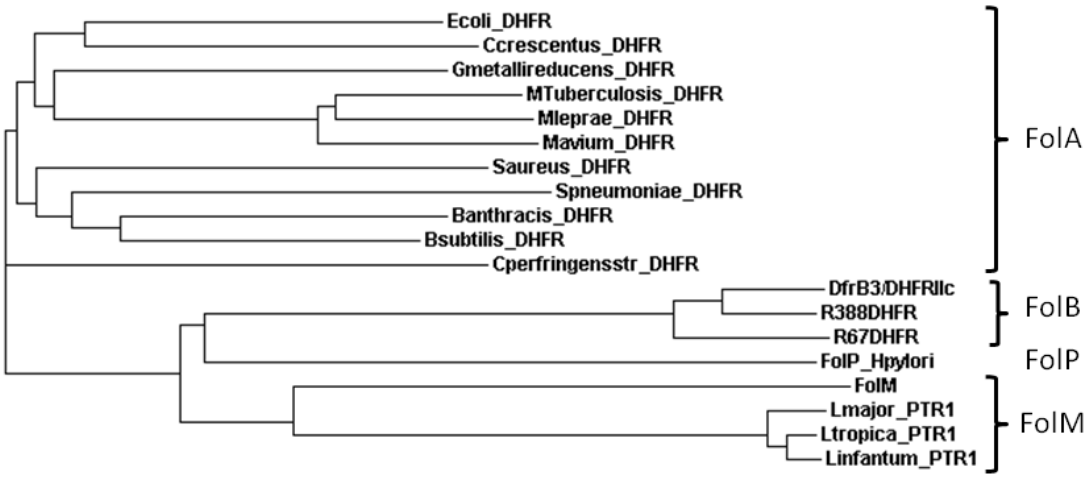

Figure I.6 Phylogenetic tree from ClustalW 2.2

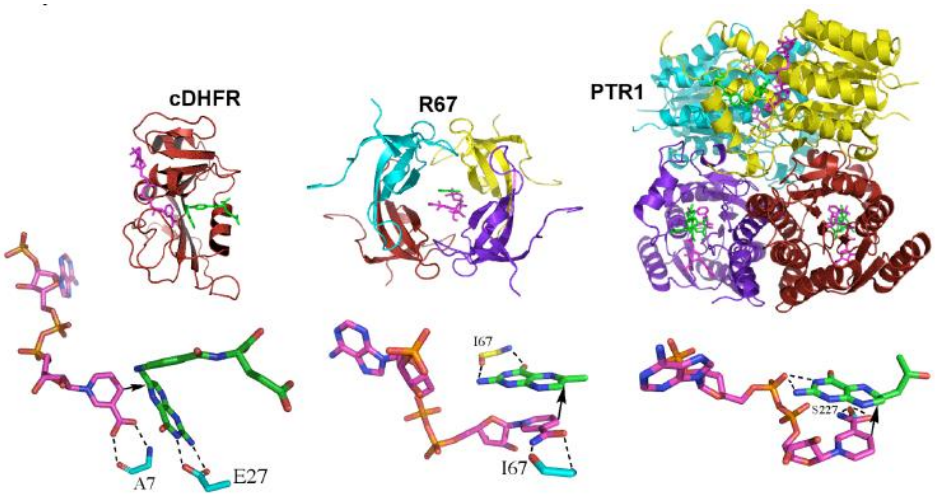

Figure I.7 A comparison of the structures of three types of DHFRs. From left, cDHFR (PDB ID: 1RX2), R67 DHFR (PDB ID: 2RK1) and PTR1 (PDB ID: 2BFP) are shown on the top. The folate and nicotinamide ligands are in green and magenta, respectively. Importantly, not only are the proteins' structures and scaffolds different (top) but the reactants' orientations also differ (bottom). The reactants in cDHFR are in an exo-orientation, while in R67 DHFR and PTR1 they are in an endo-orientation. In cDHFR and R67DHFR the *re*-face, while in PTR1 it is the *si*-face.

CHAPTER II

MICROSCALE SYNTHESIS AND KINETIC ISOTOPE EFFECT ANALYSIS OF NADPH ISOTOPOLOGUES

Section I. Microscale Synthesis and Kinetic Isotope Effect Analysis of (*4R*)-[AD-^{14}C, 4-^{2}H] NADPH and (*4R*)-[AD-^{3}H,4-^{2}H] NADPH

This section was published in the journal *Journal of Labelled Compounds and Radiopharmaceuticals* [Atsushi Yahashiri, Arundhuti Sen, and Amnon Kohen (2009), 52 11-12, 463-466 Microscale synthesis and kinetic isotope effect analysis of (*4R*)-[AD-^{14}C, 4-^{2}H] NADPH and (*4R*)-[AD-^{3}H,4-^{2}H] NADPH] copyright 2009, John Wiley & Sons, Ltd.

Summary

We present a one-pot chemo-enzymatic microscale synthesis of NADPH with two different patterns of isotopic labels: (*4R*)-[Ad-^{14}C,4-^{2}H] NADPH and (*4R*)-[Ad-^{3}H,4-^{2}H] NADPH. These co-factors are required by an enormous range of enzymes, and isotopically labeled nicotinamides are consequently of significant interest to researchers. In the current procedure, [Ad-^{14}C] NAD^+ and [Ad-^{3}H] NAD^+ were phosphorylated by NAD^+ kinase to produce [Ad-^{14}C] $NADP^+$ and [Ad-^{3}H] $NADP^+$, respectively. *Thermoanaerobium brockii* alcohol dehydrogenase was then used to stereospecifically transfer deuterium from C2 of isopropanol to the *re* face of C4 of $NADP^+$. After purification by HPLC, NMR analysis indicated the deuterium content at the 4R position is more than 99.7 %. The labeled cofactors were then used to successfully and sensitively

measure kinetic isotope effects for R67 dihydrofolate reductase, providing strong evidence for the utility of this synthetic methodology.

Introduction

Reduced β-nicotinamide adenine dinucleotide 2' phosphate (NADPH, Scheme II.1) and its oxidized form ($NADP^+$) are essential cofactors for a huge range of enzymes, including dihydrofolate reductase (DHFR), glucose dehydrogenase (GDH), and others involved in crucial biosynthetic pathways. The development of efficient methods for the synthesis of a variety of NADPH molecules with different isotopic labelling patterns is of interest to a broad range of biochemical, pharmacological, and mechanistic research. For example, recent kinetic isotope effects studies (KIEs) of DHFR have used six different isotopic labelling patterns to investigate the dynamics of this important model enzyme.[42, 65]

KIE studies have proved to be a valuable probe of the chemical step of enzymatic reactions, yielding information regarding fundamental catalytic processes like C-H bond activation.[66] KIE measurements determine the relative reaction rates (or rate constants) for isotopologues**, and can be performed either non-competitively (where reaction rates are measured separately for each isotopologue) or competitively (isotopologues react together in one vessel). In comparison to non-competitive experiments, competitive KIE measurements are generally considered to be more reliable and sensitive, frequently due to the use of radiolabeled compounds.[67] Competitive measurements of hydride transfer isotope effects in type A (*pro-R* specific) NADPH-

** Isotopologues are molecules that differ only in their isotopic composition.

dependent enzymes, for example, utilize two isotopologues of NADPH, each labeled at the *pro-R* position of the C4 of the nicotinamide with one of the three isotopes of hydrogen, *viz.* ^{1}H (H), ^{2}H (D) and ^{3}H (T). Conventionally, the lighter isotopologue is traced using a ^{14}C label at a position on the molecule remote from the reaction center, and ^{3}H is used as the heavier isotope, and (depending upon the mixture of isotopes used) the measured KIEs can be k_H/k_T (H/T), k_H/k_D (H/D) or k_D/k_T (D/T). Other combinations are possible, but not commonly utilized.[68]

Given the ubiquity of NADPH-dependent enzymes, and the requirement of labeled NADPH molecules for kinetic measurements, there is a continuous need for efficient synthetic methods for the production of stereospecifically labeled NADPH. In particular, 4*R* deuterated NADPHs with remote radiolabeling are essential for competitive H/D and D/T KIE studies.[53] However, the synthesis of radiolabeled 4R deuterated NADPH requires extra caution. Proton contamination at the 4R position can cause serious artifacts in H/D KIE measurements, so the deuterium content in the labeled compounds needs to be high enough so these artifact will be below the noise of the measurement (commonly > 99.5 % D). We have previously reported syntheses for *(4S)*-[4-^{3}H]-NADPH, and *(4R)*-[4-^{3}H]-NADPH using type B (*pro-S* specific) glucose dehydrogenase from *Cryptococcus uniguttulatus* (Schemes II.2 and II.3a).[69] However, this procedure requires a long reaction time, and involves four separate enzymatic reactions, making it unappealing for the synthesis of deuterated compounds. We have also reported the synthesis of (*4R*)-[4-^{3}H]-NADPH using type A alcohol dehydrogenase from *Thermoanaerobactor brockii* (*tb*ADH) in a large scale reaction.[70] Here we present an optimized procedure for a two-step, one-pot, chemo-enzymatic microscale synthesis of

doubly isotopically labeled (*4R)*-[Ad-^{14}C,4-^{2}H]-NADPH, and (*4R)*-[Ad-^{3}H,4-^{2}H]-NADPH (Scheme II.2, and II.3b), and their use in the measurement of competitive primary (1°) KIEs. First, radiolabeled NAD^+ was phosphorylated by NAD^+ kinase to produce labeled $NADP^+$. *tb*ADH was then used to stereospecifically catalyze a deuteride transfer from d_8-isopropanol (99.7 % D at the 2 position) to the radiolabeled $NADP^+$, followed by HPLC purification and preservation. The isotopic purity of the radioactive compounds was confirmed by NMR analysis (99.7 % D). Finally, measurements of H/D, and D/T 1˚ KIEs for plasmid-encoded R67 DHFR indicated that any contamination was low enough not to affect the measurements.

Materials and Methods

Materials

Reagent-grade chemicals were used as purchased unless specified otherwise. *β*-nicotinamide [Ad-^{14}C] adenine dinucleotide ([Ad-^{14}C]-NAD^+; 267 mCi/mmol), and *β*-nicotinamide [2,5',8-^{3}H] adenine dinucleotide ([Ad-^{3}H]-NAD^+; 25.0 Ci/mmol) were purchased from Amersham Pharmacia. Monobasic potassium phosphate, Tris (hydroxymethyl)aminomethane, $MgCl_2$, and Microcon YM-30 regenerated cellulose centrifugal filters (3000 Molecular Weight Cut-off) were purchased from Fisher. Ultima Gold liquid scintillation cocktail was purchased from PerkinElmer. All other materials were purchased from Sigma.

Methods

HPLC Analysis and Separation

Analytical HPLC separations were performed using an Agilent Technologies 1100 Series HPLC, fitted with a Supelco Discovery C-18 reverse-phase column (250 x 4.6 mm, 5 μm). A semi-preparative Supelco Discovery C18 reverse-phase column (250 x 10 mm, 5 μm) was used for the purification of the synthesized NADPH, and eluted peaks were analyzed using an online UV diode array detector or a Packard 500TR Series flow scintillation analyzer (HPLC-FSA). When more sensitive analysis was necessary, fractions were collected and analyzed by a Packard 2900 TR Series Liquid Scintillation Counter (LSC). The details of the HPLC method used have been described elsewhere.[71, 72]

Synthesis of (R)-[Ad-^{14}C,4-^{2}H]-NADPH and (R)-[Ad-^{3}H,4-^{2}H]-NADPH

Radiolabeled NAD^+ solution (500 μL, 12.5 μCi, for [Ad-^{14}C]-NAD^+, and 250 μL, 62.5 μCi, for [Ad-^{3}H]-NAD^+) was lyophilized, then the following were added to a total final volume of 450 μl: 250 mM Tris, 130 μM creatine phosphate disodium salt tetrahydrate, 800 μM NAD^+, 20 mM $MgCl_2$ (final concentrations). The pH was adjusted to 6.7, and ATP was added to a final concentration of 2.4 mM. 400 units of creatine phosphokinase, and 50 units of NAD^+ kinase were then added to initiate the phosphorylation step. The reaction mixture was incubated with occasional mixing at 35 °C until the reaction was complete as determined by HPLC-FSA analysis.

Upon completion of the phosphorylation step, the pH of the reaction mixture was adjusted to 8.0 (the intended product, NADPH, is more stable at this pH) and 5 μl of 2-

propanol-d_8 along with 7 units of *tb*ADH were added. The reaction was incubated anaerobically at 43 °C for 15 min under argon. After the completion of the reaction, as determined by HPLC-FSA analysis, the enzymes were removed with a Microcon YM-30 centrifugal filter device at 4 °C. The product was purified via semi-preparative HPLC, and the total radioactivity was determined by LSC. The synthesized NADPH was lyophilized and stored at -80 °C. The proton contamination at the 4R position in both synthesized NADPHs was examined by ^{1}H-NMR measurement using a 600 MHz NMR (Bruker Avance-600 probe) for 10000 scans in D_2O (Figure II.1).

Competitive KIE Experiments.

For 1° D/T KIE experiments (*4R*)- [Ad-^{14}C,4-^{2}H]-NADPH and (*4R*)-[4-^{3}H]-NADPH were combined in a 1:6 DPM ratio of ^{14}C:^{3}H (to compensate for the lower efficiency of ^{3}H scintillation counting), and copurified using reverse-phase HPLC to remove impurities. For 1° H/D KIE experiments, [Ad-^{14}C] NADPH and (*4R*)-[Ad-^{3}H,4-^{2}H] NADPH were combined in either a 1:4, or 1:9 DPM ratio. The two ratios were examined in order to assure no experimental artifacts on the KIE values (theoretically these ratios should not affect the KIE, if the experiment is artifact free). The co-purified radiolabeled NADPH was divided into aliquots containing 360,000 DPM of ^{14}C, and flash frozen for short-term storage (up to 3 weeks) at -80 °C. Measurements of KIEs on R67 DHFR were conducted as described elsewhere.[34] The fractional conversion (*f*) of NADPH was determined as per equation II.1, from the ratio of ^{14}C in the product to the total amount of ^{14}C in both product and reactant peaks:

Equation II.1 Fractional Conversion.

$$f = \frac{[\text{Ad-}^{14}\text{C}]\text{NADP}^+}{[\text{Ad-}^{14}\text{C}]\text{NADP}^+ + [\text{Ad-}^{14}\text{C}]\text{NADPH}}$$

The observed KIEs were calculated according to equation II.2:[73]

Equation II.2 Observed Kinetic Isotope Effects

$$KIE = \frac{\ln(1-f)}{\ln\left[1-f\left(\frac{Rt}{R\infty}\right)\right]}$$

where R_t is the ratio of ^{3}H to ^{14}C in products at fractional conversion *f*, and R_∞ is that ratio at 100 % conversion. The percentage error from the average KIE value at each temperature was plotted versus the fractional conversion, since most artifacts would result in increasing or decreasing trends in such a plot (Figure II.2a).

Results and Discussion

Synthesis of (4R)-[Ad-^{14}C,4-^{2}H]-NADPH and (4R)-[Ad-^{3}H,4-^{2}H]-NADPH

(*4R*)-[Ad-^{14}C, 4-^{2}H]-NADPH and (*4R*)-[Ad-^{3}H, 4-^{2}H]-NADPH were each synthesized from the relevant NAD^+ precursor in two steps, *viz*. phosphorylation of adenine-radiolabeled NAD^+ to $NADP^+$, followed by the stereospecific reduction of $NADP^+$ with d_8-isopropanol and *tb*ADH. In the phosphorylation step, a combination of two enzymes was used in the reaction mixture. NAD^+ kinase catalyzed the phosphorylation of NAD^+ to form $NADP^+$ by transferring phosphate from ATP (Scheme II.2). Since one of the products, ADP, is a potent inhibitor of NAD^+ kinase, the creatine phosphate/creatine phosphokinase system was concomitantly used to regenerate ATP, minimizing the amount of ATP required and preventing the accumulation of ADP. The

completion (> 99 %) of the phosphorylation reaction is very important for subsequent applications, since NAD^+ and NADPH cannot be well separated in later purification steps.

Prior to the *tb*ADH reaction, the pH was adjusted to 8.0 because NADPH is more stable at higher pH (> 7.5) while NAD^+ and $NADP^+$ are stable at lower pH. *tb*ADH was then used to catalyze a deuteride transfer from commercially available deuterated isopropanol (< 0.3 % H on alcoholic carbon) to the *re* face of nicotinamide of radiolabeled $NADP^+$ to form *(4R)*-[Ad-^{14}C,4-^{2}H]NADPH or *(4R)*-[Ad-^{3}H,4-^{2}H]NADPH in a single step. The overall yields in radioactivity for (*4R*)-[Ad-^{14}C,4-^{2}H]-NADPH and (*4R*)-[Ad-^{3}H,4-^{2}H]-NADPH were 70 %, and 60 %, respectively. Deuteration was over 99.7 % complete, as determined by NMR analysis (Figure II.1). Our previously reported labeling procedure used type B glucose dehydrogenase and required three steps following the phosphorylation step (Scheme II.3a), but this reduction by *tb*ADH stereospecifically labels the 4*R*-position of radiolabeled NADPH in H_2O with just one step after phosphorylation of the NAD^+ (Scheme II.3b).

Analysis of D/T and H/D KIEs values vs. Fractional Conversion

Competitive KIE measurements are a sensitive application that can identify the quality of the labeled materials. Almost any problem, like H-contamination, would result in a trend when using the linearized equation for KIEs (Equation II.2). In competitive KIE measurements, two different isotopically labeled substrates (^{3}H and ^{14}C) are mixed, and the fractionation of the light and heavy isotopes in the products is compared as a function of different fractional conversions. Competitive KIEs are a useful tool in studies

of enzyme mechanisms, and in cases where the enzyme is NADPH-dependent, deuterated NADPH can be used with tritium or proton labeled NADPH to determine D/T and H/D KIEs, thus aiding the investigation of various mechanistic questions.[53] In this case, in order to determine the extent of proton contamination at the 4R position in the deuterated products, both 1° H/D and 1˚ D/T KIE values were measured and plotted as function of *f*. The synthesized (*4R*)-[Ad-^{14}C, 4-^{2}H] NADPH was co-purified with (*4R*)-[4-^{3}H]-NADPH, and the mixture used in the competitive measurement of 1° D/T KIEs, while the synthesized (*4R*)-[Ad-^{3}H,4-^{2}H]-NADPH was co-purified with [Ad-^{14}C]-NADPH to determine 1° H/D KIEs in the reaction catalyzed by R67 DHFR. In case of significant H-contamination, observed KIE values should show a definite trend over a range of fractional conversions, since at lower fractional conversions it is expected that far more of the protonated material will have reacted than the deuterated (Figure II.2a). Not only was such a trend not observed, but for H/D experiments, the different ratios of ^{3}H :^{14}C radioactivity did not appear to affect the measured KIEs. Furthermore, the errors on measured KIEs from six independent experiments for the D/T KIE, and five independent experiments for the H/D value, did not show any trends caused by proton contamination over the fractional conversion range. Figure II.2b presents percentage errors *vs.* fractional conversion for both D/T and H/D KIEs. The measured KIEs are independent of fractional conversion within experimental error, indicating that the pro-*R* C4 position of NADPH is sufficiently deuterated in both cases.

Conclusion

We have successfully developed a two-step microscale chemo-enzymatic synthesis of doubly isotopically labeled *(4R)*-[Ad-^{14}C,4-^{2}H] NADPH, and *(4R)*-[Ad-^{3}H,4-^{2}H] NADPH. We have also demonstrated the utility of the synthesized materials by measuring the KIEs for the R67 DHFR catalyzed reaction: D/T and H/D KIEs were determined with high precision, and the lack of any observed trend in the relative KIE over a range of fractional conversions indicates that any H-contamination, if present, is too small to affect the sensitive competitive measurement. This labeling pattern can also be used, if necessary, in the kinetic study of many other NADPH dependent enzymes.

(*4R*)-[Ad-^{14}C,4-^{2}H]-NADPH, together with (*4R*)-[4-^{3}H]-NADPH can be used to measure primary D/T KIEs, and (*R*)-[Ad-^{3}H,4-^{2}H]-NADPH together with [Ad-^{14}C]-NADPH to measure primary H/D KIEs for any type A NADPH-dependent enzyme. Alternatively, these compounds can be used to measure secondary (2˚) KIEs with any type B enzyme. The procedure described here can be easily modified to synthesize other labeled nicotinamides, including *(R)*-[carbonyl-^{14}C,4-^{2}H] NADPH, and ^{32}P or ^{33}P-labeled 2'-phosphate *(4R)*-[4-^{2}H]NADPH.

Section II. Single-step Enzymatic Synthesis of *R*-[4-^{3}H] NADPH

This section is in preparation for submission to the *Journal of Labelled Compounds and Radiopharmaceuticals* [Atsushi Yahashiri, Hyun Jo, and Amnon Kohen]

Summary

We report a single-step enzymatic microscale synthesis of stereospecifically labeled *R*-[4-^{3}H] NADPH. Application of glucose dehydrogenase from *Thermoplasma acidophilum* enables a transfer of tritium from [1-^{3}H] D-glucose to the *re*-face of C4 of $NADP^+$. Enzymatic analysis showed that the synthesized NADPH is over 99.8 % stereomerically pure, and the counting of the radioactivity indicated final yield of 72 %. This single-step synthesis is advantageous compared with previously reported chemical and enzymatic synthetic procedures because of its high stereopurity and simplified procedure. The product can be used in a variety of experiments, such as the determination of the stereospecificity of enzymes and the measurement of kinetic or equilibrium isotope effects in enzymatic reactions.

Introduction

Reduced β-nicotinamide adenine dinucleotide 2' phosphate (NADPH) is an essential reducing cofactor in various biosynthetic pathways. Radiolabeled NADPHs are of practical use in studying the mechanisms of nicotinamide-dependent enzymes, and particularly, tritium (^{3}H) labeling has been applied in a broad range of chemical, biochemical, and pharmacological research due to its stability and sensitivity.[42, 53, 54, 57, 74-

[76] Its half-life of twelve years is advantageous for quantitative analyses, and low energy emission is beneficial for the development of biomolecular assays.[77, 78] Furthermore, the accuracy and sensitivity of radioactivity analyses in liquid scintillation counting (LSC) assays provides versatility in experimental design.[15, 79, 80]

Stereospecific labeling with tritium at the C4 position of the nicotinamide ring (Figure II.1) is of interest because of its applications in mechanistic studies of NADPH-dependent enzymes. Such labeled cofactor is useful in the determination of the enzymes' stereospecificity and measurements of primary or secondary competitive kinetic isotope effects (KIEs). Understanding the stereochemistry of enzymatic reactions is essential in the design of enzyme targeting drugs in pharmacological and medicinal fields. In fact, *R*-[4-^{3}H] NADPH is a frequently used compound in the determination of stereospecificity of NADPH dependent enzymes.[34] Analyses of the products of enzymatic reactions can provide clear evidence of the stereospecificity of these enzymes, classified as type A (pro-*R* specific), type B (pro-*S* specific), or non-stereospecific enzymes. NADPH dependent type A enzymes only transfer the ^{3}H to the product when *R*-[4-^{3}H] NADPH is used, and produce cold [4-^{1}H] NADP^{+}, whereas type B enzymes transfer ^{1}H to the product and yield [4-^{3}H]NADP^{+}.[34, 71, 72, 81, 82]

Another important use of labeled nicotinamides is in measuring KIEs, namely the relative reaction rates (or rate constants) for different isotopologues. The measurements of KIEs can expose the nature of the catalytic reaction and details of the location and charge of the reaction's transition state.[18, 64, 82-84] In competitive KIE measurements of hydrogen, a mixture of isotopologues reacts together in the same reaction pot, and the isotopic fractionation in the products is analyzed. As the lighter isotope reacts faster or

slower than the heavier one, the product is depleted or enriched with the heavy isotope, respectively. Consequently, measuring the isotopic fractionation in the product at different time points, relative to that at time infinity, affords the ratio of rates, i.e., the KIE. The competitive method determines isotope effects on k_{cat}/K_M because the mixed isotopologues are competitive inhibitors of the others.[15] This measurement leads to a highly accurate KIE determination and is applied to determine not only primary (1˚) isotope effects, (isotope effect on atoms involved in bond cleavage or formation during the reaction), but also secondary (2˚) isotope effects (isotope effects on atoms more distant from the reactive center).[15]

Furthermore, while non-competitive measurements of H/D KIEs (i.e., measuring the rate of each isotopologue independently) are very common and do not require T-labeling, the measured KIEs often do not truly represent the intrinsic KIEs on the H-transfer reaction. This phenomenon is called kinetic complexity, and results from other enzymatic steps (i.e. substrate binding, isomerization, conformational changes, and product release) partially involved in limiting the rate of enzymes. As a result, the isotopically sensitive chemical step is masked, and depleted KIEs are observed. One possible procedure that enables assessment of intrinsic KIE values is the Northrop method that depends on T-labeled cofactor. That method requires comparison of all the isotopes of hydrogen, via determination of two different KIEs on the same chemical step. For example, numeric solution of the relation between k_H/k_T (H/T KIE) and k_D/k_T (D/T KIE) can lead to a good assessment of their intrinsic KIEs.[80-82] 1˚ H/T and D/T KIE determinations for type A enzyme, and the determination of 2˚ KIEs for type B enzymes share *R*-[4-^{3}H] NADPH as a common cofactor.[34, 38] Given the frequent usage of tritium

labeled NADPH as an essential enzymatic substrate for KIE determination, the development of effective synthetic methods is of interest.

Several methods have been reported for the synthesis of *R*-[4-^{3}H] NADPH, but all suffered from various shortcomings.[69, 70, 85, 86] When synthesizing radio-labeled substrates, microscale enzymatic syntheses are preferred methods due to the small scale, mild reaction conditions, and the resultant high yield and stereopurity. Agarwal et al. synthesized *R*-[4-^{3}H] NADPH in two steps by reducing acetone to [2-^{3}H]-isopropanol with [^{3}H]-$NaBH_4$, and using it to reduce $NADP^+$ with thermophilic alcohol dehydrogenase from *Thermoanaerobium brockii* (*tb*ADH) (Scheme II.4a).[70] In this procedure, on the top of the need to synthesize [2-^{3}H]-isopropanol, it is difficult to prevent the formation of *S*-[4-^{3}H] NADPH, which is caused by oxygen contamination in the reaction mixture.[70] McCraken et al. reported a three-step synthetic procedure: reduction of $NADP^+$ by type B glucose dehydrogenase from *Cryptococcus uniguttulatus* (*cu*GDH) and [1-^{3}H]-glucose; an oxidation by the *R*-specific *tb*ADH and acetone to form [4-^{3}H]-$NADP^+$; and again reduction by *cu*GDH and cold glucose to yield the final product (Schemes II.4b).[69] The procedure requires careful control of the ratio between [1-^{3}H]-glucose, acetone, and cold glucose, and its reproducibility and yield are limited by its complexity. Alternatively, a filtration step (~1hr) was required to eliminate *tb*ADH prior to the final reduction of [4-^{3}H] -$NADP^+$ to *R*-[4-^{3}H]-NADPH. Additionally, at present (June, 2010) *cu*GDH is no longer commercially available. Whereas glucose dehydrogenase from *Bacillus megaterium* has been currently used as a substitute in our lab,[35] the development of new synthetic procedures for *R*-[4-^{3}H] NADPH is of obvious need. Here we report a new synthesis using type A glucose dehydrogenases from

Thermoplasma acidophilum (Scheme II.4c), and the examination of the synthesized material in stereospecificity experiments.

Materials and Methods

Materials

Reagent-grade chemicals were used as purchased unless otherwise specified. Tris was purchased from Fisher. 7,8-Dihydrofolate (H_2F) was prepared as described by Blakely.[87] Ultima flo, and Ultima Gold liquid scintillation cocktail were from PerkinElmer. All other materials were purchased from Sigma.

Methods

HPLC Analysis and Separation

Analytical HPLC separations were performed using an Agilent Technologies 1100 Series HPLC fitted with a Supelco Discovery C18 reverse-phase column (250 x 4.6 mm, 5 μm). Purifications were performed using a semi-preparative Supelco Discovery C18 reverse-phase column (250 x 10 mm, 5 μm). The eluted peaks were analyzed using an online UV diode array and a Packard 500TR Series flow scintillation analyzer (HPLC-FSA). When more sensitive analysis was necessary, fractions were collected and analyzed by a Packard 2900 TR Series Liquid Scintillation Counter (LSC). The details of the HPLC method used have been described elsewhere.[71, 72]

Synthesis of R-[4-^{3}H] NADPH

The synthesis of *R*-[4-^{3}H] NADPH is illustrated in Scheme II.4c. The enzyme solution was prepared by diluting 10 µL (1.5 units) of *ta*GDH purchased from Sigma into 50 µL of 100 mM potassium phosphate buffer at pH 8.0. Nitrogen was blown over 0.2 mCi (10 nmol, specific radioactivity: 20 Ci/mmol) of [1-^{3}H] D-glucose, evaporating the solvent to dryness. The dried [1-^{3}H] D-glucose was dissolved into the reaction mixture contained 100 mM potassium phosphate buffer (pH 8.0), 500 µM [1-^{1}H] D-glucose, 1 mM $NADP^{+}$ as the final concentration. The pH was adjusted to 8.0, and the volume was adjusted to 280 µL. The reaction was initiated by adding 20 µL (0.6 units) of the preincubated enzyme solution, and the reaction was conducted anaerobically under argon. The reaction mixture was incubated with occasional mixing at 40 °C for 30 min. The completion of the reaction was determined by HPLC-FSA analysis. After the completion of the reaction, the product was purified *via* semi-preparative HPLC, and the total radioactivity was determined by LSC. The synthesized NADPH was lyophilized and stored in a dry container at -80 °C .[71]

Stereopurity Test for Synthesized R-[4-^{3}H]] NADPH

The synthesized *R*-[4-^{3}H] NADPH was repurified by analytical HPLC column prior to the experiment. The repurified *R*-[4-^{3}H] NADPH was incubated with 10 mM H_2F, and 100 units of dihydrofolate reductase (DHFR) from *E. coli* at 25 ˚C for 30 min. Then, the reaction mixture was bubbled with O_2 gas for 15 min to oxidize the product tetrahydrofolate which overlaps with the NADPH peak in HPLC-LSC separation. The product was analyzed by HPLC and fractions were collected and analyzed by LSC as

described elsewhere.[65, 71] The LSC analysis was used because it has much higher sensitivity than that of the HPLC-FSA.

Results and Discussion

This paper presents a *single-step* synthesis of *R*-[4-^{3}H] NADPH using commercially available substrates and enzymes: *ta*GDH catalyzes a tritium transfer from D-[1-^{3}H] glucose to the *re* face of the nicotiamide of $NADP^{+}$ to form *R*-[4-^{3}H] NADPH. The overall yield was 72 % as determined from the conversion of radioactivity from glucose to NADPH, and the stereopurity was over 99.8 % as determined by the DHFR catalyzed reaction. The stereopurity experiments followed by the sensitive HPLC-LSC analysis indicated that *S* tritiated NADPH, was undetected (Figure II.3). The synthetic procedure presented is advantageous relative to previously reported procedures due to the simplification of the process (Table II.1). In the previously reported two-step chemo-enzymatic synthesis using *tb*ADH, it was hard to control the production of *(S)*-[4-^{3}H] NADPH resulting from non-stereospecific chemical oxidation of *R*-[4-^{3}H] NADPH to [4-^{3}H] $NADP^{+}$.[70] The enzymatic reduction of [4-^{3}H] $NADP^{+}$ yields *S*-[4-^{3}H] NADPH that interferes with any potential use of that material. In another enzymatic synthetic procedure, *R*-[4-^{3}H] NADPH was synthesized using type B *cu*GDH.[69] In this three-step procedure, the first two steps yielded [4-^{3}H] $NADP^{+}$, after which enzymes were removed by a filtration step (~1 hr) to eliminate *tb*ADH, leading to substantial losses of the labeled intermediate. In that procedure, the [4-^{3}H] $NADP^{+}$ was finally reduced with the *cu*GDH using excess cold D-glucose, which further complicated the synthetic and purification procedures. The new one-step synthesis using *ta*GDH is advantageous relative to the two

procedures mentioned above in terms of the simplicity, length, yield, and stereopurity (Table II.1).

Conclusion

In summary, a new single-step microscale enzymatic synthesis of *R*-[4-^{3}H] NADPH is described. The yield (in terms of radioactivity) was 72 %, and the stereopurity was > 99.8 % as determined by consuming the product with *R*-specific DHFR . The potential for applications is broad. Beyond the examples presented above, *R*-[4-^{3}H] NADPH together with [Ad-^{14}C]NADPH or together with *R*-[Ad-^{14}C;4-^{2}H] NADPH can be used to measure 1˚ H/T KIEs or D/T KIEs for type A NADPH dependent enzymes as well as 2˚ KIEs with type B enzymes, and in measurements of equilibrium effects. More broadly, the labeled compound can be used in the determination of new enzymatic mechanisms to examine where the labeling will end up during new enzymatic reaction.[76] The procedure described here can be easily modified to synthesize other labeled nicotinamides. For example, *R*-[4-^{2}H] NADPH can be synthesized using the same procedure with D-[1-^{2}H] glucose.

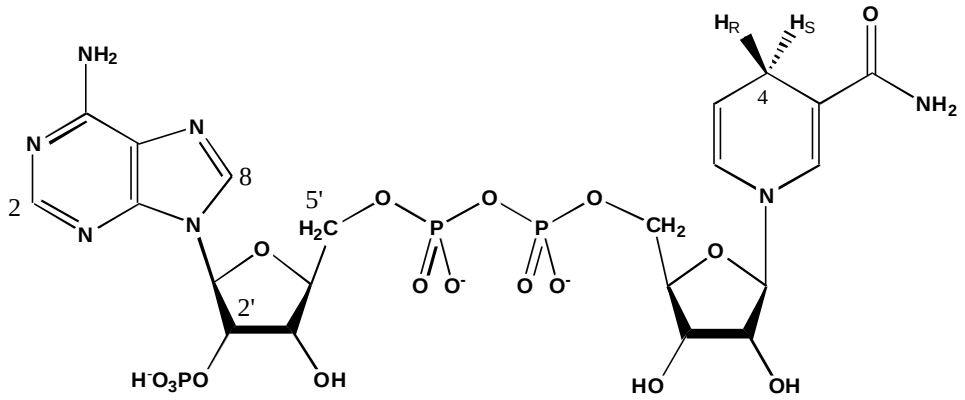

Scheme II.1 Structure of NADPH ($H_R = H_S = {}^1H$), (*R*)-[Ad-^{14}C,4-^{2}H] NADPH ($H_R = {}^2H$, $H_S = {}^1H$), and (*R*)-[Ad-2,5',8-^{3}H,4-^{2}H] NADPH ($H_R = {}^2H$, $H_S = {}^1H$). (*R*)-[4-^{3}H] NADPH (H_R = T, H_S = H), and (*S*)-[4-^{3}H] NADPH (H_R = H, H_S = T).

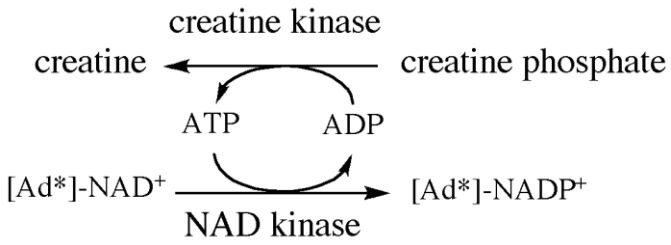

Scheme II.2 Phosphorylation of radiolabeled NAD^+ using creatine recycling system.

(a) Three-steps synthesis

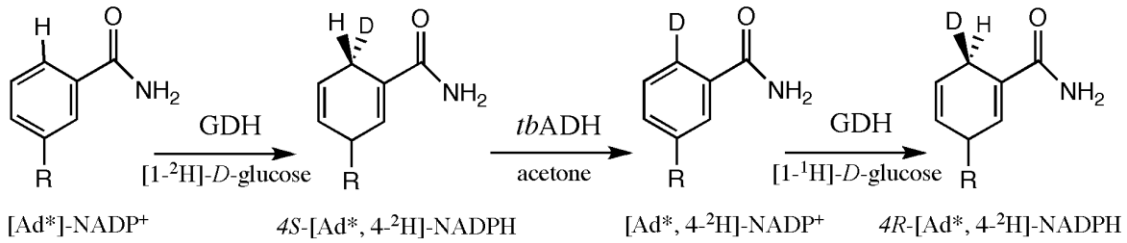

[Ad*]-NADP+ 4S-[Ad*, 4-2H]-NADPH [Ad*, 4-2H]-NADP+ 4R-[Ad*, 4-2H]-NADPH

(b) One- step synthesis

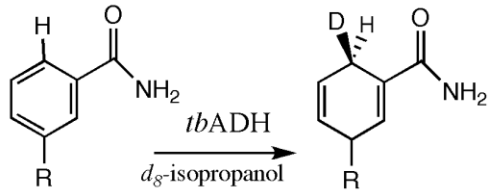

[Ad*]-NADP+ 4R-[Ad*, 4-2H]-NADPH

Scheme II.3 Chemoenzymatic synthesis of isotopically labeled *(R)*-[Ad-^{14}C,4-^{2}H] NADPH, and (*R)*-[Ad-^{3}H,4-^{2}H] NADPH. R represents adenine-2'-phosphate-ribose-5'pyrophosphate-ribose. (a) Three steps synthesis using Type B glucose dehydrogenase and alcohol dehydrogenase[69] (b) One-step synthesis using tbADH.

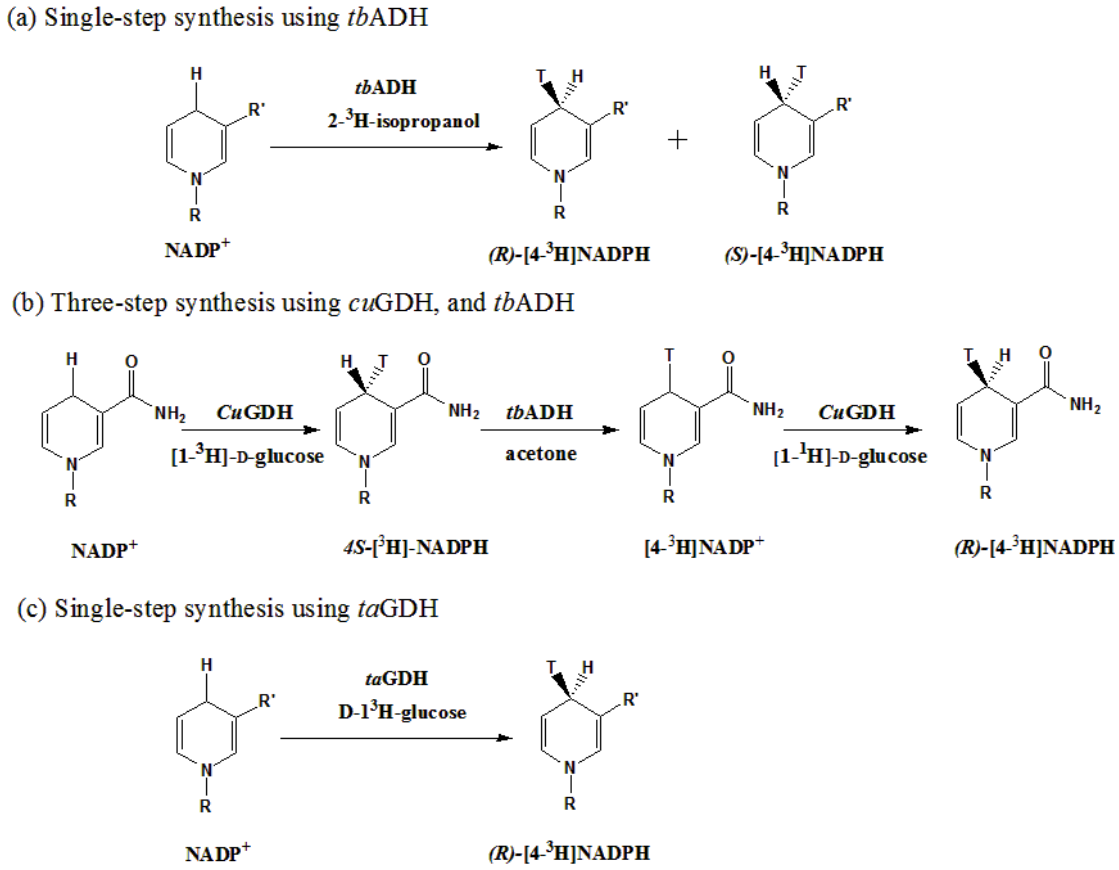

Scheme II.4 Different enzymatic syntheses of isotopically labeled *R*-[4-^{3}H] NADPH. R represents adenine dinucleotide 2' phosphate. (a) A two-step synthesis using type A *tb*ADH; (b) A three-step synthesis using type B *cu*GDH and *tb*ADH[69]; (c) A one-step synthesis using type A *ta*GDH.

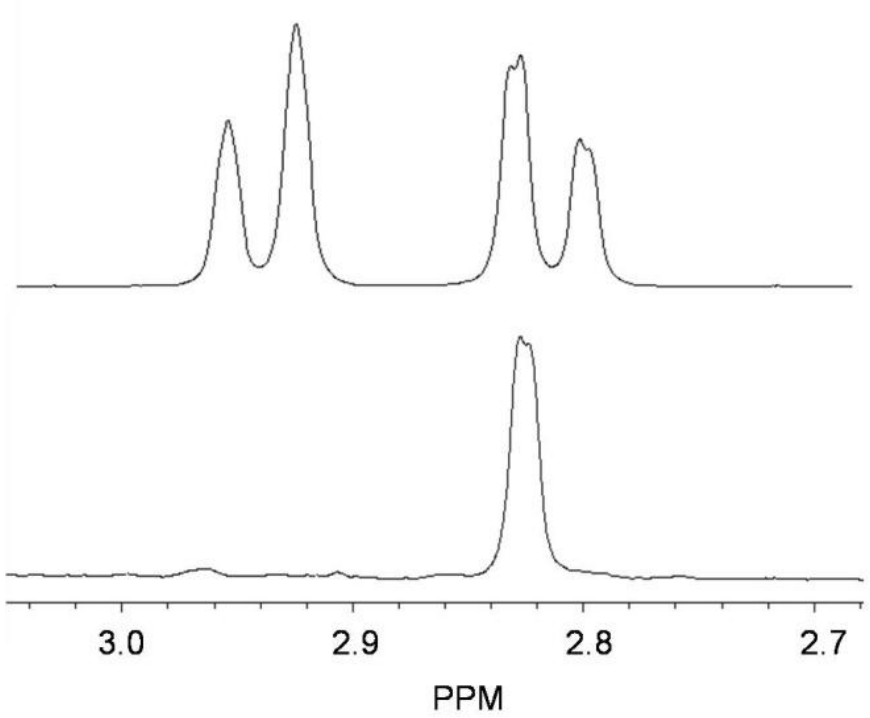

Figure II.1 ^{1}H-NMR spectrum of (a) NADPH, (b) (*4R*)-[Ad-^{14}C,4-^{2}H]-NADPH. The peaks shown represent the hydrogens at C4 of the product with the pro-*R* hydrogen at 2.935 PPM and the pro-*S* hydrogen at 2.822 PPM. In spectrum b, integration of the noise at and around 2.935 PPM indicated that up to 0.3 % ^{1}H contamination would have been detectable if present. Since none is detected the H-contamination is less than 0.3 %.

(a)

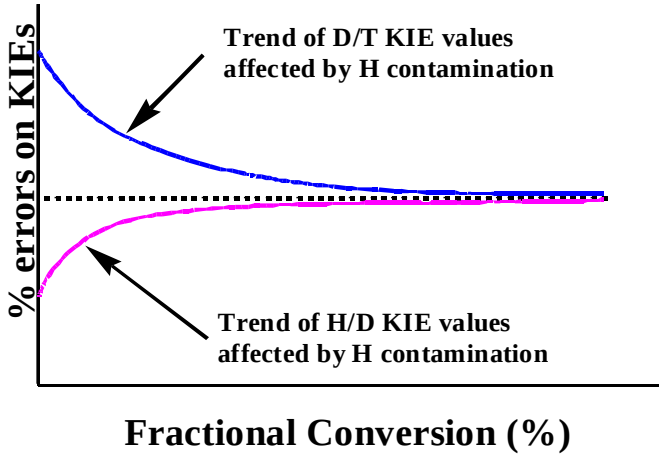

(b)

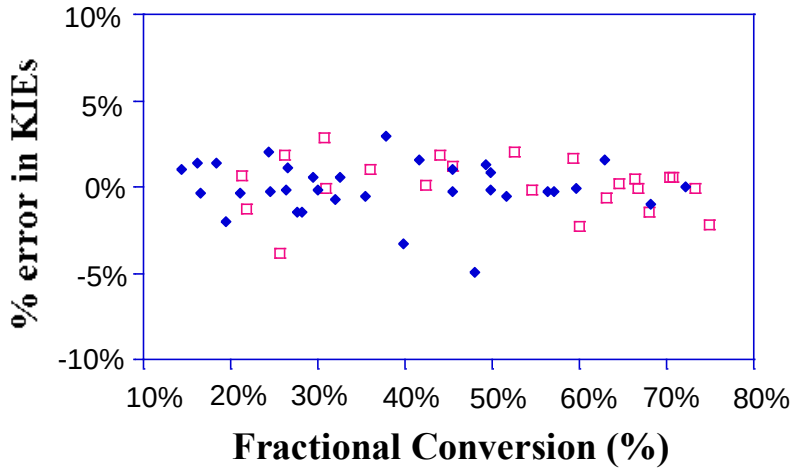

Figure II.2 Schematic illustration of the effects of H contamination on observed KIE values over fractional conversion. **(a)** Dotted line represents % error of KIEs with no H contamination (*f* independent KIEs). Solid lines represent the trends of affected H/D and D/T KIEs distribution due to the artifacts of H contamination. **(b)** Experimental data: Deviations of D/T (♦) and H/D (□) KIEs from their average values are plotted vs. fractional conversion (*f*).

(a)

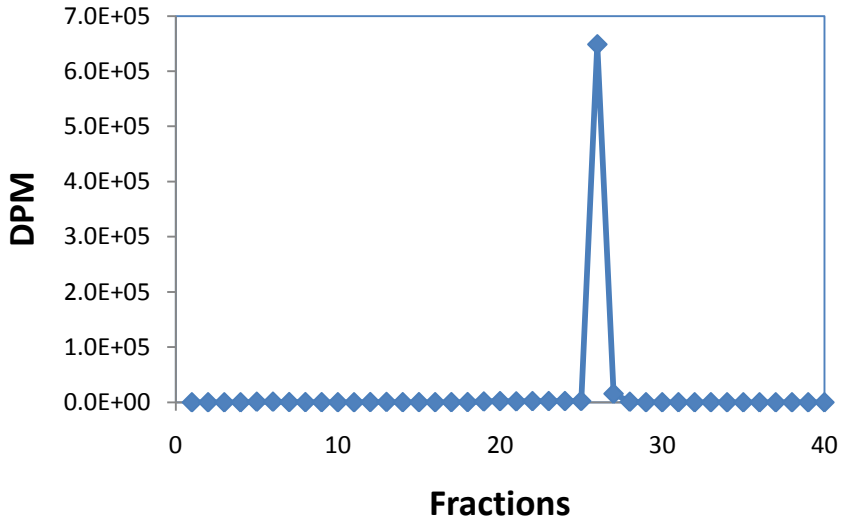

(b)

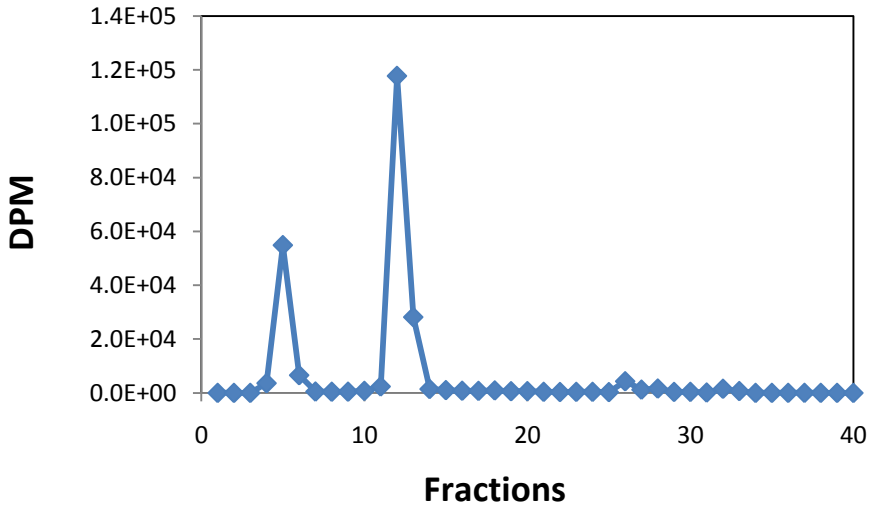

Figure II.3 Radiogram from HPLC-LSC analysis. (a) Repurified NADPH. (b) DHFR reaction products. Tritium at 4*R* position of nicotinamide was transferred on to the product tetrahydrofolate (oxidized tetrahydrofolate derivatives are eluted at 5 min, and 12 min).[71, 72] The small peaks at fractions 26, and 32 are the accumulated unreacted *R*-[4-^{3}H] NADPH, and H_4F, respectively. The formation of [4-^{3}H] $NADP^+$ at 18~21 min is below detection limits.

Synthetic procedure	*Stereopurity*
2-step synthesis using Type A *tb*ADH[a]	84 ~ 99 %
3-step synthesis using Type B *cu*GDH[b]	99.0 %
1-step synthesis using Type A *ta*GDH	99.8%

a. Ref [70],

b. Ref [69].

Table II.1 Stereopurity of synthesized products:

CHAPTER III

TRIPLE ISOTOPIC LABELING AND KINETIC ISOTOPE EFFECTS: A SENSITIVE AND ACCURATE METHOD FOR EXPOSING THE H-TRANSFER STEP IN ENZYMATIC SYSTEMS

This section is in preparation for submitting in the journal *Chem Comm*. [Arundhuti Sen, Atsushi Yahashiri and Amnon Kohen][88]

Summary

Various experimental designs for the assessment of intrinsic kinetic isotope effects in enzymatic reactions are compared. Reduction of dihydrofolate and dihydrobiopterin by two different enzymes were used as model systems, and a range of isotopic labeling patterns applied to facilitate the comparative study of these different methods.

Introduction

In 1975, Dexter Northrop proposed an elegant method to assess the value of intrinsic hydrogen kinetic isotope effects (KIEs) from observed KIEs on the second order rate constants (k_{cat}/K_M, or in short V/K) of enzymatic reactions.[89] The method involves examination of KIEs using the three isotopes of hydrogen (H, D, and T) and was later expanded to include a wide variety of experimental designs.[68] As simultaneous measurement of KIEs using all three isotopes is impractical, one must measure a combination of at least two KIEs. For example, $^{T}(V/K)_{H}$ and $^{T}(V/K)_{D}$ can be used with T as the reference isotope, or $^{D}(V/K)_{H}$ and $^{T}(V/K)_{H}$ can be used with H as the reference isotope. Since 1998,[90] these two combinations have both been used, but no comparative

studies were conducted to determine which of these combinations is advantageous. Only a direct comparison of all combinations of observed KIEs for the same system, under the same experimental conditions, can direct researchers toward the preferred combination. Here we present such an experimental comparison, by assessing the same intrinsic KIEs using both combinations. This required the development and synthesis of a new stereospecific labeling pattern of a reduced nicotinamide cofactor (NADPH) (Figure III.1), enabling competitive measurements of $^{D}(V/K)_{H}$ KIEs that have not been attempted previously. We discuss the pros and cons of the different combinations of observed KIEs, and suggest some guidelines for the design of effective KIE experiments.

The study of kinetic isotope effects is a rich source of information for mechanistic chemistry and biochemistry. Regardless of the reaction being studied, KIE experiments generally follow the same basic procedure: the relevant reactant molecules are isotopically modified so as to produce the smallest perturbation of the system, and their relative reaction rates or rate constants are measured.[67, 79] This procedure permits the use of a wide array of analytical techniques and rate assays, and the design of experiments tailored to the system under investigation. A well-designed KIE experiment can effectually isolate the chemical step from complex kinetic pathways, such as those frequently seen in enzymatic reactions.[81] Since the intrinsic KIEs are often masked by other kinetic steps that are not isotopically sensitive (a phenomenon referred to as kinetic complexity), several methods have been developed to assess intrinsic values from observed KIEs. An assessment of intrinsic KIEs is of critical importance, as only these values can be compared to KIEs from molecular calculations, which in turn provide a molecular rational for experimental KIEs. Equation III.1 relates the observed and

intrinsic KIEs by accounting for the impact of kinetic complexity on the measured value of the KIE:

Equation III.1 Relationship between Observed and Intrinsic KIE

$$KIE_{obs} = \frac{KIE_{int} + C_f + C_r \bullet EIE}{1 + C_f + C_r}$$

Here, C_f and C_r are the commitments to catalysis in the forward and reverse direction, respectively, and *EIE* is the equilibrium isotope effect. The Northrop method derives Equation III.1 by elegant algebra into expressions that are used to extract intrinsic KIEs from measured values. If H/T and D/T KIEs are measured for an enzymatic reaction, intrinsic KIEs can be extracted from observed values via Equation III.2:

Equation III.2 Calculation of Intrinsic KIE using T as a Reference

$$\frac{^{T}(V/K)_{H,obs} - 1}{^{T}(V/K)_{D,obs} - 1} = \frac{(k_H / k_T)_{int} - 1}{(k_H / k_T)_{int}^{-3.3} - 1}$$

A similar equation can be written to calculate intrinsic KIEs from H/T and H/D KIEs:

Equation III.3 Calculation of Intrinsic KIE using H as a Reference

$$\frac{^{T}(V/K)_{H,obs} - 1}{^{D}(V/K)_{H,obs} - 1} = \frac{(k_H / k_T)_{int} - 1}{(k_H / k_T)_{int}^{-1.4} - 1}$$

The only restrictions on the use of the Northrop method are that, for the reaction under consideration, the KIE_{obs} must be measured on an irreversible step (so $C_r = 0$), or that the EIE for the reaction must be close to 1††. Another important assumption is that

†† For nicotinamide-dependent enzymes it is generally found that the EIE does approach 1 under physiological conditions.

the intrinsic relations between KIEs follow the Swain-Schaad relationships[17] as discussed in more detail below.

Northrop has suggested that the isotope of H used as a reference in this technique may play an important role in determining the sensitivity and accuracy of such experiments.[68] Simulations of the magnitude of the propagated error with changing KIE values led to the conclusion that (assuming an intrinsic KIE of ~ 5) the use of H as the reference isotope (i.e. $^{T}(V/K)_{H,obs}$, $^{D}(V/K)_{H,obs}$ experiments) would lead to the largest errors, while T as the reference isotope ($^{T}(V/K)_{H,obs}$, $^{T}(V/K)_{D,obs}$ experiments) would have the smaller error. This is an intriguing result since one would expect the combination of *larger* observed KIEs – i.e. with H as reference – to give smaller errors than measuring a combination of smaller KIEs, as is the case if T were used as reference (assuming the same number of experiments performed for each combination). Thus, in the absence of experimental evidence favoring one method or another, the choice of reference isotope remains to be examined empirically.

We have competitively‡‡ measured primary (1˚) KIEs using two nicotinamide-dependent enzymes from *E. coli*: chromosomal dihydrofolate reductase (cDHFR) and the R-plasmid encoded R67 DHFR. Both cDHFR and R67 DHFR catalyze the conversion of 7,8-dihydrofolate (H_2F) to 5,6,7,8-tetrahydrofolate (H_4F), with a hydride from pro-*R* C4 of reduced nicotinamide adenine dinucleotide phosphate (NADPH) transferred to the *si*-

‡‡ There are two categories of KIE experiments, competitive and non-competitive. Non-competitive KIE experiments involve separate measurements of rates for each isotopologue, whereas competitive methods measures the ratio of reaction rates, i.e., KIE, directly by reacting a mixture of isotopologues in a one-pot reaction, and following the isotopic fractionation as the reaction progresses.

face of the substrate. The two variants are unrelated both in terms of sequence and structure, and the differences in their dynamic flexibility and overall catalytic pathways have been commented upon previously.[45] In the context of this communication, it is important to note that under physiological conditions the hydride transfer step is rate-limiting in the catalytic cascade of the R67 enzyme but not in cDHFR (where hydride-transfer is partially rate-limiting at pH ≥ 8).[91]

To the best of our knowledge, these are the first examples of enzymatic systems for which all three hydrogen KIEs ($^{T}(V/K)_{H,}$ $^{T}(V/K)_{D,}$ and $^{D}(V/K)_{H,}$) have been experimentally measured. These measurements are used to assess the intrinsic KIEs for these enzymes using Equations III.2 and III.3. Such a comparative analysis allows us to evaluate the benefits of measuring one combination or the other. Since approximately a third of all enzymes catalyze some form of hydrogen transfer,[92] and since KIE studies in such systems can provide direct insight to the chemical step, these data are both timely and important.

Finally, the development of a new competitive method to measure $^{D}(V/K)_{H}$ is also interesting because most non-competitive experiments measure that value. The new method provides a point of direct comparison between competitive and non-competitive measurements for the same parameter for many nicotinamide dependent enzymes.

Materials and Methods

Materials

All materials were purchased from Sigma-Aldrich unless otherwise noted. 7,8-Dihydrofolate (H_2F) was synthesized from folic acid as described by Blakely. [Ad-^{14}C]-

NADPH, [Ad-^{3}H]-NADPH, 4*R*-[Ad-^{3}H, 4-^{2}H]-NADPH, 4*R*-[Ad-^{14}C, 4-^{2}H]-NADPH, and 4*R*-[4-^{3}H] NADPH were synthesized by previously published chemo-enzymatic methods (Figure III.1).[65, 69, 83] The synthesized co-factors were purified by semi-preparative HPLC on a Supelco Discovery C-18 RP column as described elsewhere, lyophilized and stored at -80 °C, at which temperature these are stable for two years.[71] cDHFR and R67 DHFR were expressed, purified, and stored according to well-established procedures.[93]

Methods

1° $^{T}(V/K)_{H}$ and $^{T}(V/K)_{D}$ experiments with cDHFR and R67 DHFR were performed using experimental procedures extensively described previously.[34, 44] For 1° $^{D}(V/K)_{H}$ KIE measurements, these procedures were used with some modifications. Briefly, [Ad-^{14}C]-NADPH and 4*R*-[Ad-^{3}H, 4-^{2}H]-NADPH were combined in 1:4 or 1:9 radioctivity ratios (to compensate for lower tritium efficiency during LSC counting; we have determined that varying this ratio between these values does not affect the observed KIEs), co-purified by RP HPLC, and divided into 300,000 DPM ^{14}C aliquots for short-term storage at -80 °C. These aliquots were then used in competitive $^{D}(V/K)_{H}$ KIE experiments at 25°C, pH 9 for cDHFR and pH 8 for R67 DHFR. For cDHFR, the procedure described by Wang et al.[44] was followed with one significant change: since the radioactive labels are remote from the site of hydride transfer, the tetrahydrofolate product need not be oxidized to eliminate problematic variable peaks in the ^{3}H radiogram. We experimentally verified that removal of the oxygen bubbling step did not impact the end result, and all $^{D}(V/K)_{H}$ experiments were subsequently performed without this time-consuming step. Similary, competitive $^{D}(V/K)_{H}$ KIE experiments for R67

DHFR followed the procedure described in reference 34, but without the oxidation step. For both enzymes, at least two experiments were performed for each KIE, with 5 or more data points obtained per experiment. A typical chromatogram of HPLC-LSC analysis is shown in Figure III.2. Intrinsic $^{T}(V/K)_{H}$ KIEs were calculated using the Northrop method and the appropriate form of the Northrop equation: i.e. $^{T}(V/K)_{H}$ and $^{T}(V/K)_{D}$ KIEs were input into Equation III.2, while $^{T}(V/K)_{H}$ and $^{D}(V/K)_{H}$ KIEs were used in Equation III.3, and these equations were evaluated for the intrinsic KIE. Data analysis was performed in the same manner as before.[44] Finally, we used [Ad-^{14}C]-NADPH and [Ad-^{3}H]-NADPH as substrates in a binding isotope effect (BIE) experiment with cDHFR, using the same experimental and analytical methodology described above.

Results and Discussion

Table III.1 lists the observed results, along with the intrinsic $^{T}(V/K)_{H}$ KIEs calculated from observed KIEs using the Northrop method, *viz*. numerical solutions to Equations III.2 or III.3. Since we assume that intrinsic KIEs closely follow the Swain-Schaad relationships[17], intrinsic H/D and D/T KIEs may be easily calculated from the intrinsic $^{T}(V/K)_{H}$ values. For cDHFR with dihydrofolate (H_2F), intrinsic KIEs calculated using the $^{T}(V/K)_{H}$ and $^{D}(V/K)_{H}$ KIEs combination are in complete agreement with intrinsic values calculated from $^{T}(V/K)_{H}$ and $^{T}(V/K)_{D}$ KIE combination. The error on intrinsic $^{T}(V/K)_{H}$ KIEs using H as reference (i.e., from $^{T}(V/K)_{H}$, $^{D}(V/K)_{H}$ combination) is not noticeably larger than those using T as reference (i.e., from $^{T}(V/K)_{H}$, $^{T}(V/K)_{D}$ combination). The $^{T}(V/K)_{H}$, $^{D}(V/K)_{H}$ combination was further validated by KIE measurements in cDHFR, using dihydrobiopterin (H_2B) as substrate rather than H_2F.

Here again, the agreement between $^{T}(V/K)_{H}$ intrinsic KIEs calculated by each method is remarkably good. For R67 DHFR reduction of H_2F, where the H-transfer step is rate-limiting, the validity of the method was confirmed by determining that all measured KIEs are related by the Swain-Schaad relationships as the observed and intrinsic KIEs were identical.

To address concerns that the remote-labeling at the adenine ring might give rise to binding isotope effects (BIEs), we measured a BIE for cDHFR of 1.002 ± 0.001 using [Ad-^{14}C]-NADPH and [Ad-^{3}H]-NADPH as substrates and the same analytical methodology as in a regular $^{T}(V/K)_{H}$ KIE measurement. This confirms that the remote-labeling scheme used in the $^{D}(V/K)_{H}$ measurements does not contribute significantly to the magnitude of isotope effects measured by competitive experiments in cDHFR.

By varying the position and type of the radioactive labels, we have been able to measure $^{T}(V/K)_{H}$, $^{D}(V/K)_{H}$, $^{T}(V/K)_{D}$ KIEs in two different DHFRs, using two substrates (e.g. H_2F and H_2B for cDHFR), as well as a BIE for cDHFR. The combination of competitive $^{T}(V/K)_{H}$, $^{T}(V/K)_{D}$ KIEs measurements was previously applied to study intrinsic KIEs for both enzymes.[34, 38] The data reported here show that intrinsic KIEs may be obtained with similar precision by measuring a combination of $^{T}(V/K)_{H}$, $^{D}(V/K)_{H}$ KIEs as from the $^{T}(V/K)_{H}$, $^{T}(V/K)_{D}$ combination. Furthermore, we find that in terms of experimental error, it is inconsequential which isotope (H or T) is used as a reference in the Northrop method. In cases where the KIEs are expected to be small, the $^{T}(V/K)_{H}$, $^{H}(V/K)_{D}$ combination may be the preferred choice due to the smaller size of the $^{T}(V/K)_{D}$ value, which might not be accurately measured.[35] The $^{T}(V/K)_{H}$, $^{T}(V/K)_{D}$ combination can, however, still be used if a larger number of $^{T}(V/K)_{D}$ values are measured or if the

relative experimental errors are small. Finally, the labeled nicotinamide cofactors required for each combination of experiments can be prepared with similar synthetic procedures, with no significant differences in terms of cost or effort.

Conclusion

In summary, we have shown that the competitive measurement of primary deuterium KIEs is a viable, accurate technique for determination of intrinsic KIEs in two non-homologous DHFR enzymes and with an alternative substrate. However, since the isotopic labeling is on the cofactor, the methods discussed herein are not limited to the reduction of folate derivatives. The importance of nicotinamide cofactors to enzymatic function can scarcely be over-stated as these are ubiquitous enzymatic cofactors, which extends the applicability of the findings to other nicotinamide-dependent enzymes. Furthermore, it is likely that studies with other cofactors and substrates will benefit form the findings of the current study, as the essence of these experiments is very general. Thus the labeling patterns illustrated in Figure III.1 can easily be adapted with minor modification for use to study an enormous number of enzymes, many of which are potential drug targets. In the case of nicotinamide cofactor with T-labeling on the adenine ring, such as the case of $^{D}(V/K)_{H}$ measurements, it is important that the BIE be measured for every new enzymatic system. Since BIEs are typically dependent on the environment of the binding-site,[94] it is important that such a precautionary experiment be performed each time a new remote-labeling pattern is developed, or whenever such a pattern is used to measure KIEs in a new enzymatic system.

Enzyme w/substrate	Observed H/D KIE	Observed H/T KIE	Observed D/T KIE	Intrinsic H/T KIE with T as reference	Intrinsic H/T KIE with H as reference
cDHFR w/H_2F	2.2 ± 0.1	4.9 ± 0.1	1.7 ± 0.1	6.1 ± 0.4	6.2 ± 0.1
cDHFR w/DHBP	3.5 ± 0.1	7.1 ± 0.2	2.0 ± 0.1	13.2 ± 0.9	13.3 ± 0.9
R67 DHFR w/H_2F	3.5 ± 0.1	6.0 ± 0.1	1.7 ± 0.1	6.0 ± 0.1*	6.0 ± 0.1*

* In the case of R67 DHFR, since the chemistry is rate-limiting, the observed and intrinsic KIE values are identical.

Table III.1. Observed and intrinsic V/K KIEs for cDHFR and R67 DHFR at 25°C.

No.	R	L_1	L_2	Measured isotope effect
1.	^{14}C None	^{1}H ^{3}H	^{1}H ^{1}H	1° k_H/k_T
2.	^{14}C None	^{2}H ^{3}H	^{1}H ^{1}H	1° k_D/k_T
3.	^{14}C ^{3}H	^{1}H ^{2}H	^{1}H ^{1}H	1° k_H/k_D
4.	^{14}C ^{3}H	^{1}H ^{1}H	^{1}H ^{1}H	K_H/K_T

Table III.2. Possible NADPH labeling patterns for enzymes like DHFR, which specifically use the Pro-*R* hydrogen as reducing agent (R, L_1 and L_2 as per Figure III.1). The remote radioactive label R acts as a tracer for the non-radioactive hydrogen isotopes in the adjacent columns (L_1 for primary KIEs and L_2 for secondary KIEs). The intrinsic primary KIEs are represented as k_l/k_h where l and h represent light and heavy isotopes, and the relevant binding isotope effect is assigned as K_H/K_T where the labeling is on the adenine ring of NADPH.

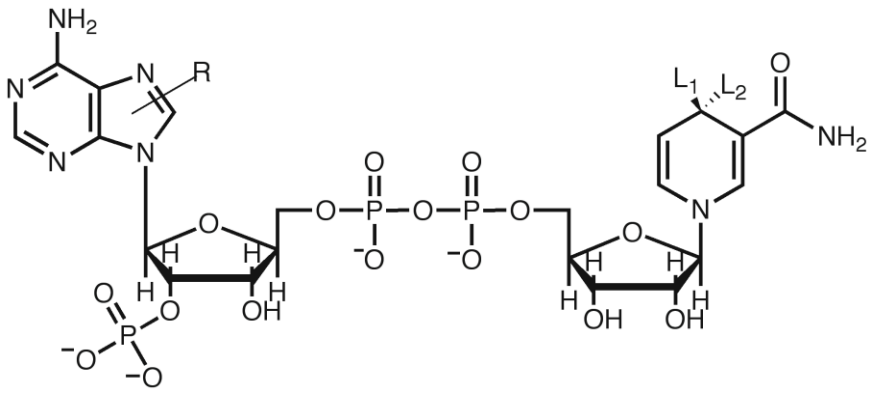

Figure III.1 Labeled NADPH. Here, L_1 and L_2 refer to labeling at the pro-R and pro-S hydrogen positions at C4 of the nicotinamide ring, while R represents the remote isotopic labeling, at one or multiple positions of the adenine ring. Note that in the case of [Ad-^{3}H], the ^{3}H is located at position 2 and 8 on the ring, and position 5' of the attached sugar. [Ad-^{14}C]-label means universal labeling of the adenine ring. Table III.2 summarizes the various labeling patterns available to determine competitive 1˚ KIEs in NADPH dependent enzymes. The pattern for NADH dependent enzymes would be the same but the 2'-phosphate would be an hydroxyl.

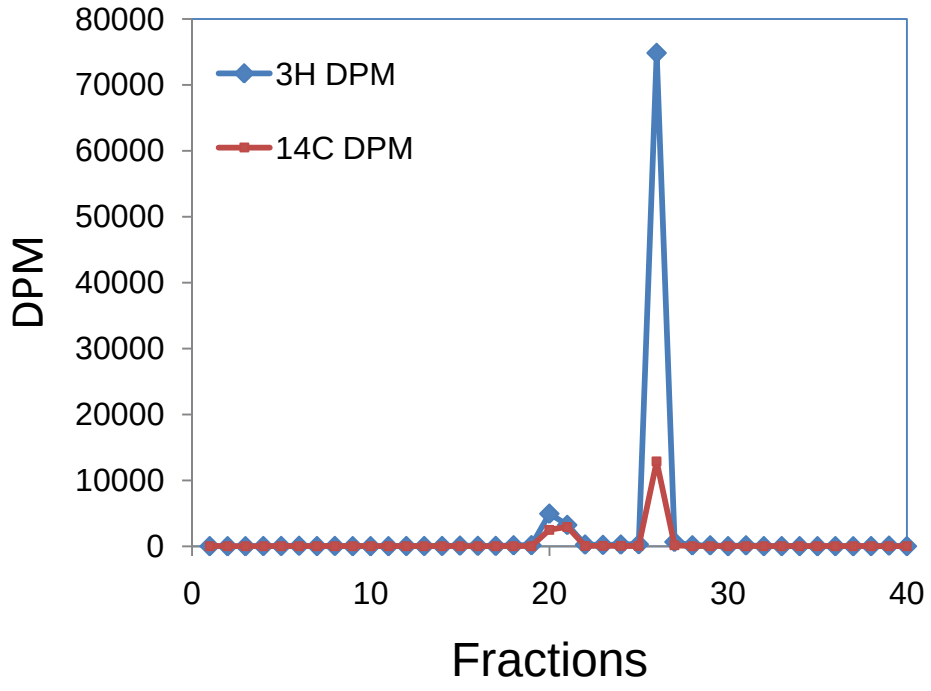

Figure III.2 Typical elution pattern from HPLC-LSC analysis for typical H/D KIE experiment. The presence of two radioactive peaks (corresponding to $NADP^+$ at 20 min and NADPH at 26 min) simplifies the analysis of the H/D experiment in comparison with the D/T or H/T measurement.

CHAPTER IV

ROLE OF EVOLUTION IN TUNING H-TRANSFER COORDINATE IN ENZYMES

This chapter was published in the journal *ChemPhysChem* [Atsushi Yahashiri, Elizabeth E. Howell, and Amnon Kohen (2009), Role of Evolution in Tuning H-Transfer Coordinate in Enzymes][34]

Summary

The nature of a H-transfer reaction catalyzed by a primitive enzyme was examined and compared to the same reaction catalyzed by a mature (highly evolved) enzyme. The findings were evaluated using two different theoretical models. The tunneling correction model[16, 95, 96]suggests that the reaction catalyzed by the mature enzyme involves extensive tunneling while that of the primitive enzyme involves no tunneling contribution. Marcus-like models,[16, 25, 95, 97] on the other hand, suggest that the reaction catalyzed by the primitive enzyme has a poorly reorganized reaction coordinate, while the mature enzyme has tuned the reaction coordinate to near perfect reorganization. The later interpretation does not indicate the degree of tunneling but it does address the level of system preparation that brings the reaction coordinate to the tunneling conformation. Importantly, the findings indicate that in contrast to the primitive enzyme, the mature one has evolved to catalyze a reaction with significant tunneling contribution or with perfectly reorganized reaction coordinate for H-tunneling (using tunneling-correction or Marcus like model, respectively).

Introduction

The current study compares the temperature dependence of intrinsic kinetic isotope effects (KIEs). This tool has been established in recent years as a critical probe for the nature of the chemical step (H-transfer in this case) in enzymatic reactions.[16, 27, 39, 40, 49, 57, 95, 98, 99] One of the unique features of this tool is that it circumvents the need for complete kinetic examination of the system under study as it directly reports on the nature of the chemical step in question. Interestingly, the temperature-independent KIEs have been reported for many highly evolved enzymes catalyzing H transfer, and it has been suggested that this phenomenon indicates that enzymes have evolved to bring the donor and acceptor to a perfect donor-acceptor-distance (DAD) for H-tunneling.[16, 38, 42-44, 57, 95, 100, 101] Typically, the same enzymes under nonphysiological conditions (e.g., low temperature[57] or following a mutation,[43, 102]) presented temperature-dependent KIEs. This provides a positive-control for the ability of temperature dependence of intrinsic KIEs to differentiate between systems that involve different degrees of tunneling and/or different levels of reorganization (according to these two theoretical approaches). While the term "evolved" implies that primitive enzymes would not have as perfect a DAD as their well-evolved counterparts, this theme has not been tested prior to the current study.

In this report, we examine the reaction catalyzed by dihydrofolate reductase (DHFR), namely the reduction of 7,8-dihydrofolate (H_2folate) to 5,6,7,8-tetrahydrofolate (H_4folate) with the stereospecific transfer of a hydride from the *pro-R* C4 position of a nicotinamide ring to the *si* face of the C6 of the pteridine ring. Highly evolved DHFRs are ubiquitous and can be found in most modern organisms. In response to antibacterial drug pressure, bacteria adopt a plasmid that encodes for a primitive enzyme that has some

DHFR activity.[45, 103] The two enzymes being compared here are the well-studied, highly evolved, chromosomal enzyme (cDHFR) from *E. coli*, and the genetically unrelated R-plasmid encoded DHFR (R67DHFR). The later is found in bacterial strains (including *E. coli*) that have developed resistance to the antibiotic drug trimethoprim (TMP - a picomolar inhibitor of cDHFR). Despite the fact that both enzymes catalyze the same reaction, they share no sequence or structural similarities (Figure IV.1).[45, 103]

The active site structure of R67 DHFR is quite different from that in cDHFR, resulting in an approximately 10^6 fold difference in K_i values for TMP.[104, 105]As R67 DHFR has been genetically selected based on its ability to confer TMP resistance, it may not have needed to be a very efficient catalyst. For example, R67 DHFR is one of the smallest enzymes known to self-assemble into an active quaternary structure; this is advantageous as it expends less energy and DNA in encoding the genetic information. On the other hand, a major limit to the catalytic efficiency of R67 DHFR arises from the 222 symmetry imposed on the single active site pore in the homotetramer.[45] This situation results in presentation of a promiscuous binding surface, which allows binding of the nonproductive DHF•DHF and NADPH•NADPH complexes as well as the catalytic DHF•NADPH complex. This "catch 222" situation leads to a low catalytic efficiency (by two orders of magnitude relative to the chromosomal DHFR) and a large entropic contribution to the activation parameters ($T\Delta S^{\ddagger}_{25} = -11.3$ compared to $\Delta H^{\ddagger} = 6.3$ kcal/mol).[48] A wide variety of structural and kinetic data also support this model,[47, 61, 66, 106, 107] including directed evolution experiments where four active-site residues of R67 DHFR can be substituted by a variety of residues.[108] Since R67 DHFR is a homotetramer with a single active site pore, this scenario results in 16 changes per active site, yet, the

mutants are as active as the wild type R67 DHFR. Such tolerance is also in accordance with a poorly evolved enzyme.[45, 108] To improve R67 DHFR function further, gene duplication or quadruplication, followed by divergence of individual gene copies likely needs to occur. Such studies with modified enzymes where the 222 symmetry has been broken[109] are under way.

A comparison of the nature of the H-transfer step catalyzed by these two enzymes is also of great interest due to their different flexibilities. An examination of the chemical step catalyzed by a rigid vs. a flexible enzyme, where both catalyze the same reaction, is of general interest in biophysical and physical chemistry in general. The mature DHFR is flexible and its motions on many different time scales (ns-ms) appear to be critical to its function.[63, 110] The R67 enzyme, on the other hand, appears to be rigid on all examined time scales.[46]

The DHFR chemical reaction serves as an excellent model system for testing the role of the protein in catalysis because many of the experimental and theoretical studies discussed below used this same system.[38, 43, 49, 99, 111, 112] Furthermore, for cDHFR, it has been demonstrated that mutations that decrease the rate of the H-transfer increase the temperature dependency of KIEs,[43] indicating poorer reorganization and a longer DAD. The nature of H-transfer in the R67 DHFR catalyzed reaction has been examined by extracting its intrinsic KIEs from their observed values across a temperature range of 5-45 °C. The findings were compared to the same studies conducted with cDHFR.[38] The only modification was quenching of the R67 DHFR reaction by addition of 5 mM Congo Red.[34] The cDHFR reaction was quenched by addition of methotrexate (a nM inhibitor of cDHFR, but not an inhibitor of R67 DHFR).

Materials and Methods

Materials

Reagent-grade chemicals were used as received unless specified otherwise. β-Nicotinamide [U-^{14}C]adenine dinucleotide (50 μCi) was purchased from Amersham Pharmacia (specific radioactivity >220 mCi/mmol), and Congo Red was obtained from Aldrich. Alcohol dehydrogenase from *Thermoanaerobium brockii* (*tb*ADH), and 2-propanol- d_8 were purchased from Sigma. 7,8-Dihydrofolate (DHF) was prepared by dithionite reduction of folic acid as described by Blakely.[87] R67 DHFR was provided from Dr. Howell. R67 DHFR was expressed, purified, and lyophilized as described elsewhere.[47]

Methods

Synthesis of Labeled Cofactors for KIEs.

(*R*)-[4-^{3}H]-NADPH, (*S*)-[4-^{3}H]-NADPH and [Ad- ^{14}C]NADPH were synthesized as described elsewhere.[69-71] (*R*)- [Ad- ^{14}C] -[4-^{2}H]-NADPH was prepared by stereospecific reduction of $NADP^+$ with 2-propanol-d_8 (> 99.8% D at C2 as determined by ^{1}H NMR) using *tb*ADH. All synthesized cofactors were purified by reverse-phase HPLC on a Supelco Discovery C18 column as described previously and lyophilized for long-term storage at -80 °C.

Determination of Stereospecificity of R67 DHFR by Stereospecifically Labeled NADPH.

Being a primitive enzyme, R67 DHFR has presented binding promiscuity, and utilizes α-NADP and thio-NADPH as cofactors.[113] Consequently, it was not clear at first

whether R67DHFR is as highly stereospecific as highly evolved enzymes. Low stereospecificity would require special treatment and would make accurate determination of KIEs more difficult, as the stereospecificity together with the 1˚ and 2˚ KIEs would have to be solved simultaneously.

We stereospecifically labeled the hydrogens at the 4 position of NADPH with ^{3}H, (T), and conducted the R67 DHFR reaction to determine stereospecificity by examination of the radioactivity in the products. For (*S*)-[4-^{3}H]-NADPH, the *pro-R* hydrogen on NADPH was transferred to the reaction product, tetrahydrofolate (H_4F), and all radioactivity remains on $NADP^+$. While using (*R*)-[4-^{3}H]-NADPH, T on the *pro-R* position was transferred, and all radioactivity was found at THF. The radioactivity at $NADP^+$ was undetectable within experimental error (<0.1%) and the same as for cDHFR, which was used as control with the same labeled substrates. As a conclusion, R67 DHFR is a type A DHFR that stereospecifically transfers the *pro-R* hydrogen from NADPH.

Determination of Competitive Kinetic Isotope Effects.

The R67 DHFR enzymatic reaction was conducted with 200 μM of DHF and 4 μM of NADPH containing cold NADPH and a trace amount of 4*R* [4-^{3}H] NADPH or 4*S* [4-^{3}H] NADPH in MTEN buffer (50 mM 2-morpholinoethanesulfonic acid, 25 mM Tris, 25 mM ethanolamine, and 100 mM NaCl) at pH 8.0. All reactions were carried out under steady state conditions to complete the NADPH consumption. After completed enzyme reactions, aliquots were immediately frozen at -78 °C on dry ice. Prior to the HPLC analysis, the sample was thawed, and oxygen was gently bubbled into the reaction mixture for 15 min to convert THF into its oxidized form.[44, 71] Aliquots were then

injected onto an HPLC equipped with a Supelco reverse phase C18 column, and the eluent was analyzed by Packard flo scintillation analyzer, or Liquid scintillation counter (LSC).[71]

Co-purification of Isotopically Labeled NADPH for Competitive KIE Experiments.

[Ad-^{14}C] NADPH and (*R*)-[4-^{3}H] NADPH (H/T experiments) or (*R*)- [Ad-^{14}C, 4-^{2}H] NADPH and (*R*)-[4-^{3}H] NADPH (D/T experiments) were combined at a radioactivity in DPM ratio close to 1:6 (^{14}C/^{3}H), compensating for the lower efficiency of tritium scintillation counting. Each of the mixtures was co-purified by reverse-phase HPLC on a Supelco Discovery C18 column (25 cm x 4.6 mm, 5 μL), divided into aliquots containing 360,000 DPM of ^{14}C, and flash frozen for short-term storage (up to 3 weeks) at -80 °C.

Competitive Kinetic Isotope Effects (KIEs).

One aliquot of the copurified NADPH was thawed just before use. DHF was added to the reaction mixture to a final concentration of 200 μM (approximately 50-fold excess over the 4 μM total NADPH). The final volume was brought to 990 μL by adding MTEN, and the pH was readjusted to 8.0 at the experimental temperature. Before starting the enzyme reaction, two 80 μL samples (t_0) were withdrawn for quality control for radiolabeled NADPHs. The reaction was initiated by addition of R67 DHFR enzyme solution, and reacted for up to 40 min. At various time points, 80 μL aliquots which have varied fractional conversions (*f*) ranging from 15 to 85% as determined from the distribution of ^{14}C between NADPH and NADP^{+}, were withdrawn, and quenched with 20 μl of Congo Red (final concentration of 5 mM). To ascertain complete fractional

conversion, *c*DHFR (approximately 0.2 unit) was added to the residue of the mixture, and two aliquots for t_∞ samples were quenched after 20 min additional incubation. All quenched samples were immediately frozen and stored at -80 °C.

HPLC Analysis

The detailed HPLC analysis followed reference 71. In short, prior to HPLC-LSC analysis, the samples were thawed and oxidized through bubbling of oxygen for 15 min at room temperature. The samples were then injected into the reverse-phase HPLC system. Fractions (0.8 mL) were collected, mixed with 10 mL of Ultima Gold liquid scintillation cocktail (PerkinElmer), and stored in the dark for 24 h before radioactivity determination in LSC analysis (Packard Tricarb Tr2900 LSC).

The fractional conversion (*f*) of NADPH was determined using Equation II.1. The observed KIEs were calculated according to the following Equation II.2.[73] Experiments at one temperature point were performed at least in triplicate. The observed KIEs were plotted according to the Arrhenius plot (Equation I.7) for KIEs and fitted with exponential regression using KaleidaGraph.

Results and Discussion

Both H/T and D/T KIEs on the second order parameter (k_{cat}/K_M) were measured across a temperature range of 5-45 °C (Table IV.1). In contrast to cDHFR, for which the chemical step was not rate-limiting (and the intrinsic KIEs had to be extracted using the Northrop Method),[68] the H-transfer step is the rate-limiting step in the R67 DHFR catalyzed reaction for both first and second order enzymatic rate constants (k_{cat} and

k_{cat}/K_M, respectively).[47] This is indicated by a logarithmic ratio between observed H/T and D/T KIEs (3.3 ± 0.1 across the temperature range). Furthermore, the H/D KIE we measured for k_{cat} at 25˚C (see reference 47) is also within the predicted Swain–Schaad relations. This further indicates that the observed KIEs for R67-DHFR are also the intrinsic KIEs. In Figure IV.2, the temperature dependence of the intrinsic KIEs for R67 is compared to that of the KIEs measured for cDHFR.[38]

The fitting of the experimental data to the Arrhenius equation for KIEs (prior to averaging the values at each temperature) yields the isotope effects on the activation parameters for both enzymes. The cDHFR KIEs were practically temperature – independent (ΔEa = -0.1 ± 0.3 kcal/mol) and their intercept value (the isotope effect on the pre-exponential factor) was similar to the observed KIEs at the experiment temperature (A_H/A_T = 7.4 ± 4.0).[38] The data for R67 DHFR, on the other hand, resulted in a temperature-dependent KIE (ΔEa = 0.87 ± 0.03 kcal/mol) and an isotope effect on the Arrhenius pre-exponential factor (intercept in Figure IV.2) that is much smaller (A_H/A_T = 1.36 ± 0.07).

Theoretical models using a tunneling correction to transition state theory would interpret these findings as indicative of extensive tunneling in the mature *c*DHFR reaction and no-tunneling in the primitive R67 DHFR reaction. [16, 27, 96] In recent years, Marcus-like models have been developed that take a different approach to rationalizing temperature-independent and temperature-dependent KIEs.[16, 25, 95, 102] According to these models, the temperature-independent KIEs indicate a perfectly reorganized reaction coordinate, and the average DAD of the reactive conformation is ideal for tunneling of both light and heavy isotopes (Figure IV.3). In this model, temperature-dependent KIEs

indicate poor reorganization of the reaction coordinate, for which the average DAD is too long for efficient tunneling. In these cases, fast fluctuations of that distance (a phenomenon denoted as gating) sample more conformations that enable tunneling at higher temperatures. Since the light isotope tunnels from a longer distance than the heavy one, the KIEs increase with decreasing temperature.

$$k = Ce^{\frac{-(\Delta G^{\circ}+\lambda)^2}{4\lambda RT}} \int_{DAD_0}^{DAD_1} e^{F(m)} e^{\frac{-E_{F(m)}}{k_b T}} dDAD$$

Equation I.10 (shown above) presents a general Marcus-like model[16, 25, 95, 102] where the first exponential term is the traditional Marcus-term and is not isotopically sensitive (see Figure IV.3). The second exponential term is the Franck-Condon term describing the H-tunneling (isotopically sensitive but temperature independent, illustrated by the red probability function in Figure IV.3). The last exponential term describes the DAD fluctuations (the gating coordinate) and is both isotopically and temperature sensitive.

Conclusion

In summary, the nature of the chemical steps catalyzed by the highly evolved, flexible, cDHFR and the primitive, rigid, R67 enzyme were compared. The cDHFR appears to have a perfectly reorganized reaction coordinate or otherwise efficient H-tunneling. In contrast, the R67 enzyme required significant gating of its DAD prior to tunneling or otherwise no tunneling contribution to its catalyzed reaction. The findings provide supporting evidence for the notion that enzymes have evolved to optimize their reaction coordinate for efficient tunneling.

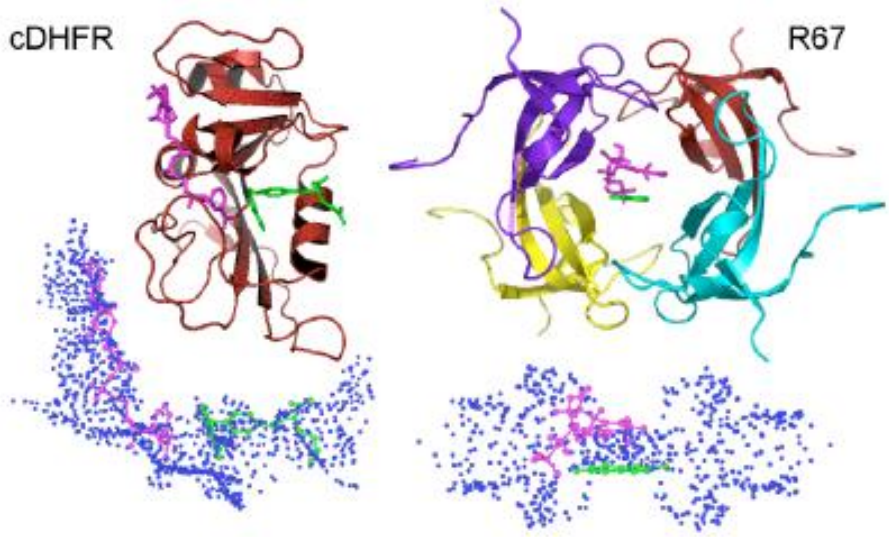

Figure IV.1 Structures of cDHFR (PDB ID R1X2; left) and R67 DHFR (PDB ID 1VIF; right) are presented at the top. For R67 DHFR, the pteridine ring position (green) of the folate was defined in the crystal structure and the nicotinamide (magenta) was docked in place using DOCK. Under each structure we present the reverse images for each active site.[45] In the reverse images, each sphere point describes a potential atom position for use by the docking algorithm. The sphere cluster for cDHFR is shown in approximately the same orientation as its structure. In contrast, the sphere cluster for R67 DHFR is shown sideways, after a 90° rotation along the y-axis.

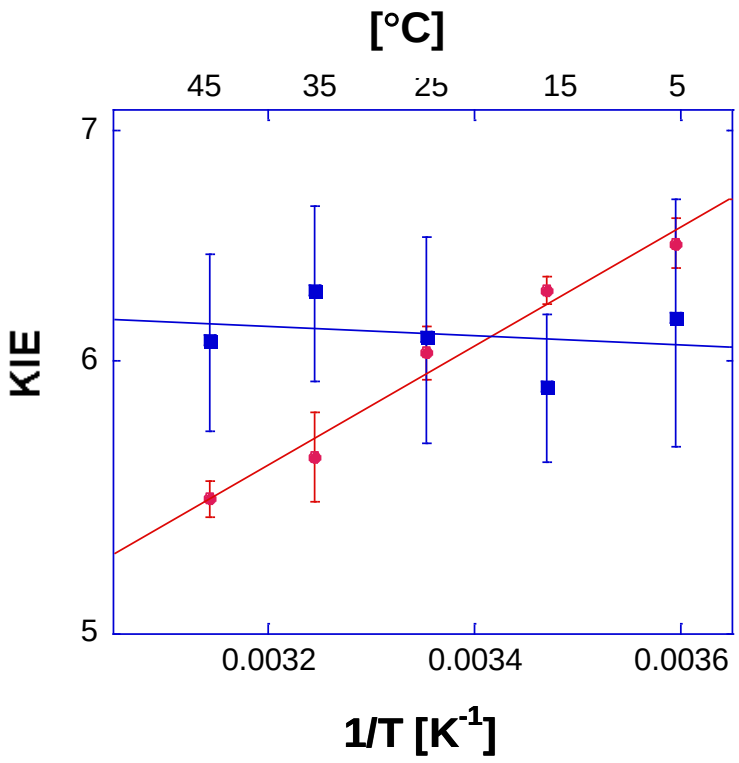

Figure IV.2 A comparative Arrhenius plot of the H/T KIEs (log scale) vs. the reciprocal of the absolute temperature (1/T). The R67 data are in red circles and the cDHFR data[38] are in blue squares. The lines present the exponential fit of the data to the Arrhenius equation. The average and standard deviation of KIEs at each temperature were determined using at least 10 KIE values from three experiments. The standard errors for R67 are much smaller than these for cDHFR because its observed KIEs were also intrinsic, while for cDHFR extensive error-propagation during calculations of intrinsic KIEs inflated the reported errors.[43]

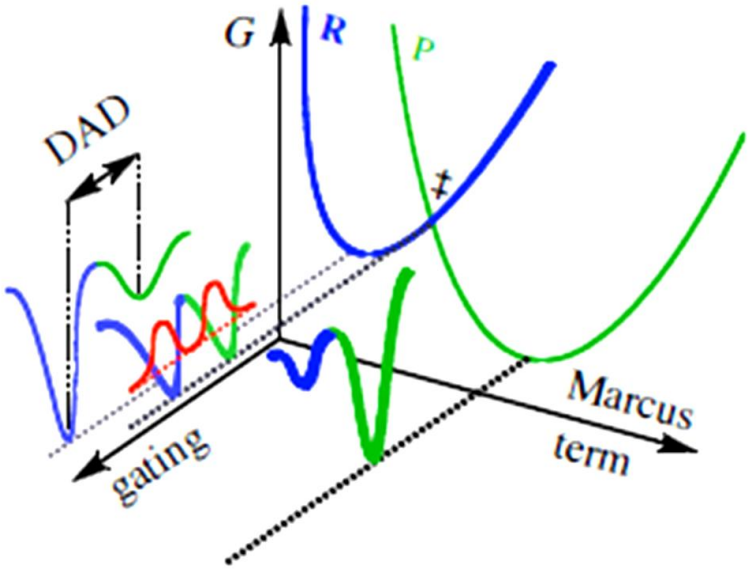

Figure IV.3 Illustration of "Marcus-like" models as expressed in Equation I.10: The orthogonal coordinates presented are the Marcus-term (isotopically insensitive), and the fluctuation of the DAD (gating, isotopically sensitive). R (blue) is the reactant state and P (green) is the product state. The Franck-Condon term presented by the probability of finding the hydrogen at the reactant or the product states is illustrated for the reactive conformation (red probability function).

Temp (°C)	H/T KIE[b]	D/T KIE[b]	H/D KIE[c]
5	6.53 ± 0.09	1.76 ± 0.03	
15	6.36 ± 0.07		
25	6.04 ± 0.11	1.73 ± 0.01	3.52 ± 0.04
35	5.56 ± 0.16		
45	5.47 ± 0.06	1.68 ± 0.02	

Table IV.1 KIEs determined at various temperatures. D/T KIEs were only measured at 25 ˚C and extreme temperatures to establish that the KIEs are within the Swain-Schaad relationship, so the chemistry is rate limiting throughout the temperature range. All the reported errors represent one standard deviation from at least 5 replicates.

CHAPTER V

EFFECT OF ELECTROSTATIC SHIELDING ON H-TUNNELING IN R67 DIHYDROFOLATE REDUCTASE

This chapter was published in the journal *ChemBioChem* [Atsushi Yahashiri, Guy Nimrod, Nir Ben-Tal, Elizabeth E. Howell, and Amnon Kohen (2010), Effect of electrostatic shielding on H-tunneling in R67 dihydrofolate reductase]

Summary

Dihydrofolate reductase (DHFR) catalyzes the hydride (H) transfer reaction between NADPH and dihydrofolate, and produces tetrahydrofolate and $NADP^+$. R67 DHFR is a plasmid encoded enzyme, and is considered a "primitive enzyme" due to its genomic, structural, and kinetic properties.[45, 103] Interestingly, kinetic studies of R67 DHFR show an enhancement in H-transfer rate with increasing ionic strength.[107] To evaluate the source of this rate enhancement, the temperature dependency of intrinsic kinetic isotope effects (KIEs) was measured and the nature of the H-transfer step was evaluated at low and high ionic strengths. At high ionic strength, the KIEs were less temperature dependent than at lower ionic strength. These findings were evaluated using a Marcus-like model, which suggests that at higher ionic strength, the donor and acceptor of the hydride were better oriented for H-tunneling than the same system at lower ionic strength. This comparison addresses the level of system preparation that brings the reaction coordinate into a tunneling-ready conformation. While the effect is small, it is statistically significant, as apparent from the comparative data and standard deviations.

These data demonstrate the high sensitivity of the methodology that was developed to study this system. The differences in electrostatic potential surface between low and high ionic strengths were calculated, and the theoretical findings add a molecular perspective to the experimental data.

Introduction

A kinetic isotope effect (KIE) is the ratio of rates or rate constants of two reactants that only differ in their isotopic composition. The temperature dependence of intrinsic KIEs is sensitive to a reaction's potential surface and dynamics. It serves as an excellent probe for quantum mechanical H-tunneling and the organization of the H-donor and acceptor at the enzyme's active site.[102, 114] One way to assess the intrinsic KIEs involves measurements of KIEs for the three isotopes of hydrogen.[15, 114 79]This methodology may evaluate the nature of the H transfer reaction in enzyme catalysis by specifically focusing on the chemical step in the complex kinetic cascade of an enzymatic reaction. Because of the large mass ratio of three different isotopes of hydrogen, ^{1}H (H), ^{2}H (D) and ^{3}H (T), large and distinct KIEs on the measurements give precious information on the reaction potential surface.[66] For instance, temperature-independent KIEs have been reported for several highly-evolved enzymes under physiological conditions. This phenomenon was interpreted as an indication of precise organization of the reaction coordinate for efficient H-tunneling. On the other hand, the same enzymes under non-physiological conditions presented temperature-dependent KIEs, indicating a poorly organized reaction coordinate.[42, 57, 111, 115-117] A primitive enzyme that was subjected to similar investigation also presented temperature dependent KIEs.[34]

As discussed in more details in the above references, the temperature dependence of KIEs can be rationalized using Marcus-like models (Figure V.1). These models can be summarized in the Equation I.10.

$$k = Ce^{\frac{-(\Delta G^\circ+\lambda)^2}{4\lambda RT}} \int_{r_0}^{r_1} e^{F(m)} e^{\frac{-E_{F(m)}}{k_b T}} dDAD$$

where *C* is the fraction of reactive complexes, and the first exponential term is the traditional Marcus-term that is not isotopically sensitive. ΔG° is the driving force for the reaction, λ is the reorganization energy, R is the gas constant and T the absolute temperature in Kelvin. The second exponential term is the Frank-Condon term representing the integrated tunneling probability of all of the relevant donor– acceptor distances as function of the mass of the transferred particle (F(m)). It is isotopically sensitive, but temperature independent. The last exponential term describes the donor-acceptor distance (DAD) fluctuations, namely the conformational space sampled by the DAD at a given temperature, were $E_{F(m)}$ is the excitation energy for the gating motion between donor and acceptor, as function of the mass of the transferring particle, and k_b is the Boltzmann constant. This term is both isotopically and temperature sensitive.[118] Based on these models, a large temperature dependence of KIEs indicates poor organization of the reaction coordinate, whereas temperature independent KIEs indicate that the enzyme has evolved to bring the donor and acceptor to an optimized hydrogen DAD for hydrogen tunneling.

The current study focuses on a plasmid encoded type of DHFR that is found in several strains of bacteria that have developed resistance to the antibiotic drug, trimethoprim (TMP). In contrast to chromosomal, *dfr*A or *fol*A coded DHFR (*c*DHFR), R67 DHFR is coded by R-plasmid *dfrB*, and shares no sequence or structural similarities

with *c*DHFR. Yet, both the chromosomal and plasmidal DHFR catalyze the same reaction: reduction of 7,8-dihydrofolate (H_2F) to 5,6,7,8-tetrahydrofolate (H_4F) with the stereospecific hydride transfer from the *pro-R* C4 position of nicotine adenine dinucleotide phosphate (NADPH) to the *S* C6 position of H_2F. In contrast to chromosomal DHFRs, R67 DHFR has a robust framework, and is considered to be a primitive enzyme.[45, 103] R67 DHFR is a double funnel like homotetramer of 78 amino acid residues, and it forms a solvent accessible large central pore as an active site. Not being sensitive to antibiotic inhibitors of chromosomal DHFRs, it allows antibiotic resistance. R67 DHFR has a two orders of magnitude lower catalytic efficiency than *c*DHFR, and a large entropic contribution to the activation parameters compared to the *c*DHFR.[48]

We previously reported that the nature of H-transfer in the R67 DHFR catalyzed reaction is very different from that of *c*DHFR: the chemical step (hydride transfer) is rate limiting, and the KIEs are temperature dependent, suggesting a poorly organized reaction coordinate and longer average DAD.[34] Interestingly, we also found that the H transfer of R67 DHFR shows unusual salt dependence.[107] The Michaelis parameters, $K_{M\,(NADPH)}$ and k_{cat}, have the expected increase in K_M with higher ionic strength, but k_{cat} is also increased at higher salt concentrations (Table V.1).[107] This phenomena is not common and not observed in the well-evolved cDHFRs for which much higher ionic strength than that of cellular environment usually has a suppressing effect.[119] This is because high ionic strength increases the effective dielectric constant of the solvent, and shields the electrostatic effects at the active site. In this paper, we examined how the primitive R67 DHFR accelerates the H-transfer rate at elevated ionic strength.

Materials and Methods

Materials

Reagent-grade chemicals were used as purchased unless specified otherwise. β-Nicotinamide [Ad-^{14}C]adenine dinucleotide (267 mCi/mmol) ([Ad-^{14}C] NAD^+), and β-nicotinamide [2,5',8-^{3}H]adenine dinucleotide (25.0 Ci/mmol) ([Ad-^{3}H] NAD^+) were purchased from Amersham Pharmacia. Glucose dehydrogenase from *Bacillus megaterium* (*Bm*GDH) was purchased from USB Corporation. Phosphate and Tris base were purchased from Fisher. Congo Red was obtained from Aldrich. Ultima Gold liquid scintillation cocktail was purchased from PerkinElmer. 7,8-Dihydrofolate (DHF) was prepared by dithionite reduction of folic acid as described by Blakley.[87] All other materials were purchased from Sigma.

Methods

Calculation of the Difference in Electrostatic Potentials on R67 DHFR.

The effect of the different salt concentrations on the electrostatic potential on the surface of the protein scaffold was calculated using established methodologies. The potential at the high ionic strength was subtracted from that at the low ionic strength and the resulting image is presented in FigureV.2. Since many possible errors in the calculations are similar in both calculations, the result presented in Figure V.2 is more reliable than each individual calculation.

Calculation of the difference in electrostatic potential on R67 DHFR was performed by Dr. Nimrod and Dr. N. Ben-Tal. In order to produce a reliable image of the electrostatic potential on the surface of the protein scaffold, missing atoms were

constructed using UCSF Chimera[120]. Tyr 69 in chain D was built by structural alignment with chain B that, among the other chains in the structure, has the least root mean square deviation (RMSD) from the Cα atoms of chain D.

The *p*-aminobenzoyl moiety of the DHF molecule (for which no electron density is defined in the crystal structure) was reconstructed as follows. Using Ligand Expo[121], PDB entries with DHF molecules were searched, and each of the molecules in these entries was superimposed on the atoms available for the DHF molecule in the original structure. Out of these alignments, we selected the one which formed the minimum number of atom clashes with R67 DHFR. Finally, we rotated the torsion angle defined by C6-C9-N10-C14, in order to avoid any atom clashes. Out of the resulting conformations, the one with the highest LigScore[122] value was selected using the Accelrys Discovery Studio package (v2.1).

Both the $NADP^+$ and the DHF molecules are mostly buried within the R67 DHFR pore and participate in hydrogen bonds with protein residues. Therefore, we assumed that the titratable groups of the ligands changed their protonation state and are neutral (but polar). Assuming a replacement of $NADP^+$ with NADPH does not induce a conformational change in R67 DHFR, we examined the effect of this replacement on the electrostatics of the complex. To this end, we repeated the calculations when the nicotinamide in $NADP^+$ is represented as in NADPH. However, the differences in the electrostatics of the complexes were negligible (data not shown).

The electrostatic potential on the protein surface was calculated by assigning partial charges and radii to each atom in the structure using the PDB2PQR server[123] and the AMBER force field[124]. The electrostatic potential was calculated with the Adaptive

Poisson-Boltzmann Solver[125] using the Python molecular viewer[126]. The calculations were conducted with the nonlinear Poisson Boltzmann equation at low and high salt concentrations (μ = 0.15 and 0.42 M, respectively).

Enzyme Preparation.

R67 DHFR was provided from Dr. Howell. R67 DHFR was expressed, purified and lyophilized as described elsewhere.[47]

Synthesis of Labeled Cofactors for KIEs.

[Ad- ^{14}C] NADPH, (*R*)-[4-^{3}H] NADPH, and (*R*)-[4-^{2}H;Ad-^{3}H] NADPH were synthesized as described elsewhere[69, 83, 88]. Briefly, [Ad- ^{14}C]NAD^{+} was phosphorylated with NAD^{+} kinase in creatine recycling system, and stereospecifically reduced at 4-pro*S* position on nicotinamide with *Bm*GDH in the presence of glucose. Similarly, (*R*)-[4-^{2}H;Ad-^{3}H] NADPH was prepared with phosphorylation followed by 4*R* stereospecific reduction of NADP^{+} with 2-propanol-d_8 (> 99.7% D at C2 as determined by ^{1}H NMR) using alcohol dehydrogenase from *Thermoanaerobium brockii*. All synthesized cofactors were purified by reverse-phase HPLC on a Supelco Discovery C18 column as described previously and lyophilized for long-term storage at -80 °C[71, 72].

Co-purification of Isotopically Labeled NADPH for Competitive KIE Experiments.

[Ad-^{14}C]NADPH and (*R*)-[4-^{3}H]- NADPH (H/T experiments) were combined at a radioactivity in DPM ratio close to 1:6 (^{14}C/^{3}H), or [Ad-^{14}C]NADPH and (*R*)-[4-^{2}H;Ad-^{3}H]-NADPH (H/D experiments) were combined at a ratio close to 1:4 to compensate for

the lower efficiency of tritium scintillation counting. Each of the mixtures was co-purified by reverse-phase HPLC on a Supelco Discovery C18 column (25 cm x 4.6 mm, 5 μL), divided into aliquots containing 360 000 DPM of ^{14}C, and flash frozen for short-term storage (up to 4 weeks) at -80 °C.

Competitive H/D and H/T Kinetic Isotope Effects Measurements.

The synthesis of labeled substrates and the kinetic measurements followed the methods we established in the past for the same enzyme.[34] All experiments at high ionic strength were conducted in TE buffer (10 mM Tris, 1 mM EDTA, and 400 mM NaCl) at pH 8.0. Since the reported KIEs at physiological ionic strength were determined in MTEN buffer (μ = 0.15 M) [105, 127], as control experiments, the effects of buffer components were also examined, but they did not affect intrinsic KIE values.

In each competitive KIE experiment, one aliquot of the copurified labeled NADPH was thawed immediately before use. DHF was added to a final concentration of 200 μM, approximately 50-fold excess over 4 μM of NADPH. The reaction was initiated by the addition of R67 DHFR enzyme solution, and incubated for up to 40 min. At various time points, 80 μL aliquots, which contained varied fractional conversions (*f*: Equation II.1) ranging from 15 to 85% as determined from the distribution of ^{14}C between NADPH and $NADP^+$, were withdrawn and quenched with 20 μl of Congo Red (final concentration of 5 mM). To ascertain complete fractional conversion, R67 DHFR was added to the residue of the mixture and two aliquots for t_∞ samples were quenched after 20 min of additional incubation after the completion of the NADPH consumption. All quenched samples were immediately frozen and stored at -80 °C.

Prior to the HPLC analysis, the sample was thawed, and oxygen was gently bubbled into the reaction mixture for 15 min to convert THF into its oxidized form.[44, 71] Aliquots were then injected onto an HPLC equipped with a Supelco reverse phase C18 column, and the eluent was analyzed by Packard flo scintillation analyzer, or Liquid scintillation counter (LSC).[71] The detailed HPLC analysis followed references 71, 72.. In short, prior to HPLC-LSC analysis, the samples were thawed and oxidized through bubbling of oxygen for 15 min at room temperature. The samples were then injected into the reverse-phase HPLC system. Fractions (0.8 mL) were collected, mixed with 10 mL of Ultima Gold liquid scintillation cocktail (PerkinElmer), and stored in the dark for 24 h before radioactivity determination by LSC analysis (Packard Tricarb Tr2900 LSC). The fractional conversion (*f*) of NADPH was determined by the Equation II.1 from the ratio of ^{14}C in the product to the total amount of ^{14}C. The observed KIEs were calculated according to the Equation II.2.[73] Experiments at one temperature point were performed at least in duplicate. The intrinsic KIEs were fitted to the Arrhenius equation for KIEs (Equation I.7), and the isotope effects on the activation parameters were calculated using KaleidaGraph.

Results and Discussion

To understand this unusual effect of ionic strength on R67 DHFR, we combined theoretical and experimental approaches. The differential electrostatic potential surface of the R67 DHFR-NADPH-H_2F ternary complex[61] between physiological ionic strength (μ = 0.15 M) and high ionic strength (μ = 0.42 M)[107] was calculated. The calculations suggested that at a low ionic strength, the enzyme's active site is more positively charged,

while the exterior of the protein is more negatively charged at the lower ionic strength (Figure V.2a and b). The calculations confirmed that at high ionic strength the effective charges in the whole system are reduced, and thus the electrostatic repulsion between the nicotinamide and pterin rings (hydrogen donor and acceptor) at the active site is also reduced (Figure V.2c). Based on these results, we hypothesized that the DAD might be reduced by this change, leading to a more organized reaction coordinate that is better poised for H-tunneling.

To test this hypothesis, we compared the nature of the H-transfer at high and low ionic strengths. We used competitive KIE experiments with R67 DHFR at high ionic strengths (μ = 0.42 M) using a modification of a method we have previously reported for R67 DHFR. [34, 127] Both primary H/D and H/T KIEs on the second order parameter (k_{cat}/K_M) were measured across a temperature range of 5-45 °C (Table V.2). The current determination of KIEs is more sensitive than previously reported due to the analysis of the larger H/D (0.87 % deviation) rather than the smaller D/T KIE (1.2 % deviation, see Table IV.1). A significant improvement in the methodology results from having all the radioactive labeling on the nicotinamide derivatives and none on the product H_4F or its derivatives. The relation between H/D and H/T KIEs clearly follows the semiclassical Swain-Schaad relationship,[17] and serves as a strong indication that the observed KIEs are the intrinsic KIEs across the temperature range. The observed KIE in this case (competitive experiment) is on the second order rate constant, denoted as $^{D}(V/K)$ and $^{T}(V/K)$ for H/D and H/T, respectively. Its relation to the intrinsic KIE follows Equation V.1:

Equation V.1 Relationship between Intrinsic KIEs and Observed KIEs in DHFR reaction

$$^{X}(V/K) = (^{X}k + C) / (1 + C)$$

where ^{X}k is the intrinsic KIE, X is D or T, and C the commitment to catalysis, representing the kinetic complexity (this is a simplified term but the full term will not change the trend in question). For all normal KIEs, the intrinsic H/D KIE is smaller than the intrinsic H/T KIE ($^{D}k < {}^{T}k$). Since C is the ratio between the isotopically sensitive rate of H-transfer in one direction to the isotopically non-sensitive steps in the opposite direction, it is the same for the observed H/D and H/T. Consequently, the observed H/D will be deflated by the commitment (relative to its intrinsic value) more than H/T, and the observed Swain-Schaad relations (also denoted the Swain-Schaad exponent) will be inflated:

Equation V.2 Swain-Schaad exponent using Hydrogen as a reference

$$\frac{\ln^{T}(V/K)}{\ln^{D}(V/K)} > \frac{\ln^{T}k}{\ln^{D}k} = 1.44$$

As discussed in many books and reviews from the 1970s up through ref 2, this is a very sensitive probe as it can range from an intrinsic value of 1.44 up to ∞ due to commitment (in contrast to H/T vs. D/T that only varies between an intrinsic value of 3.3 to unity due to commitment). As found for low ionic strength,[34] the H-transfer step is the rate-limiting step at high ionic strength, and no kinetic-complexity is masking the reported data.

The intrinsic H/T KIEs were evaluated using an Arrhenius plot, and the findings were compared to the same studies conducted at low ionic strength. The fitting of the

experimental data to the Arrhenius equation for KIE provides the isotope effects on the activation parameters for both conditions of ionic strength (Figure V.3). At low ionic strength, R67 DHFR KIEs showed steeper temperature-dependence than at high ionic strength ($\Delta E_a = 0.80 \pm 0.03$ vs. $\Delta E_a = 0.87 \pm 0.03$ kcal/mol at high and low salt, respectively). The isotope effects on the pre-exponential factor were a little smaller at low ionic strength ($A_H/A_T = 1.49 \pm 0.08$ vs. $A_H/A_T = 1.36 \pm 0.07$ at high and low salt, respectively). These differences are at the limit of the detection of the improved methodology, but are statistically, and quantitatively significant (Table V.3).[42]

Here, a small change (2.5 fold) in H-transfer rate in two different ionic strengths seems to be associated with a change in the temperature dependence of intrinsic KIEs. Additionally, at high ionic strength, the intrinsic KIEs became somewhat smaller. In accordance with Marcus-like models, a reduced temperature dependency in KIEs suggests that the average DAD at the tunneling-ready conformation at high salt is shorter and requires less "gating" than at low ionic strength. Together, these findings support the hypothesis suggested above, namely that the average DAD[128] is shorter at high ionic strength due to reduced electrostatic repulsion. Our findings indicate that at the active site of R67 DHFR, the electrostatic shielding provided by the increased salt improves the orientation of the donor and acceptor at the tunneling-ready conformation and increases k_{cat}.

Conclusion

In summary, a modified analysis of the nature of H-transfer in the reaction catalyzed by R67 DHFR improved the sensitivity limits and exposed the effect of high

ionic strength on the intrinsic properties of the catalyzed chemistry. The findings revealed a small but significant alteration of organization of the system and the DAD for H-tunneling as result of altering salt concentration. The combination of calculations and kinetic studies suggests that at high ionic strength, the reduced electrostatic repulsion leads to shorter DAD for H-tunneling.

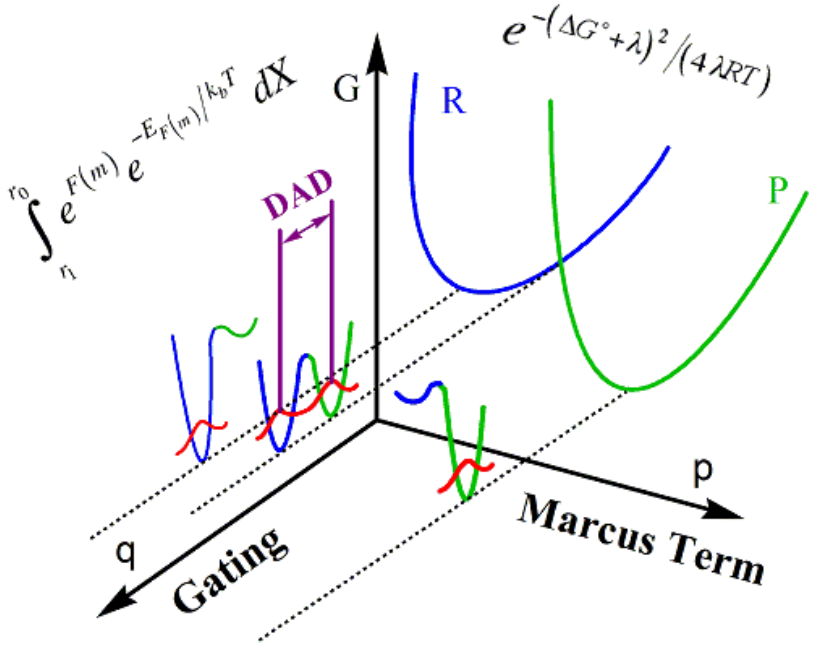

Figure V.1 Three-dimensional illustration of Marcus-like models: Energy surface of environmentally coupled H tunneling. Two orthogonal coordinates are presented: p, the environmental energy parabolas for the reaction state (R: blue) and the product state (P: green), and q, the gating coordinate, along which the red lines represent the hydrogen's probability wavefunction. Thermal fluctuations in the DAD along the q coordinate lead to the temperature dependence of KIE.[34]

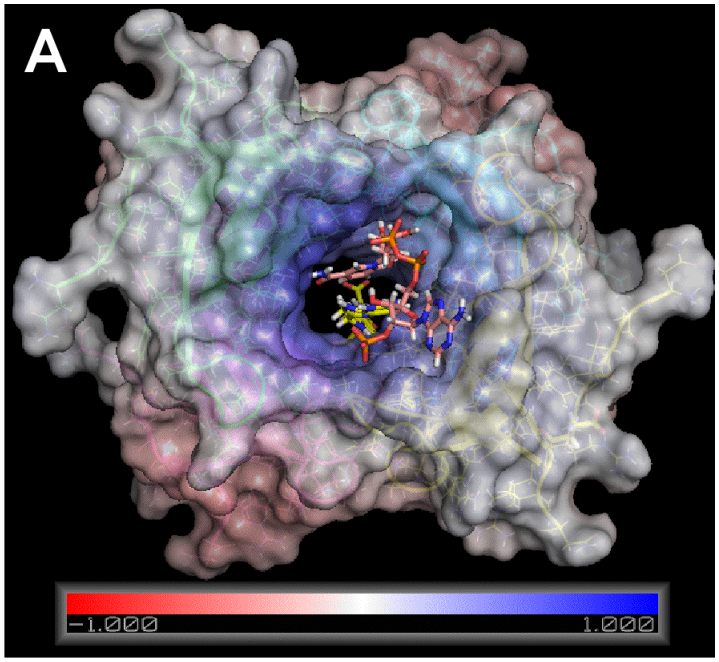

Figure V.2 The change in the electrostatic potential of R67-DHFR at different salt concentrations. The electrostatic potential at $\mu = 0.15$ minus the potential at $\mu = 0.42$ is mapped onto the molecular surface of the protein, according to the color scale on the left. By this scale, blue surfaces indicate that the charge is higher at $\mu = 0.15$ M, while red surfaces indicate that the charge is higher at 0.42 M salt. The figure was produced using PyMol (DeLano, W.L., The PyMOL Molecular Graphics System (2002) DeLano Scientific, San Carlos, CA, USA (http://www.pymol.org)).[129]

NADPH binding domain is more positively charged at high ionic strength.

A) NADPH binding domain.

B) H_2F binding domain.

C) The active site of the enzyme.

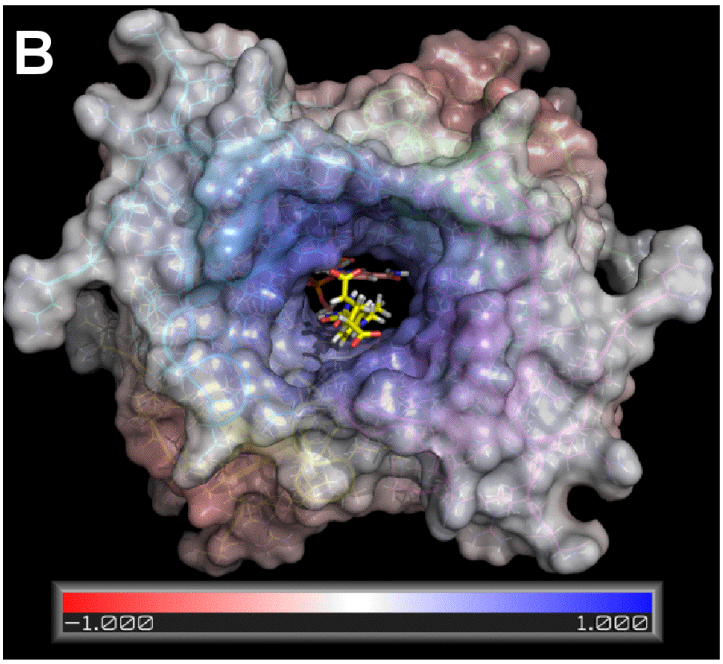

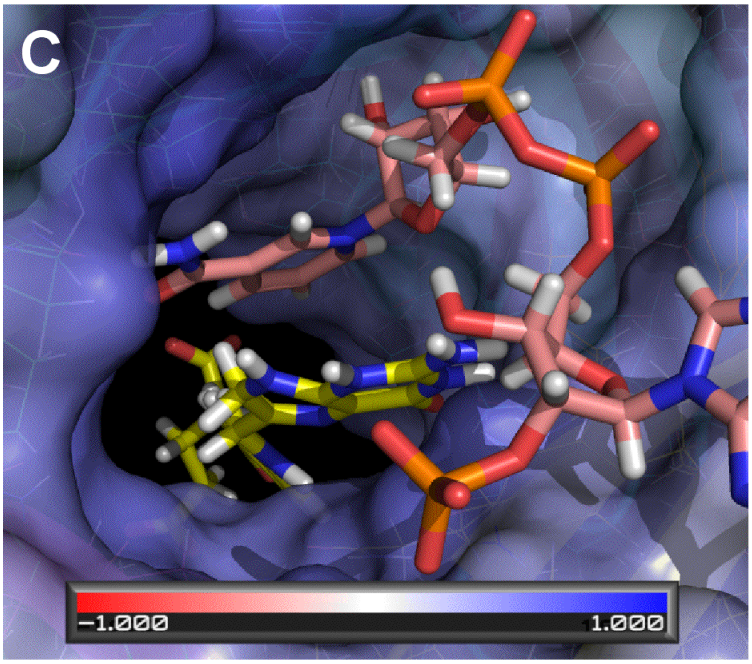

Figure V.2-continued

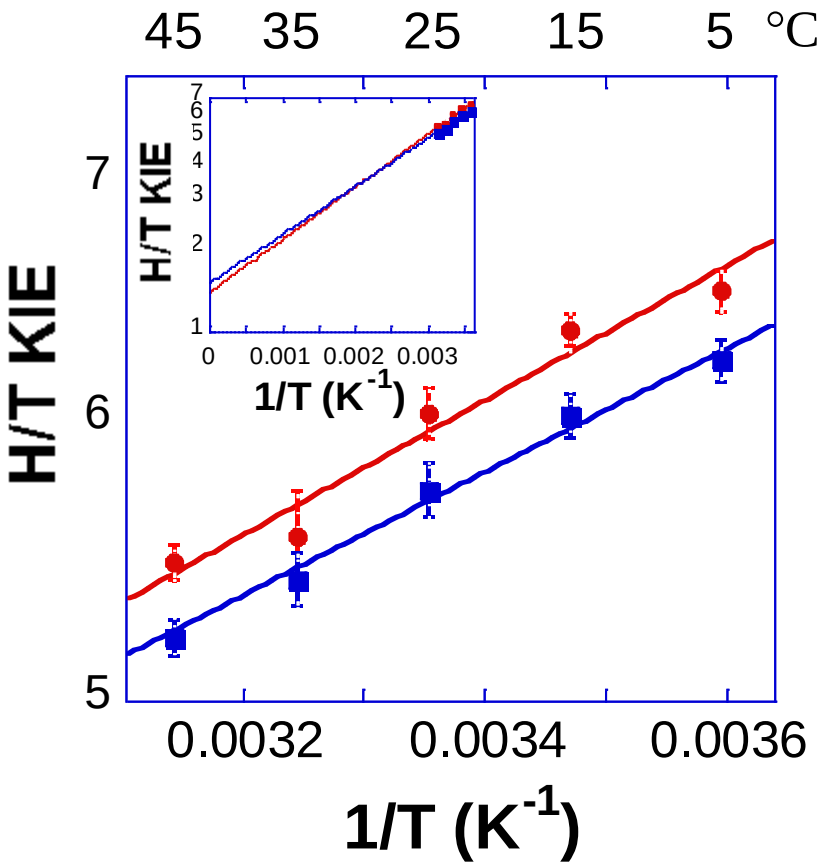

Figure V.3 A comparison of Arrhenius plots for the H/T KIEs (log scale) vs. the reciprocal of the absolute temperature at low ionic strength (●) and at high ionic strength (■). The average and standard deviation of KIEs at each temperature were determined using at least 8 KIE values from multiple experiments.

[NaCl]	$K_{m(\mathrm{NADPH})}$	$K_{m(\mathrm{DHF})}$	k_H
0.13 M (μ = 0.15)	8.7 ± 0.4	13 ± 1	1.5 ± 0.1
0.20 M (μ = 0.22)	13 ± 1	29 ± 2	2.0 ± 0.1
0.30 M (μ = 0.32)	26 ± 1	54 ± 3	2.8 ± 0.1
0.40 M (μ = 0.42)	41 ± 2	81 ± 4	3.7 ± 0.2
	[a] TE buffer contains 10 mM Tris and 1 mM EDTA, [b] Kinetic parameters from reference 107		

Table V.1 Steady-state kinetic values for R67 DHFR in TE buffer in the presence of NaCl.[a,b] All the reported errors represent 1σ standard deviation from at least 5 replicates.

Ionic strength	μ = 0.42		μ = 0.15		
Temp (°C)	H/T KIE[a]	H/D KIE[a]	H/T KIE[b]	D/T KIE[b]	H/D KIE[c]
5	6.24 ± 0.08	3.55 ± 0.04	6.53 ± 0.09	1.76 ± 0.03	
15	6.02 ± 0.08		6.36 ± 0.07		
25	5.73 ± 0.10	3.40 ± 0.03	6.04 ± 0.11	1.73 ± 0.01	3.52 ± 0.04
35	5.41 ± 0.09		5.56 ± 0.16		
45	5.21 ± 0.06	3.14 ± 0.04	5.47 ± 0.06	1.68 ± 0.02	
	[a] This work, [b] reference 34, and [c] reference 83				

Table V.2 KIEs determined at various temperatures. D/T KIEs were only measured at 25 ˚C and extreme temperatures to establish that the KIEs are within Swain-Schaad relationship, so the chemistry is rate limiting throughout the temperature range.[§§]

[§§] All the reported errors represent 1s standard deviation from at least 5 replicates. The observed KIE in this case (competitive experiment) is on the second order rate constant, denoted as $^{D}(V/K)$ and $^{T}(V/K)$ for H/D and H/T, respectively. As discussed in many books and reviews from the 1970s up through ref 2, this is a very sensitive probe as it can be ranged from an intrinsic value of 1.44 up to ∞ due to commitment (in contrast to H/T vs. D/T that only varies between an intrinsic value of 3.3 to unity due to commitment).

	R67 DHFR (Ionic strength)	
Ionic Strength	μ = 0.42 M	μ = 0.15 M[a]
A_H/A_{T_T}	1.49 ± 0.08	1.36 ± 0.07
$\Delta\Delta E_{aA\text{-}B}$ (kcal/mol)	0.80 ± 0.03	0.87 ± 0.03
Fold in k_H[b]	2.5	1
	[a] reference 34 [b] Fold in k_H is relative to k_H at μ = 0.15 M	

Table V.3 Comparison of the isotope effect on the Arrhenius pre-exponential factors in accordance with the differences in k_{cat} relative to the wild-type chromosomal DHFR.All the reported errors represent 1σ standard deviation from at least 5 replicates.

CHAPTER VI

COMPARATIVE CROSS-REACTIVITY KINETIC STUDIES OF PTERIDINE REDUCTASE AND DIHYDROFOLATE REDUCTASE

This chapter is in preparation to submit to the journal *ChemPhysChem* [Atsushi Yahashiri, Michael J. Toraason, Asad Hashmi, Robert Nixon III, Nikhil Manjunath, Arundhuti Sen and Amnon Kohen]

Summary

Pteridine reductase 1 (PTR1) primarily catalyzes the reduction of biopterin and dihydrobiopterin (H_2B) with NADPH and produces tetrahydrobiopterin (H_4B) and $NADP^+$. It has been suggested that PTR1 has some dihydrofolate reductase (DHFR) activity, reduction of dihydrofolate (H_2F) to tetrahydrofolate (H_4F).[130] Chromosomal DHFR from *E. coli* (cDHFR) is an efficient enzyme in catalyzing the reduction of H_2F, however, its catalytic activity toward H_2B was not known. In order to study kinetic properties of both enzymes, we first purified the enzymes using a methotrexate-agarose affinity chromatography. This method is advantageous relative to previously reported PTR1 purification methods because of the fewer purification steps. In H_2B reduction, a strict stereospecificity to the pro-*S* 4H of NADPH was observed for PTR1 whereas pro-*R* specificity was found for cDHFR. To compare the cross reactivity between H_2B and H_2F reductases, steady state kinetic Michaelis-Menten parameters for both H_2B and H_2F were determined for PTR1 and cDHFR. In the PTR1 reaction, the parameters for H_2F and H_2B were very similar; on the other hand, k_{cat} and K_m for H_2B reduction by cDHFR was ~ 500

fold slower and weakly interact relative to H_2F reduction. These results suggest PTR1 did not show a significant substrate-selectivity although it slightly prefers the reduction of the natural substrate. cDHFR, however, presented significant selectivity toward its natural substrate. These findings indicate that the *p*-aminobenzoyl-glutamate (pAB-glu) moiety of H_2F contributes to both binding and product release rates (the rate limiting step on k_{cat}) for DHFR but has insignificant roles in PTR1 catalysis. To test the effect whether the missing pAB-glu in the cDHFR catalyzed H_2B reaction also affects the nature of the H-transfer reaction we examined the temperature dependence of the intrinsic KIEs using *R*-labeled NADPH. Interestingly, the enzymatic reduction of H_2B showed inflated KIEs that were more temperature dependent than the reaction of H_2F. In accordance with Marcus-like models,[16, 25, 95] these findings suggest that the unnatural substrate reduction occurs from an ensemble of confirmations that is not as well tuned for H-tunneling as the natural substrate. Together, the findings indicate that the lack of the interaction provided by the pAB-glu tail of the natural substrate, reduced not only binding affinity but also disturbed the reorganization of the donor and acceptor of the reactive conformations, from which H-tunneling can occur.

Introduction

The chromosomal dihydrofolate reductase from *E. coli* (cDHFR) has been studied as a model system of H transfer reaction in enzymology. cDHFR catalyzes the reduction of dihydrofolate (H_2F) to tetrahydrofolate (H_4F) using NADPH, by the stereospecific transfer of a hydride from the pro-*R* C4 position of a nicotinamide ring to the *si*-face of C6 of the 7,8-dihydropteridine ring.[91] cDHFR is a flexible enzyme with a complex

kinetic cascade,[45] and it is proposed to be a well-evolved enzyme because of its high efficiency.[131] Experimental and theoretical studies of cDHFR suggested that a network of coupled promoting motions participates in the rate enhancement in catalysis.[3, 41, 43, 132, 133] In accordance with temperature independent intrinsic KIEs with its natural substrates, it is suggested that cDHFR has a fine-tuned active site for H tunneling.[38, 43]

Recently, DHFR activity has been reported in several different enzymes,[134] and these alternative DHFRs compensate the DHFR activity in the organisms that lack chromosomal DHFR (*FolA*). One of these enzymes, pteridine reductase 1 from *Leishmania major*[***] (PTR1) primarily catalyzes the reduction of biopterins (B) and dihydrobiopterin (H_2B) to tetrahydrobiopterin (H_4B) using NADPH whereas it also reduces dihydrofolate (H_2F) to tetrahydrofolate (H_4F) using NADPH (Figure VI.1).[130] This residual DHFR activity of PTR1 supports the resistance of *Leishmania* against some antibiotic treatments targeting DHFR.[130] Genetically PTR1 is proposed to be classified as a *FolM* DHFR family member, and thus it is remotely related to other *FolA* (chromosomal DHFRs) and *FolB* (plasmid-coded DHFR) families (Figure I.6).[62] Given the reduced sensitivity against DHFR targeting antibiotics, the structure of PTR1 is quite different from the chromosomal (*FolA*) DHFRs. PTR1 is a rather large homotetramer (130 kD) with four active sites whereas *FolA* DHFR is a small monomer (18 kD) and has a single active site per enzyme (Figure I.7).[45, 62] The active site structure of PTR1 suggested that the pro-*S* 4H of NADPH faces toward the substrate whereas *FolA* and

[***] Leishmaniasis is a parasitic disease caused by the infection of *Leishmania* species.[135] Over 12 million people in 88 countries currently suffer from Leishmaniasis, which is a serious health threat worldwide.

FolB DHFRs maintain strict pro-*R* stereospecificity as evident from both structural studies and isotopic labeling experiments.[34]

Here we report comparative investigations of H-transfer reaction of two different substrates by two different enzymes. First, we developed a new purification procedure for PTR1 using methotrexate-agarose (MTX-agarose) affinity chromatography (Scheme VI.1b). The Michaelis-Menten parameters using PTR1 with H_2F and H_2B were then compared with their values for DHFR. We determined the intrinsic primary (1°) KIEs and their temperature dependence in the reduction of its unnatural substrate H_2B by cDHFR and the findings were compared to those with the natural substrate H_2F and rationalized using Marcus-like models.

Materials and Methods

Materials

Reagent-grade chemicals were used as purchased unless specified otherwise. Methotrexate was purchased from MP biochemicals LLC. Sodium chloride, phosphate and Tris base were purchased from Research Product International Corp. H_2B was purchased from Schircks Laboratories. Ultima Gold liquid scintillation cocktail was purchased from PerkinElmer. DE52 anion exchange chromatography resin was purchased from Whatman. H_2F was prepared by dithionite reduction of folic acid as described.[87] All other materials were purchased from Sigma.

Methods

Expression of PTR.

The PTR1 expression system was a gift from Dr. Stephen M. Beverley at Washington University in St. Louis.[136] The transformed strain was inoculated into 5 mL of the Lysogeny broth with 100 μg/mL of ampicillin (LB amp^+). The first seed culture was grown at 37 °C on a rotating wheel at 200 rpm in the incubator. Then, 0.5 mL of seed culture was inoculated into 50 mL LB amp^+ medium and cells were grown at 37 °C with shaking at 200 rpm for 10 hours. 15 mL of seed culture were inoculated into 1.5 L LB media. Cells were grown at 37 °C with shaking at 120 rpm until the optical density at 600 nm was about 0.8. Temperature was adjusted to 25 °C and 10 μl of 1 M filter-sterilized isopropyl-β-D-thiogalactopyranoside solution was added to start expressing the PTR1. Cells were grown at 30 °C for 20 h with shaking at 120 rpm, and harvested by centrifugation and stored at -20°C.

Purification of PTR1.

Subsequent procedures were carried out at 4 °C. PTR1 activity was determined by tracing the oxidation of NADPH with H_2B by following the reduction in absorbance at A_{340}. One unit of enzyme corresponds to the oxidation of 1 μM of NADPH per minute. Cells were thawed and resuspended in 50 mM Tris-HCl, pH 7.0, 20 mM 2-mercaptoethanol, 1 mM phenylmethylsulfonyl fluoride.[130] Lysis was initiated by lysozyme treatment and sonication, and the debris was then removed by centrifugation (8000 g for 60 min). The supernatant was directly loaded onto DE52 anion exchange column equilibrated with 20 mM Tris HCI (pH 7.0) and PTR1 was eluted with a 0-0.3 M

NaCl gradient. The active fractions were directly applied to a MTX-agarose affinity column equilibrated with 20 mM Tris-HCl (pH 7.0), 0.12 M NaCl (Buffer A). PTR1 was eluted with buffer A with 0-10 mM folate gradient with 10 % (w/w) glycerol. The active fractions were combined and dialyzed against 2 L of buffer A twice to remove folate. The enzyme solution was again applied onto DE52 chromatography in order to remove residual folate. Purified fractions were pooled and condensed using a Millipore filter Ultracel 10K. Purity of PTR1 was examined by SDS PAGE and total protein was quantified with the Bradford assay with BSA standards. Purified PTR1 was stored in -80 °C. DHFR was purified using similar procedure. Purified DHFR and its active sites were quantified by Bradford assay and MTX active site titration, respectively.[137]

Enzyme Kinetics.

The kinetic parameters K_m and k_{cat} for dihydrofolate and dihydropteridine were measured in a spectrophotometric assay with NADPH as described elsewhere.[138, 139] Enzyme assay was conducted in MTEN buffer (50 mM 2-morpholinoethanesulfonic acid, 25 mM Tris, 25 mM ethanolamine, and 100 mM NaCl) at pH 9.0 and Michaelis parameters (K_m and k_{cat}) were determined. Kinetic data were evaluated by fitting to the Michaelis-Menten equation using the Sigma Plot Enzyme Kinetics Module (Systat Software Inc, San Jose, CA, USA).

Determination of Stereospecificity by Stereospecifically Labeled NADPHs.

Radiolabelled NADPH isotopologues were synthesized as described elsewhere.[35, 69, 83, 140] All synthesized cofactors were purified by reverse-phase HPLC on a Supelco

Discovery C18 column as described previously and lyophilized for long-term storage at -80 °C.[71] (*R*)-[4-^{3}H]-NADPH, (*S*)-[4-^{3}H]-NADPH and [Ad- ^{14}C]NADPH were synthesized as described elsewhere.[69, 140] Due to the instability of the products H_4F and H_4B, the reaction mixture was completely oxidized by O_2 bubbling prior to HPLC analysis, followed by Flow Scintillation Counter or Liquid Scintillation Counter (LSC).

Competitive Kinetic Isotope Effects (KIEs).

[Ad-^{14}C]NADPH and (*R*)-[4-^{3}H]- NADPH (H/T KIE measurements) were combined at a radioactivity in DPM ratio close to 1:6, compensating for the depletion of T in products and the lower efficiency of tritium scintillation counting. Similarly, (*R*)-[Ad-^{14}C] NADPH and (*R*)-[Ad-^{3}H 4-^{2}H] NADPH were combined for H/D KIE measurements. Each of the mixtures was copurified by reverse-phase HPLC on a Supelco Discovery C18 column (25 cm x 4.6 mm, 5 μL), divided into aliquots containing 360,000 DPM of ^{14}C, and flash frozen for short-term storage (up to 3 weeks) at -80 °C.

All experiments were carried out with MTEN buffer at pH 9.0 at which the H-transfer step is more rate-determining.[91] One aliquot of the copurified NADPH was thawed just before use. H_2B was added to the reaction mixture to a final concentration of 2 mM. The final volume was brought to 990 μL by adding MTEN and the pH was readjusted to 9.0 at each experimental temperature. Before starting the enzymatic reaction, two 80 μL of samples (t_0) were withdrawn as a blank. The reaction was initiated by addition of either DHFR or PTR1 enzyme solution and reacted for up to 40 min. At various time points, 80 μL aliquots of varied fractional conversions (*f*) ranging from 15 to

85% were removed and quenched by adding MTX solution (100 μM final concentration). *f* was determined from the distribution of ^{14}C between NADPH and $NADP^+$. To ascertain complete fractional conversion, DHFR (approximately 0.2 units) was added to the residue of the mixture, and two aliquots for t_∞ samples were quenched after 20 min additional incubation. All quenched samples were immediately frozen and stored at -80 °C. The quenched samples were analyzed by HPLC-LSC, and the KIEs were determined. The detailed methods are described elsewhere.[44, 83, 88]

Results and Discussion

Enzyme Purification using MTX-agarose Affinity Chromatography

The purification of recombinant PTR1 has been previously reported by several groups.[130, 136] In the most recent report, Nare et al. purified PTR1 in 7 steps using four different columns including several ion exchange and size exclusion chromatographies (Scheme VI.1a).[136] The development of a more efficient purification method of PTR1 is beneficial for the studies of the enzyme. In order to shorten the purification scheme, the combination of two DE52 anion exchange chromatographies and MTX-agarose affinity chromatography was applied. The first anion exchange column is needed to remove cDHFR, which is a major unwanted contaminant to also be bound to the MTX-column. cDHFR not only binds to MTX, but would also adversely affect the kinetic studies of PTR1. In the first DE52 chromatography, we successfully removed endogenous cDHFR from the *E. coli* competent cell with a NaCl gradient. PTR1 was eluted first at around 0.12 M NaCl, whereas cDHFR was eluted at 0.25 M (Figure VI.2). The active fractions were directly loaded onto MTX-Agarose affinity column and PTR1 was eluted with 10

mM folate in 10 % (w/w) glycerol (Figure VI.3). Fractions with PTR1 activity were pooled and subsequent dialysis step and the second DE52 anion exchange chromatography were required for the removal of excess folate in the elution buffer of the affinity column.

This procedure yields 41 mg of pure PTR1 from 9 liters of LB media for *E. coli* growth (Table VI.1). SDS PAGE analysis (Figures VI.4 and VI.5) indicates that PTR1 (31 kD monomer) was sufficiently pure for the following kinetic experiments described here. Figure VI.5 indicates that the PTR1 was the major protein appearing, and most importantly that the band correspond to cDHFR at ~18k was not observed even in the overloaded SDS PAGE.

Stereospecificity in H_2B Reduction by PTR1 and cDHFR

The stereospecificity of the reduction of H_2B by PTR1 and cDHFR was examined using radiolabeled NADPHs (Figure VI.6). PTR1 selectively transfers the pro-*S* hydrogen on *R*-[4-^{3}H] NADPH to the reaction product, and ^{3}H remained at 4 position on $NADP^+$ (Figure VI.6b). The stereospecificity analysis with *S*-[4-^{3}H] NADPH also supported the pro-*S* 4H specificity of PTR1. Transferring the pro-*S* 4H of NADPH agreed with the expectation based on the PTR1 crystal structure.[62] In the cDHFR reduction of H_2B, on the other hand, ^{3}H from *R*-[4-^{3}H] NADPH was transferred and all radioactivity was found in H_4B oxidized derivatives that are eluted at 5 min, and 12 min in Figure VI.6c.[56, 140] Interestingly, the stereospecificity of the cDHFR reaction was not affected by the lack of the pAB-glu tail, as H_2F reduction is also pro-*R* specific.[91] It is also interesting to note

that the stereospecificity of PTR1 is quite unique, as R67 DHFR, another major family of DHFR *Fol*B, is also a pro-*R* specific enzyme.[34]

Cross-reactivity Analyses for PTR1 and cDHFR in the Reduction of H_2F and H_2B

Kinetic assay was performed in MTEN buffer at pH 9.0 since many KIE experiments have been done at this pH.[42-44] The Michaelis-Menten parameters for both PTR1 and DHFR with the two substrates (H_2B and H_2F) were determined (Table VI.2). Apparently, PTR1 prefers the natural substrate, H_2B, but does not strongly discriminate between the two substrates. Its k_{cat} and $k_{cat}/K_{m(H2X)}$ are higher by 1.8 fold, and 3.3 fold for its natural substrate H_2B, respectively. This implies that interactions of PTR1's active site with the pAB-glu tail of H_2F are not very important for binding and product release. If H-transfer is rate limiting at pH 9, that tail also does not affect the chemical transformation. These findings are in accordance with the crystal structure of PTR1 in which pAB-glu tail is directed away from the active site, and into the bulk solvent.[62] cDHFR, however, showed a clear preference toward its natural substrate H_2F. In H_2B reduction cDHFR has a poor catalytic ability with a significantly weak interaction (K_m), smaller rate constant (k_{cat}) and lower efficiency (k_{cat}/K_m) by 420, 520, and 2.2 x 10^5-fold, respectively. This is also in accordance with its structure,[63] where the *p*-aminobenzoyl moiety (although not the glutamate moiety) strongly interacts with the active site.

The K_m for H_2B reduction by cDHFR was inflated indicating a significantly weakened binding interaction relative to H_2F. This finding can easily be rationalized by examination of the many crystal structures of cDHFR, where the interaction between the

enzyme and the tail of the folic ligand is clear and substantial. The 520-fold slower k_{cat} also suggests a faster product release, as product release is partly rate limiting on k_{cat} even at elevated pH. Additionally, it may also indicate a direct effect of the altered binding in the H-tunneling at the active site. To test these possibilities, we first attempted to measure the rate of the H transfer using a stopped-flow spectrophotometer; however, this was not successful due to the poor binding of H_2B, which requires substrate concentration that was too high for the spectrophotometric measurements. Consequently, we turned to a more laborious but more meaningful approach, and determined the intrinsic primary (1°) KIEs and their temperature dependence using cDHFR and its unnatural substrate H_2B.

Determination of KIEs and their Temperature Dependence in the Reduction of H_2B by cDHFR.

The observed KIEs across the temperature range (5 to 45 °C) were determined (Table VI.3). These observed KIEs for H/T, H/D, and D/T did not follow the Swain-Schaad relationship, and this indicates that the chemistry is not fully rate-limiting even at pH 9. The intrinsic KIEs were calculated throughout the temperature range using the Northrop Method regarding H, D, or T as a standard (see chapter III).[68, 88] Exponential fitting of the intrinsic KIEs to the Arrhenius equation (prior to averaging the values at each temperature) yields the isotope effects on the activation parameters for H_2B reduction. Intrinsic H/T, H/D, and D/T KIEs over a temperature range from 5 to 45 °C were plotted on a logarithmic scale vs. the reciprocal of the absolute temperature (Figure VI.7). The comparison in the fittings of the intrinsic H/T KIEs for the two substrates (Table VI.4) is shown in Figure VI.8 (the same trend was observed for the intrinsic H/D

and D/T KIEs). In H_2B reduction, KIEs were apparently larger and have more temperature dependency ($\Delta E_{a\ H/T} = 0.4 \pm 0.1$ kcal/mol) than in H_2F reduction (-0.1 ± 0.3 kcal/mol).[38] In the H_2B reaction, the intercept value (A_H/A_T), representing the isotope effect on the pre-exponential factor was, within experimental error, the same as in the H_2F reduction.[38]

The 520-fold reduction in H transfer rate for the alternative substrate, H_2B, seems to be associated with an increase in temperature dependence of intrinsic KIEs. The intrinsic KIE data provide experimental support for the hypothesis that the abolishment of the tail of H_2F not only affects binding and release, but also directly affects the catalyzed chemical step by changing the rearrangement of the enzymatic complex at the tunneling ready states (TRS). In accordance with Marcus-like models, cDHFR-NADPH-H_2F ternary complex is well rearranged so that the ensemble of conformations leads to DAD that support tunneling of all three isotopes regardless of thermal activation of DADs' fluctuations (i.e., "gating").[43] The finding that the binding contribution of the pAB-glu moiety of H_2F (missing on H_2B) is important to effectively form TRS was not anticipated from simple inspection of various crystal structures. Since the pterin ring itself seems to be well packed in the active site, the lack of interactions away from the reactive center could substantially affect binding, but not chemistry. The inflated KIEs and slight temperature dependency are both common indicators for longer average DAD. If the average DAD (from the gating term in Equation I.10) is longer for H_2B reduction than for H_2F reduction, then the enzymatic complex at TRS will explore more conformations from which the light isotope can be transferred by tunneling. However, TRS will not provide the ideal distance for the heavier isotopes, thus leading to inflated KIEs.

Furthermore, the overlap of the isotope effect on Arrhenius preexponential factors for both substrates indicates that more conformations from which both isotopes can tunnel will be populated *via* Boltzmann thermal distribution, and thus the KIEs will decrease at elevated temperature. In accordance with studies of cDHFR remote mutations,[43, 44] this new finding further demonstrates the importance of structural and dynamic components of the whole enzyme (rather than only its active site) in catalyzing chemical transformations.

Substrate dependence of KIE values was observed in other enzymes. Kinetic studies on horse liver alcohol dehydrogenase (ADH) showed that the natural substrate ethanol has a faster rate, and its H/D KIE is 3.2 whereas unnatural substrate inflated H/D KIE values were reported for benzyl alcohol, 6.1.[141] Whereas yeast ADH has an intrinsic H/D KIE of 3.2 for ethanol, it has 5.7 for a poor substrate 2-propanol.[142] Interestingly, but controversially, the temperature dependence of KIEs from pre-steady state non-competitive measurements using NAD^+ and $NADP^+$ was recently reported for pentaerythritol tetranitrate reductase.[143] In this case, NADH, that presented relatively larger and temperature independent KIEs was actually slower by 17-fold in comparison to NADPH, that showed temperature dependence in KIEs. To understand and rationalize the correlation of experimental data (the reaction rates, sizes and temperature-dependence of KIEs) and active site dynamics, further investigations by experimental and theoretical approaches are necessary.

Conclusion

In summary, the four-step purification method using MTX-agarose affinity chromatography step has proven to be effective and has significantly reduced the number of steps relative to previously reported procedures. The NADPH stereospecificity and kinetic analysis supported the distinct mechanistic differences between cDHFR and PTR1, as pro-*R* specific type A and pro-*S* specific type B nicotinamide dependent enzymes, respectively. The comparison of the nature of H-transfer in the reduction of two substrates by cDHFR indicated that the cDHFR appears to have a perfectly organized ensemble of DADs for an efficient H-tunneling at the TRS with its natural substrate, H_2F, but a poorly organized one for a substrate that lacks the pAB-glu tail. This supports the hypothesis that the appropriate binding of substrate affects not only binding and release, but also the rearrangement of the reaction coordinate toward tunneling-ready conformations. These observations suggest two potential future directions. The comparative evaluations of the nature of H transfer reactions in the reduction of natural and unnatural substrate for cDHFR, and design of selective inhibitors for PTR1. Importantly, the mechanistic differences between cDHFR and PTR1 support the possibility of the design of selective inhibitors for PTR1 with reduced toxicity. This could be a promising project that may lead to a new class of antibiotic drugs against not only Leishmaniasis, but antibiotic-resistant bacteria supported with *FolM* enzymes.[144]

(a) Nare's procedure

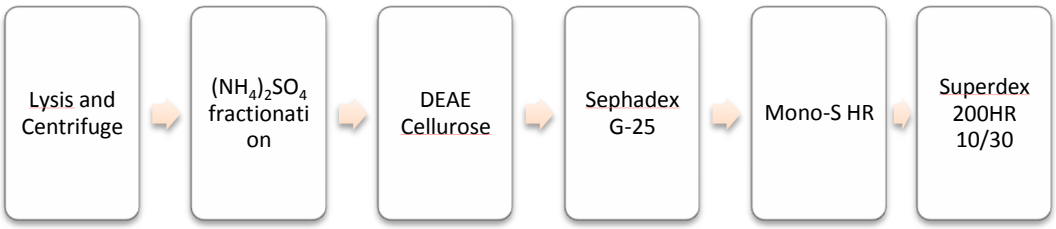

(b) 4-step purification

Scheme VI.1 Comparison of two purification strategies for PTR1.

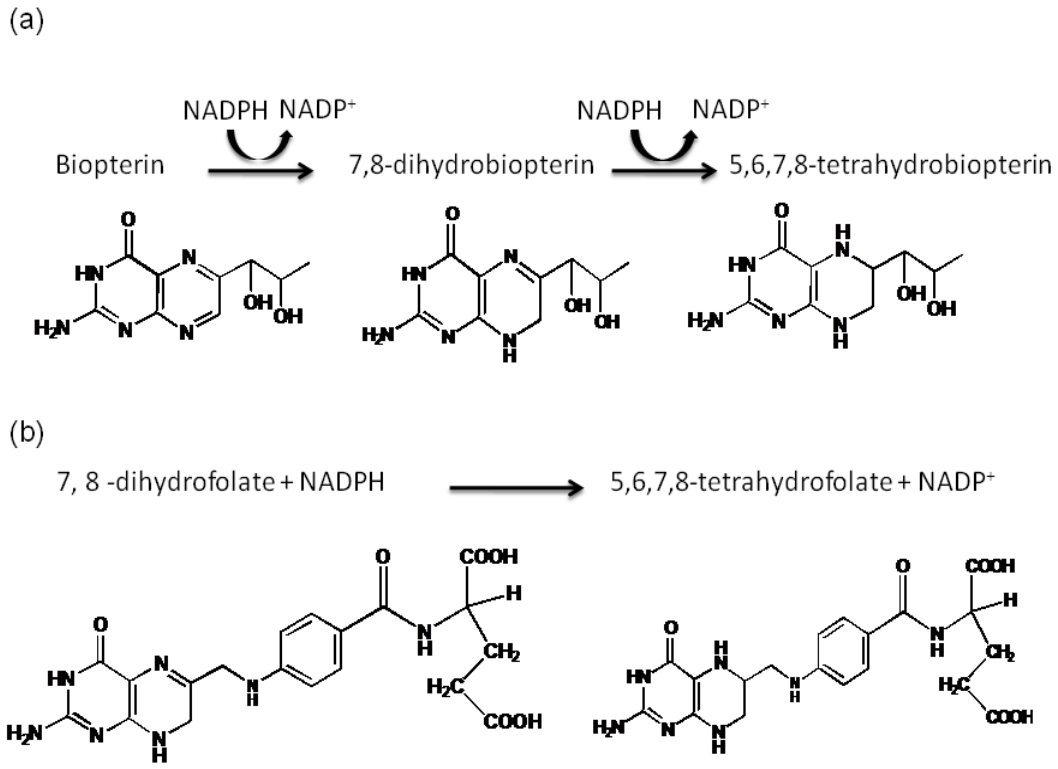

Figure VI.1 Chemical Reactions Catalyzed by PTR1. Pterins are fragments of folates where a *1,2*-propanediol replaces the methylene *p*-aminobenzoyl-glutamate (pAB-glu) tail of folates.

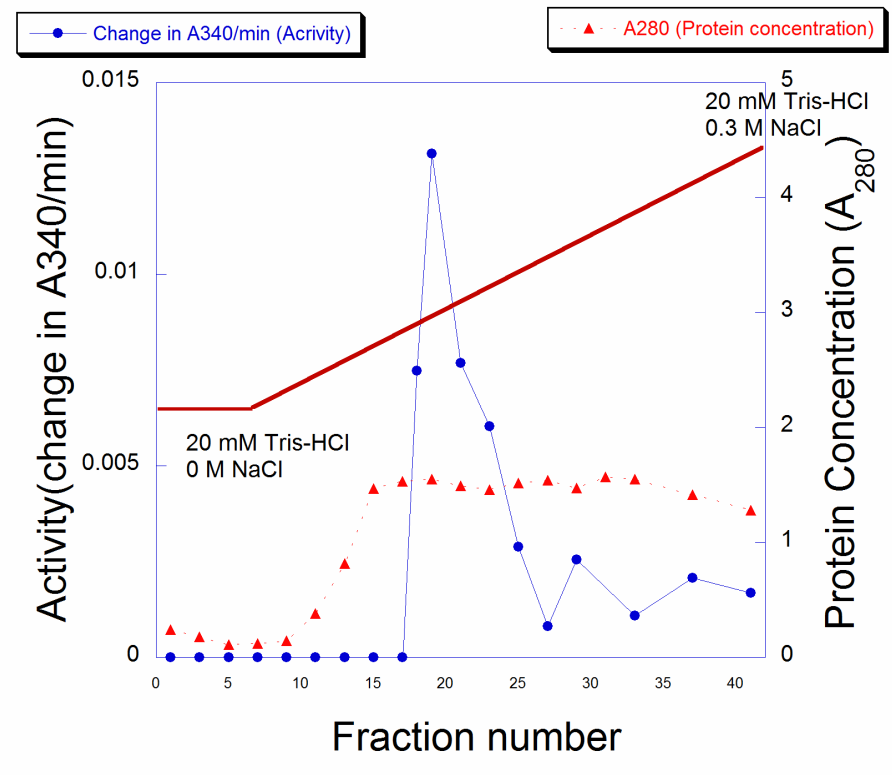

Figure VI.2 Elution profile of the first DE52 column chromatography. (●) and (▲) represent PTR1 activity (ΔA_{340}/min) and protein concentration (A_{280}), respectively.

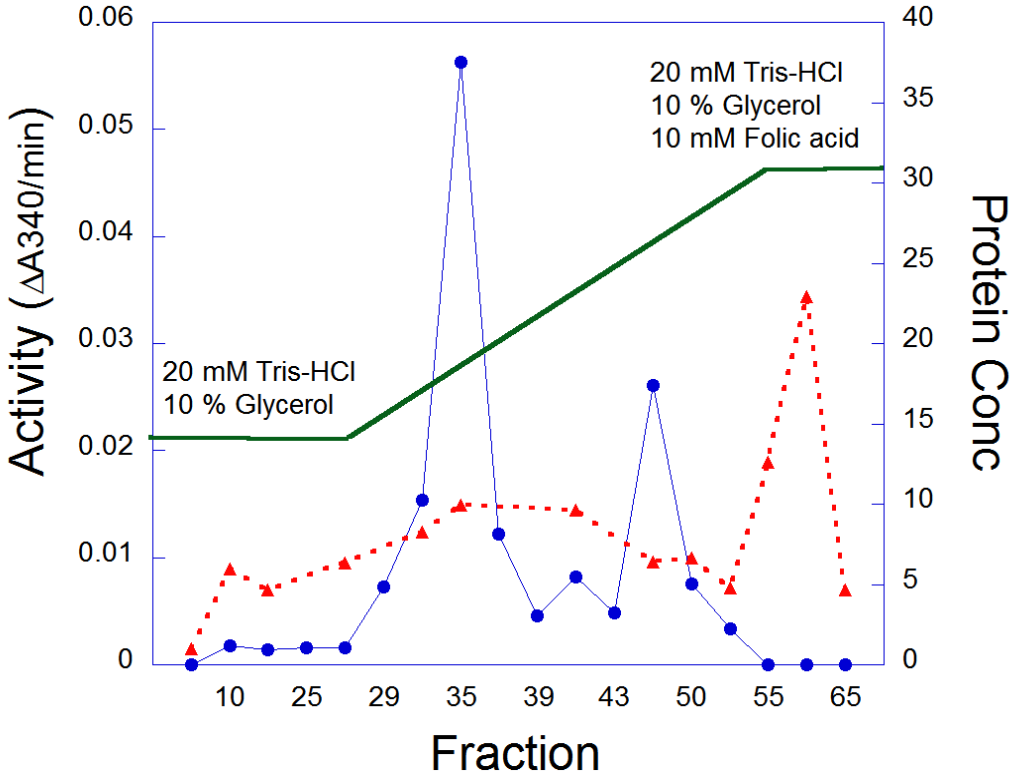

Figure VI.3 Elution profile of MTX-agarose affinity chromatography. (●) and (▲) represent PTR1 activity (ΔA_{340}/min) and protein concentration (μg/mL), respectively.

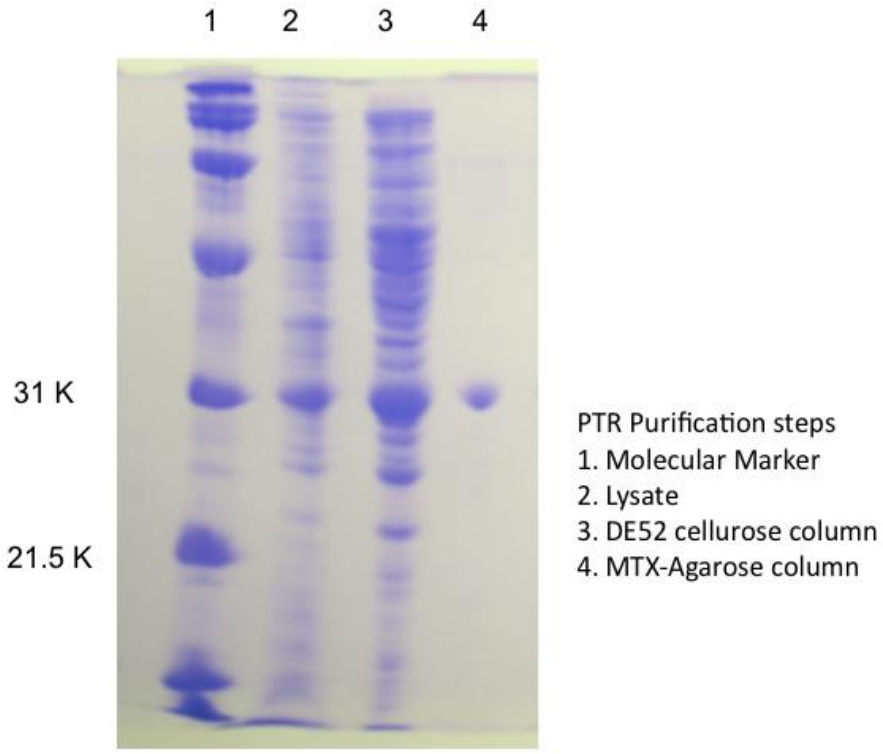

Figure VI.4 SDS PAGE of each purification step

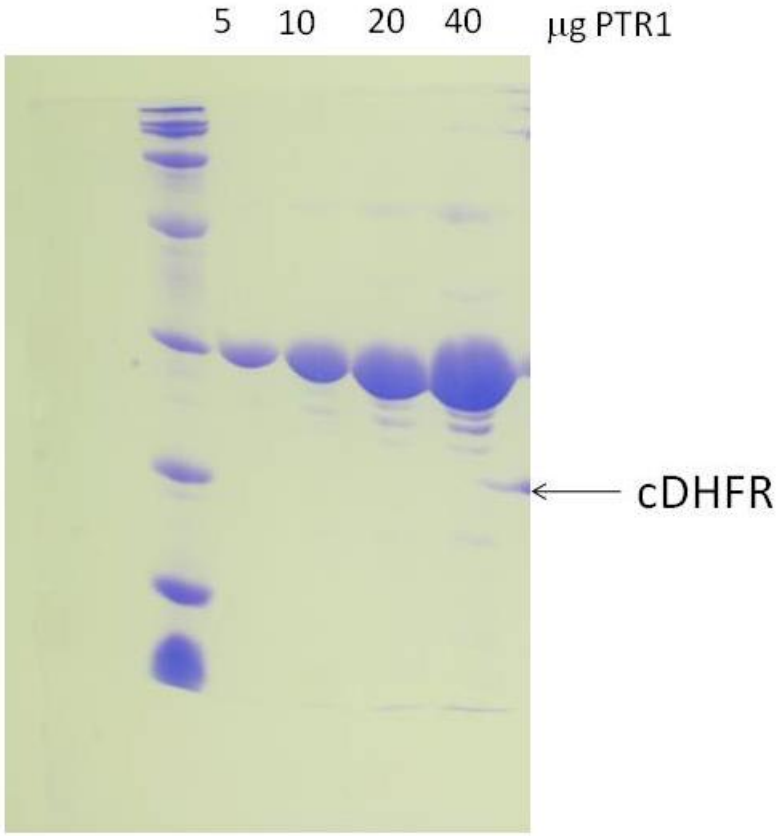

Figure VI.5 SDS PAGE of overloaded purified PTR1. At the right edge of the gel cross contamination of cDHFR standard is shown. However, there is no trace of contamination from overloaded PTR1 lane. Purity of PTR1 is over 95 %.

Steps	Protein (mg)	Total activity (Units*)	Relative Specific Activity
Lysate	**6694**		
Centrifugation	**4045**		
1st DE52	**930**	**252.6**	**1**
MTX	**86.0**	**132.3**	**5.7**
2nd DE52	**40.6**	**46.5**	**4.2**

*One unit of enzyme activity corresponds to the reduction of 1µmol of NADPH per minute.

Table VI.1 PTR1 purification table.

		Dihydrofolate (H_2F)	*Dihydrobiopterin (H_2B)*
cDHFR	k_{cat} **(s^{-1})**	**2.8**[1]	**0.0054 ± 0.0005**
	$K_{m\ H2X}$ **(μM)**	**1.2**[2]	**500 ± 99**
	$K_{m\ NADPH}$ **(μM)**	**0.94**[2]	**1.50 ± 0.34**
PTR1	k_{cat} **(s^{-1})**	**0.022 ± 0.006**	**0.039 ± 0.001**
	$K_{m\ H2X}$ **(μM)**	**5.6 ± 0.1**	**3.0 ± 0.8**
	$K_{m\ NADPH}$ **(μM)**	**6.3 ± 1.4**	**10.0 ± 3.5**

[1] Reference 145

[2] Reference 138

Table VI.2 Steady state parameters for PTR1 in MTEN buffer at pH 9.0, 25 °C.

(a)

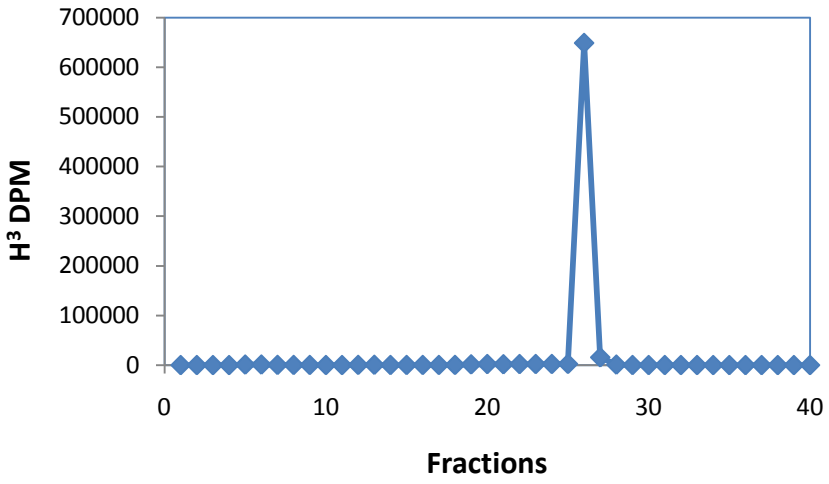

(b)

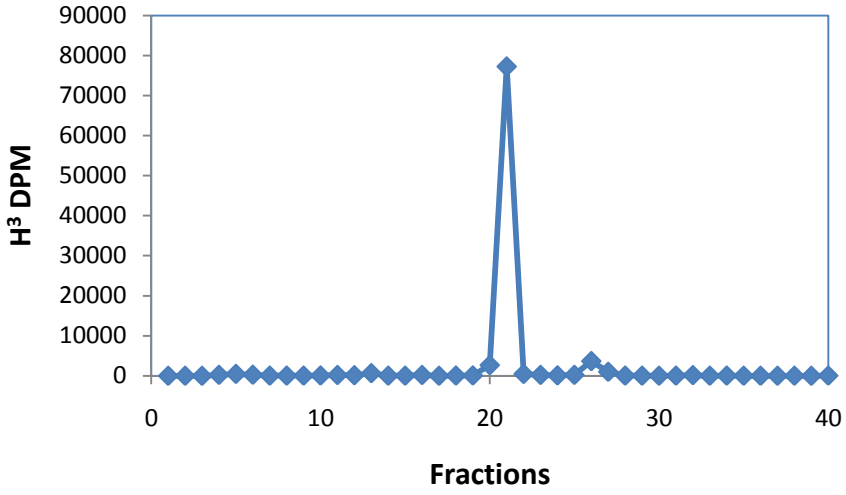

Figure VI.6 Radiogram from HPLC-LSC analysis: (a) *R*-[4-^{3}H]NADPH, (b) PTR1 reaction product, and (c) DHFR reaction products. Tritium at 4*R* position of nicotinamide was transferred on to the product H_4B (oxidized H_4B derivatives are eluted at 5 min, and 12 min), as also found for these derivatives of H_4F.[71, 72] The small peaks at 26 min is residual unreacted *R*-[4-^{3}H] NADPH.

(c)

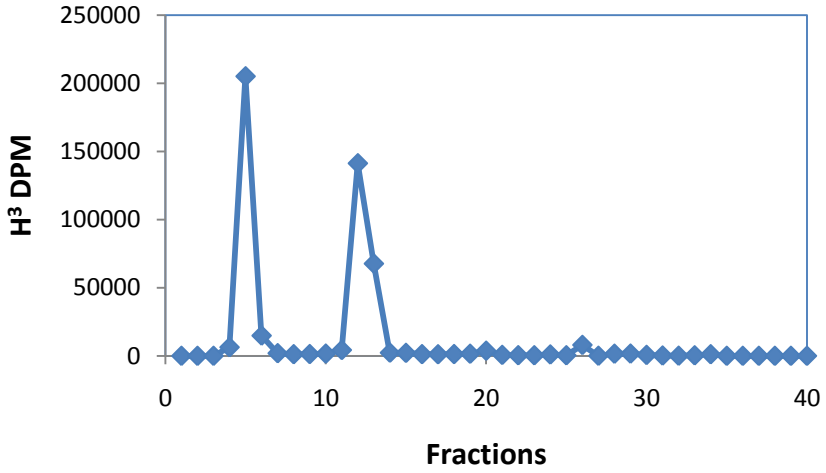

Figure VI.6-continued

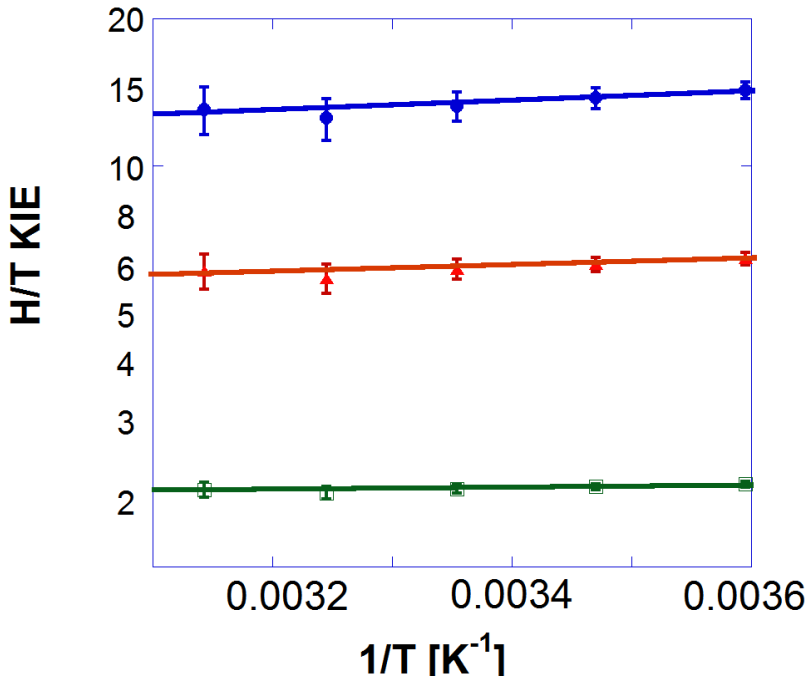

Figure VI.7 Arrhenius plot of the intrinsic H/T, H/D, and D/T KIEs (log scale) vs. the reciprocal of the absolute temperature (1/T). The H/T data are in blue circles, the H/D data are in red triangle, and D/T data are in green squares. The lines present the exponential fit of the data to the Arrhenius equation.

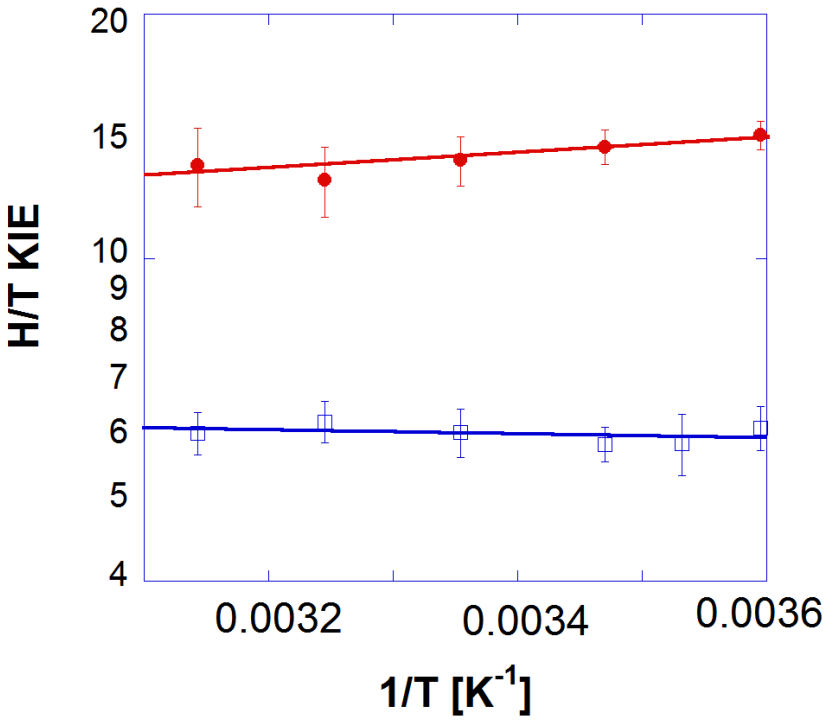

Figure VI.8 A comparative Arrhenius plot of the H/T KIEs (log scale) vs. the reciprocal of the absolute temperature (1/T). The H_2B data are in red circles and the H_2F data are in blue squares. The lines present the exponential fit of the data to the Arrhenius equation.

	Observed KIE (H_2B)		*Observed KIE (H_2F)*[a]
°°C	**H/T**	**H/D**	**H/T**
5	**7.99 ± 0.04**	**3.87 ± 0.03**	**3.06 ± 0.10**
15	**7.46 ± 0.02**	**3.68 ± 0.03**	**4.76 ± 0.04**
25	**7.09 ± 0.16**	**3.55 ± 0.02**	**4.85 ± 0.09**
35	**6.84 ± 0.15**	**3.48 ± 0.01**	**4.80 ± 0.12**
45	**6.49 ± 0.16**	**3.30 ± 0.02**	**4.82 ± 0.10**

[a] Ref [38]

Table VI.3 Observed KIEs for DHFR on H_2F and H_2B.

°C	***H/T for H_2B***	***H/T for H_2F[a]***
5	**14.3 ± 0.6**	**6.2 ± 0.4**
15	**13.7 ± 0.7**	**5.9 ± 0.3**
25	**13.2 ± 0.9**	**6.1 ± 0.4**
35	**12.5 ± 1.2**	**6.3 ± 0.4**
45	**13.0 ± 1.5**	**6.1 ± 0.4**

a. From reference 38

Table VI.4 Intrinsic KIEs for DHFR on H_2F and H_2B used to plot Figure VI.10.

CHAPTER VIII

SUMMARY AND FUTURE DIRECTIONS

Summary

Enzymes are sophisticated catalytic devices that facilitate the rate of numerous chemical reactions in physiological solutions, and are also the target of many, if not most, drugs. Consequently enzymes have been the center of research for many years.[1, 3] Many factors including essential amino acid residues, protein scaffold, hydrogen bonds, steric interaction, electrostatics, and substrate/protein dynamics have been proposed to explain the catalytic power of enzymes. It has been observed that some enzymes undergo conformational changes during catalysis through kinetic states including binding, isomerization, chemical barriers, and product release.[3] Furthermore, primitive enzymes show minor conformational changes during a turnover and enhance the rate of a reaction several orders of magnitude less than more dynamic isozymes.[45] How do these enzymes with different structures and dynamics accelerate the rate of the same chemical reactions? In this dissertation, we tried to understand and answer this fundamental question by the comparative studies of genetic families, ionic strengths, and alternative substrates.

In order to study these topics, we at first tackled the improvement and optimization of KIE determination procedures.[34, 35, 83] Various labeled NADPHs were synthesized by applying enzymatic synthetic strategy.[35, 140] A novel competitive H/D KIE experiment was examined and applied in determination of the intrinsic KIEs using the Northrop method by a combinational approach with H/T KIEs.[88] The nature of H transfer between dihydrofolate (H_2F) and NADPH as catalyzed by R67 DHFR (*FolB*)

was examined and compared with the same conversion catalyzed by cDHFR (*FolA*).[34] The primitive enzyme, R67 DHFR, has temperature dependent intrinsic KIEs and this indicates the requirement of significant fluctuations between hydrogen donor and acceptor distance, i.e., DAD prior to hydride transfer. The well-evolved cDHFR, however, shows temperature independent KIEs, indicating an ideal DAD. A combination of theoretical and experimental approaches was applied to investigate an unusual enhancement of hydride transfer rate by R67 DHFR with increasing ionic strength.[35] The electrostatic potential surfaces at high and physiological ionic strengths (calculated by a collaborator) indicated a reduction of charge on the enzyme surface at high ionic strength. Slightly decreased KIE values and their temperature dependency provided evidences of an improved DAD at the TRS at high ionic strength.

In another study, we aimed at the comparison of the same reaction between cDHFR and an enzyme, pteridine reductase 1 (PTR1), for which a residual DHFR activity was proposed.[134] A new purification procedure of PTR1 from *Leishmania major* (*FolM*) was developed and the enzyme produced in mg quantities.[146] The Michaelis-Menten parameters for DHFR and PTR1 with H_2F and dihydropterin (H_2B), both natural and cross residual activities, were determined. It was revealed that PTR1 catalyzes H_2F and H_2B with similar rate parameters, whereas cDHFR showed significant preference in the reduction of its natural substrate, H_2F. Further investigation of the cDHFR catalyzed reaction with the unnatural substrate, H_2B, revealed that in contrast to its reaction with H_2F, the H-transfer and DAD organization are not optimized for this unnatural substrate.[56]

Future Directions

Research will continue on the enzymatic synthesis of radiolabeled coenzymes, competitive KIE methods, and comparative studies among the DHFR related enzymes. First, as described in Chapter III, the HPLC chromatograms on H/D experiments indicate the possibility of alternative analytical procedure for the simplified chromatogram on H/D experiments. The development of an effective analytical procedure will improve both cost-performance and bench time per KIE experiment. Second, as proposed in chapter VI, an effective purification procedure of PTR1 was performed through three columns. A more efficient method would apply the Δ*folA E. coli* (*fol*A gene deleted) expression system for PTR1 expression. This might lead to the elimination of the first DE52 column, and makes a two-step purification possible. Third, the development of synthetic procedures for the radiolabeled isotopologues is required to enhance studies of the pro-*S* stereospecificity of PTR1. The combinations of new combinations of isotopologues, i.e., [Ad-^{14}C] NADPH and (*S*)-[4-^{3}H] NADPH for 1˚ H/T KIEs; (*4S*)-[Ad-^{14}C,4-^{2}H] NADPH and (*S*)-[4-^{3}H] NADPH for 1˚ D/T KIEs and [Ad-^{14}C] NADPH and (*4S*)-[Ad-^{3}H,4-^{2}H] NADPH for 1˚ H/D KIEs should be examined. The determination and evaluation of the intrinsic KIEs and their temperature dependence will reveal the nature of H transfer in the PTR1 reaction with either its natural substrate H_2B or H_2F. Fourth, in order to explore the network of coupled dynamics that contribute the rate enhancement of these enzymes, "primitive" H_2B reduction by cDHFR is of interest. Whereas it has been suggested that cDHFR has perfect organizations and ideal H-DAD distance at TRS using its natural substrate (H_2F), as described in Chapter VII, cDHFR appears not to be well

tuned for catalyzing H_2B reduction. Therefore, accelerated *in vitro* evolution of DHFR toward better H_2B reductase is of interest.

Lastly, the methodologies developed here to study various DHFRs, could be applied in studies of many other nicotinamide dependent enzymes. Such studies will enhance our understanding of enzyme catalysis in general and may lead to advances in enzymology, rational drug design, design of biomimetic catalysts, and other aspects of chemical catalysis in the broadest sense.

BIBLIOGRAPHY

1. Kraut, J., How do enzymes work? *Science* **1988,** 242, 533-540.

2. Garcia-Viloca, M.; Gao, J.; Karplus, M.; Truhlar, D. G., How enzymes work: Analysis by modern rate theory and computer simulations. *Science* **2003,** 303, 186-195.

3. Benkovic, S. J.; Hammes-Schiffer, S., A perspective on enzyme catalysis. *Science* **2003,** 301, 1196-1202.

4. Fischer, E., *Ber. Dtsch. Chem. Ges.* **1895,** 28, 1508.

5. Horst, K., Emil Fischer - Unequalled classicist, master of organic chemistry research, and inspired trailblazer of biological chemistry. *Angew. Chem. Int. Ed.* **2002,** 41, 4439-4451.

6. Pauling, L., The nature of forces between large molecules of biological interest. *Nature* **1948,** 161, 707-709.

7. Koshland, D. E., Application of a theory of enzyme specificity to protein synthesis. *Proc. Nat. Acad. Sci. U.S.A.* **1958,** 44, 98-104.

8. Gilbert, H. F.; Jencks, W. P., Mechanisms for enforced general acid catalysis of addition of thiol anions to acetaldehyde. *J. Am. Chem. Soc.* **1977,** 99, 7931-7947.

9. Bruice, T. C.; Benkovic, S. J., Chemical basis for enzyme catalysis. *Biochemistry* **2000,** 39, 6267-6273.

10. Cha, Y.; Murray, C. J.; Klinman, J. P., Hydrogen tunneling in enzyme reactions. *Science* **1989,** 243, 1325-1330.

11. Schramm, V. L., Introduction: Principles of enzymatic catalysis. *Chem. Rev.* **2006,** 106, 3029-3030.

12. Henzler-Wildman, K.; Kern, D., Dynamic personalities of proteins. *Nature* **2007,** 450, 964-972.

13. Eisenmesser, E. Z.; Bosco, D. A.; Akke, M.; Kern, D., Enzyme dynamics during catalysis. *Science* **2002,** 295, 1520-1523.

14. Wolf-Watz, M.; Thai, V.; Henzler-Wildman, K.; Hadjipavlou, G.; Eisenmesser, E. Z.; Kern, D., Linkage between dynamics and catalysis in a thermophilic-mesopholic enzyme pair. *Nat. Struc. Molec. Biol.* **2004,** 11, 945-949.

15. Cleland, W. W., Enzyme mechanisms from isotope effects. In *Isotope effects in chemistry and biology*, Kohen, A.; Limbach, H. H., Eds. Taylor & Francis, CRC Press: Boca Raton, FL, 2006; Vol. Ch. 37, pp 915-930.

16. Kohen, A.; Limbach, H. H., *Isotope effects in chemistry and biology*. Taylor & Francis, CRC Press: Boca Raton, FL, 2006.

17. Swain, C. G.; Stivers, E. C.; Reuwer, J. F.; Schaad, L. J., Use of hydrogen isotope effects to identify the attacking nucleophile in the enolization of ketones catalyzed by acetic acid. *J. Am. Chem. Soc.* **1958,** 80, 5885-5893.

18. Kohen, A., Probes for hydrogen tunneling and coupled motion in enzymatic systems. In *Hydrogen-Transfer Reactions*, Hynes, J. T.; Klinman, J. P.; Limbach, H. H.; Schowen, R. L., Eds. 2007 WILEY-VCH Verlag GmbH & Co.: Weinheim, 2007; Vol. 4, pp 1311-1340.

19. Kohen, A., Kinetic isotope effects as probes for hydrogen tunneling, coupled motion and dynamics contributions to enzyme catalysis. *Prog. React. Kin. Mech.* **2003,** 28, 119-156.

20. Streitwieser, A.; Jagow, R. H.; Fahey, R. C.; Suzuki, S., Kinetic isotope effects in the acetolyses of deuterated cyclopentyl tosylates1,2. *J. Am. Chem. Soc.* **1958,** 80, 2326-2332.

21. Kohen, A.; Klinman, J. P., Enzyme catalysis: beyond classical paradigms. *Acc. Chem. Res.* **1998,** 31, 397-404.

22. Stojkovic, V.; Kohen, A., Enzymatic H transfers: quantum tunneling and coupled motion from kinetic isotope effect studies. *Isr. J. Chem.* **2009,** 49, 163-173.

23. Villa, J.; Warshel, A., Energetics and dynamics of enzymatic reactions. *J. Phys. Chem. B* **2001,** 105, 7887-7907.

24. Sutcliffe, M. J.; Scrutton, N. S., A new conceptual framework for enzyme catalysis. Hydrogen tunneling coupled to enzyme dynamics in flavoprotein and quinoprotein enzymes. *Eur. J. Biochem.* **2002,** 269, 3096–3102 and many cited therein.

25. Marcus, R. A., H and other transfers in enzymes and in solution: Theory and computations, a unified view. 2. Applications to experiment and computations. *J. Phys. Chem. B* **2007,** 111, 6643-6654.

26. Marcus, R. A.; Sutin, N., Electron transfer in chemistry and biology. *Biochem. Biophys. Acta* **1985,** 811, 265-322.

27. Kuznetsov, A. M.; Ulstrup, J., Proton and hydrogen atom tunneling in hydrolytic and redox enzyme catalysis. *Can. J. Chem.* **1999,** 77, 1085-1096.

28. Borgis, D.; Hynes, J. T., Dynamical theory of proton tunneling transfer rates in solution - general formulation. *Chem. Phys.* **1993,** 170, 315-346.

29. Borgis, D.; Hynes, J. T., Molecular-dynamics simulation for a model nonadiabatic proton transfer reaction in solution. *J. Chem. Phys.* **1991,** 94, 3619-3628.

30. Schowen, R. L., Hydrogen tunneling. Goodbye to all that. *Eur. J. Biochem.* **2002,** 269, 3095.

31. Knapp, M. J.; Klinman, J. P., Environmentally coupled hydrogen tunneling - Linking catalysis to dynamics. *Eur. J. Biochem.* **2002,** 269, 3113-3121.

32. Caratzoulas, S.; Schwartz, S. D., A computational method to discover the existence of promoting vibrations for chemical reactions in condensed phases. *J.Chem.Phys* **2001,** 114, 2910-2918.

33. Antoniou, D.; Schwartz, S. D., Internal enzyme motions as a source of catalytic activity: rate-promoting vibrations and hydrogen tunneling. *J. Phys. Chem. B* **2001,** 105, 5553-5558.

34. Yahashiri, A.; Howell, E. E.; Kohen, A., Tuning of the H-transfer coordinate in primitive versus well-evolved enzymes. *Chemphyschem* **2008,** 9, 980-982.

35. Yahashiri, A.; Nimrod, G.; Ben-Tal, N.; Howell, E. E.; Kohen, A., The effect of electrostatic shielding on H tunneling in R67 dihydrofolate reductase. *ChemBioChem* **2009,** 10, 2620-2623.

36. Giladi, M.; Altman-Price, N.; Levin, I.; Levy, L.; Mevarech, M., FolM, a new chromosomally encoded dihydrofolate reductase in *Escherichia coli*. *J. Bacteriol.* **2003,** 185, 7015-7018.

37. Levin, I. Alternative pathways for de novo tetrahydrofolate biosynthesis in bacteria and archaea. Tel Aviv University, 2007.

38. Sikorski, R. S.; Wang, L.; Markham, K. A.; Rajagopalan, P. T. R.; Benkovic, S. J.; Kohen, A., Tunneling and coupled motion in the *E. coli* dihydrofolate reductase catalysis. *J. Am. Chem. Soc.* **2004,** 126, 4778-4779.

39. Hammes-Schiffer, S., Hydrogen tunneling and protein motion in enzyme reactions. *Acc. Chem. Res.* **2006,** 39, 93-100.

40. Hammes-Schiffer, S., Kinetic isotope effects for proton-coupled electron transfer reactions. In *Isotope effects in chemistry and biology*, Kohen, A.; Limbach, H. H., Eds. CRC Press: Boca Raton, FL, 2006; pp 499-520.

41. Hammes-Schiffer, S.; Benkovic, S. J., Relating protein motion to catalysis. *Annu. Rev. Biochem.* **2006,** 75, 519-541.

42. Wang, L.; Goodey, N. M.; Benkovic, S. J.; Kohen, A., The role of enzyme dynamics and tunneling in catalyzing hydride transfer: Studies of distal mutants of dihydrofolate reductase. *Phil. Trans. R. Soc. B* **2006,** 361, 1307-1315.

43. Wang, L.; Goodey, N. M.; Benkovic, S. J.; Kohen, A., Coordinated effects of distal mutations on environmentally coupled tunneling in dihydrofolate reductase. *Proc. Nat. Acad. Sci. USA* **2006,** 103, 15753-15758.

44. Wang, L.; Tharp, S.; Selzer, T.; Benkovic, S. J.; Kohen, A., Effects of distal mutation on active site chemistry. *Biochemistry* **2006,** 45, 1383-1392.

45. Howell, E. E., Searching Sequence Space: Two Different Approaches to Dihydrofolate Reductase Catalysis. *ChemBioChem* **2005,** 6, 590-600.

46. Pitcher, W. H.; DeRose, E. F.; Mueller, G. A.; Howell, E. E.; London, R. E., NMR studies of the interaction of a type II dihydrofolate reductase with pyridine nucleotides reveal unexpected phosphatase and reductase activity. *Biochemistry* **2003,** 42, 11150-11160.

47. Park, H.; Zhuang, P.; Nichols, R.; Howell, E. E., Mechanistic Studies of R67 Dihydrofolate Reductase. EFFECTS OF pH AND AN H62C MUTATION. *J. Biol. Chem.* **1997,** 272, 2252-2258.

48. Chopra, S.; Lynch, R.; Kim, S. H.; Jackson, M.; Howell, E. E., Effects of temperature and viscosity on R67 dihydrofolate reductase catalysis. *Biochemistry* **2006,** 45, 6596-6605.

49. Masgrau, L.; Roujeinikova, A.; Johannissen, L. O.; Hothi, P.; Basran, J.; Ranaghan, K. E.; Mulholland, A. J.; Sutcliffe, M. J.; Scrutton, N. S.; Leys, D., Atomic description of an enzyme reaction dominated by proton tunneling *Science* **2006,** 312, 237-241.

50. Basran, J.; Sutcliffe, M. J.; Scrutton, N. S., Enzymatic H-transfer requires vibration-driven extreme tunneling. *Biochemistry* **1999,** 38, 3218-3222.

51. Basran, J.; Sutcliffe, M. J.; Scrutton, N. S., Deuterium isotope effects during carbon-hydrogen bond cleavage by trimethylamine dehydrogenase - Implications for mechanism and vibrationally assisted hydrogen tunneling in wild-type and mutant enzymes. *J. Biol. Chem.* **2001,** 276, 24581-24587.

52. Harris, R. J.; Meskys, R.; Sutcliffe, M. J.; Scrutton, N. S., Kinetic studies of the mechanism of carbon-hydrogen bond breakage by the heterotetrameric sarcosine oxidase of arthrobacter sp. 1-IN. *Biochemistry* **2000,** 39, 1189.

53. Agrawal, N.; Hong, B.; Mihai, C.; Kohen, A., Vibrationally enhanced hydrogen tunneling in the *E. coli* thymidylate synthase catalyzed reaction. *Biochemistry* **2004,** 43, 1998-2006.

54. Hong, B.; Haddad, M.; Maley, F.; Jensen, J. H.; Kohen, A., Hydride transfer versus hydrogen radical transfer in thymidylate synthase. *J. Am. Chem. Soc.* **2006,** 128, 5636 - 5637.

55. Basran, J.; Harris, R. J.; Sutcliffe, M. J.; Scrutton, N. S., H-tunneling in the multiple H-transfers of the catalytic cycle of morphinone reductase and in the reductive half-reaction of the homologous pentaerythritol tetranitrate reductase. *J. Biol. Chem.* **2003,** 278, 43973-43982.

56. Yahashiri, A.; Nixon, R. I.; Manjunath, N.; Hashmi, A.; Sen, A.; Kohen A., The H-transfer coordinate for natural versus unnatural substrates: inflated kinetic isotope effects in the E. coli dihydrofolate reductase catalysis on unnatural substrate **in preparation**.

57. Kohen, A.; Cannio, R.; Bartolucci, S.; Klinman, J. P., Enzyme dynamics and hydrogen tunneling in a thermophilic alcohol dehydrogenase. *Nature* **1999,** 399, 496-499.

58. Bandarian, V.; Reed, G. H., Hydrazine cation radical in the active site of ethanolamine ammonia-lyase: Mechanism-based inactivation by hydroxyethylhydrazine. *Biochemistry* **1999,** 38, 12394-12402.

59. Cheng, M.-C.; Marsh, E. N. G., Isotope effects for deuterium transfer between substrate and coenzyme in adenosylcobalamin-dependent glutamate mutase. *Biochemistry* **2005,** 44, 2686-2691.

60. Knapp, M. J.; Rickert, K.; Klinman, J. P., Temperature-dependent isotope effects in soybean lipoxygenase-1: Correlating hydrogen tunneling with protein dynamics. *J. Am. Chem. Soc.* **2002,** 124, 3865-3874.

61. Krahn, J. M.; Jackson, M. R.; DeRose, E. F.; Howell, E. E.; London, R. E., Crystal structure of a type II dihydrofolate reductase catalytic ternary complex. *Biochemistry* **2007,** 46, 14878-14888.

62. Gourley, D. G.; Schuttelkopf, A. W.; Leonard, G. A.; Luba, J.; Hardy, L. W.; Beverley, S. M.; Hunter, W. N., Pteridine reductase mechanism correlates pterin metabolism with drug resistance in trypanosomatid parasites. *Nat. Struct. Mol. Biol.* **2001,** 8, 521-525.

63. Sawaya, M. R.; Kraut, J., Loop and subdomain movements in the mechanism of *Escherichia coli* dihydrofolate reductase: crystallographic evidence. *Biochemistry* **1997,** 36, 586-603.

64. Kohen, A.; Klinman, J. P., Hydrogen tunneling in biology. *Chem. Biol.* **1999,** 6, R191-198.

65. Markham, K. A.; Sikorski, R. S.; Kohen, A., Synthesis and utility of ^{14}C-labeled nicotinamide cofactors. *Anal. Biochem.* **2004,** 325, 62-67.

66. Chopra, S.; Dooling, R. M.; Horner, C. G.; Howell, E. E., A balancing act between net uptake of water during dihydrofolate binding and net release of water upon NADPH binding in R67 dihydrofolate reductase. *J. Biol. Chem.* **2008,** 283, 4690-4698.

67. Parkin, D. W., In *Enzyme Mechanism from Isotope Effects*, Cook, P. F., Ed. Ed.; CRC Press: Boca Raton, FL, 1991; pp 269-290.

68. Northrop, D. B., Intrinsic isotope effects in enzyme catalyzed reactions. In *Enzyme mechanism from isotope effects*, Cook, P. F., Ed. CRC Press: Boca Raton, Fl., 1991; pp 181-202.

69. McCracken, J. A.; Wang, L.; Kohen, A., Synthesis of R and S tritiated reduced b-nicotinamide adenine dinucleotide 2' phosphate. *Anal. Biochem.* **2003,** 324, 131-136.

70. Agrawal, N.; Kohen, A., Microscale synthesis of 2-tritiated isopropanol and 4*R*-tritiated reduced nicotinamide adenine dinucleotide phosphate. *Anal. Biochem.* **2003,** 322, 179-184.

71. Markham, K. A.; Sikorski, R. S.; Kohen, A., Purification, analysis, and preservation of reduced nicotinamide adenine dinucleotide 2'-phosphate. *Anal. Biochem.* **2003,** 322, 26-32.

72. Markham, K. A.; Kohen, A., Analytical procedures for the preparation, isolation, analysis and preservation of reduced nicotinamides. *Curr. Anal. Chem.* **2006,** 2, 379-388.

73. Melander, L.; Saunders, H. W., *Reaction rates of isotopic molecules*. Krieger Pub. Co.: Malabar, FL., 1987.

74. Okazaki, R.; Okazaki, T.; Sakabe, K.; Sugimoto, K.; Kainuma, R.; Sugino, A.; Iwatsuki, N., In vivo mechanism of dna chain growth. *Cold Spring Harbor Symp. Quant. Biol.* **1968,** 33, 129-.

75. Okazaki, R.; Okazaki, T.; Sakabe, K.; Sugimoto, K.; Sugino, A., Mechanism of DNA chain growth .I. Possible discontinuity and unusual secondary structure of newly synthesized chains. *Proc. Nat. Acad. Sci. U.S.A.* **1968,** 59, 598-&.

76. Koehn, E. M.; Fleischmann, T.; Conrad, J. A.; Palfey, B. A.; Lesley, S. A.; Mathews, I. I.; Kohen, A., An unusual mechanism of thymidylate biosynthesis in organisms containing the thyX gene. *Nature* **2009,** 458, 919-923.

77. Matthiesen, S.; Bahulayan, A.; Holz, O.; Racke, K., MAPK pathway mediates muscarinic receptor-induced human lung fibroblast proliferation. *Life Sci.* **2007,** 80, 2259-2262.

78. Nowak, P.; Zagzil, T.; Konecki, J.; Szczerbak, G.; Szkilnik, R.; Niwinski, J.; Gorzalek, J.; Kostrzewa, R. M.; Brus, R., Trimetazidine increases [H^3] glucose uptake in rat brain. *Pharmacol. Reports* **2006,** 58, 559-561.

79. Cook, P. F.; Cleland, W. W., *Enzyme Kinetics and Mechanism*. Taylor & Francis Group, LLC.: New York, 2007.

80. Northrop, D. B., Determining the absolute magnitude of hydrogen isotope effects. In *Isotope effects on enzyme-catalyzed reactions*, Cleland, W. W.; O'Leary, M. H.; Northrop, D. B., Eds. University Park Press: Baltimore, MD., 1977; pp 122-152.

81. Sen, A. K., A., Quantum effects in enzyme kinetics. In *Quantum Tunnelling in Enzyme Catalyzed Reactions*, Allemann, R. K.; Scrutton, N. S., Eds. Royal Society of Chemistry: London, UK, 2009; pp 164-181.

82. Sen, A.; Kohen, A., Enzymatic tunneling and kinetic isotope effects: chemistry at the crossroads. *J. Phys. Org. Chem.* **Accepted for publication**.

83. Yahashiri, A., Sen A. and Kohen A., Microscale synthesis and kinetic isotope effect analysis of (*R*)-[4-^{2}H; Ad-^{14}C] NADPH and (*R*)-[4-^{2}H; Ad-^{3}H] NADPH. *J. Label. Compd. Radiopharm.* **2009,** 52, 463-466.

84. Roston, D.; Kohen, A., Elusive transition state of alcohol dehydrogenase unveiled. *Proc. Nat. Acad. Sci. U.S.A.* **2010,** 107, 9572-9577.

85. Moran, R. G.; Sartori, P.; Reich, V., A rapid and convenient preparation of [4-^{3}H]NADP and stereospecifically tritiated NADP^{3}H. *Anal. Biochem.* **1984,** 138, 196-204.

86. Ichinose, K.; Leeper, F. J.; Battersby, A. R., Preparation of [4*R*-^{3}H]NADH, [4*R*-^{3}H]NADPH and the corresponding 4*S*-isomers all with substantial specific activities. *J. Chem. Soc., Perkin Trans. 1* **1993**, 1213-1216.

87. Blakley, R. L., Crystalline dihydropteroylglutamic acid. *Nature* **1960,** 188, 231-232.

88. Sen, A.; Yahashiri, A.; Kohen, A., Triple isotopic labeling and kinetic isotope effects: a sensitive and accurate method for exposing the h-transfer step in enzymatic systems. **in preparation**.

89. Northrop, D. B., Steady-state analysis of kinetic isotope effects in enzymatic reactions. *Biochemistry* **1975,** 14, 2644-2651.

90. Francisco, W. A.; Abu-Soud, H. M.; DelMonte, A. J.; Singleton, D. A.; Baldwin, T. O.; Raushel, F. M., Deuterium kinetic isotope effects and the mechanism of the bacterial luciferase reaction. *Biochemistry* **1998,** 37, 2596-2606.

91. Fierke, C. A.; Johnson, K. A.; Benkovic, S. J., Construction and evaluation of the kinetic scheme associated with dihydrofolate reductase from *Escherichia coli*. *Biochemistry* **1987,** 26, 4085-4092.

92. Nagel, Z. D.; Klinman, J. P., Corrigendum: A 21st century revisionist's view at a turning point in enzymology. *Nat Chem Biol* **2009,** 5, 696-696.

93. Miller, G. P.; Wahnon, D. C.; Benkovic, S. J., Interloop contacts modulate ligand cycling during catalysis by *Escherichia coli* dihydrofolate reductase. *Biochemistry* **2001,** 40, 867-875.

94. Schramm, V. L., Binding isotope effects: boon and bane. *Curr. Opin. Chem. Biol.* **2007,** 11, 529-536.

95. Nagel, Z. D.; Klinman, J. P., Tunneling and dynamics in enzymatic hydride transfer. *Chem. Rev.* **2006,** 106, 3095-3118.

96. Bell, R. P., *The tunnel effect in chemistry*. Chapman & Hall: London & New York., 1980.

97. Mayer, R. J.; Chen, J. T.; Taira, K.; Fierke, C. A.; Benkovic, S. J., Importance of a hydrophobic residue in binding and catalysis by dihydrofolate reductase. *Proc. Nat. Acad. Sci. U.S.A.* **1986,** 83, 7718-7720.

98. Pu, J.; Gao, J.; Truhlar, D. G., Multidimensional tunneling, recrossing, and the transmission coefficient for
enzymatic reactions. *Chem. Rev.* **2006,** 106, 3140-3169.

99. Maglia, G.; Allemann, R. K., Evidence for environmentally coupled hydrogen tunneling during dihydrofolate reductase catalysis. *J. Am. Chem. Soc.* **2003,** 125, 13372-13373.

100. Masgrau, L.; Roujeinikova, A.; Johannissen, L. O.; Hothi, P.; Basran, J.; Ranaghan, K. E.; Mulholland, A. J.; Sutcliffe, M. J.; Scrutton, N. S.; Leys, D., Atomic Description of an Enzyme Reaction Dominated by Proton Tunneling 10.1126/science.1126002. *Science* **2006,** 312, 237-241.

101. Liu, H.; Warshel, A., Origin of the temperature dependence of isotope effects in enzymatic reactions: the case of dihydrofolate reductase. *J. Phys. Chem. B* **2007,** 111, 7852-7861.

102. Meyer, M. P.; Tomchick, D. R.; Klinman, J. P., Enzyme structure and dynamics affect hydrogen tunneling: The impact of a remote side chain (I553) in soybean lipoxygenase-1. *Proc. Nat. Acad. Sci. U.S.A.* **2008,** 105, 1146-1151.

103. Alonso, H.; Gready, J. E., Integron-sequestered dihydrofolate reductase: a recently redeployed enzyme. *Trends Microbiol.* **2006,** 14, 236-242.

104. Amyes, S. G. B.; Smith, J. T., The purification and properties of the trimethoprim-resistant dihydrofolate reductase mediated by the R-factor, R388. *Eur. J. Biochem.* **1976,** 61, 597-603.

105. Stone, S. R.; Morrison, J. F., Catalytic mechanism of the dihydrofolate reductase reaction as determined by pH studies. *Biochemistry* **2002,** 23, 2753-2758.

106. Deng, H.; Callender, R., Structure of dihydrofolate when bound to dihydrofolate reductase. *J. Am. Chem. Soc.* **1998,** 120, 7730-7737.

107. Hicks, S. N. Role of ionic interactions in the catalytic mechanism of R67 dihydrofolate reductase. Dissertation, The University of Tennessee Knoxville, Knoxville, TN, 2003.

108. Schmitzer, A. R.; Lepine, F.; Pelletier, J. N., Combinatorial exploration of the catalytic site of a drug-resistant dihydrofolate reductase: creating alternative functional configurations. *Protein Eng. Des. Sel.* **2004,** 17, 809-819.

109. Smiley, R. D.; Stinnett, L. G.; Saxton, A. M.; Howell, E. E., Breaking symmetry: Mutations engineered into R67 dihydrofolate reductase, a D-2 symmetric homotetramer possessing a single active site pore. *Biochemistry* **2002,** 41, 15664-15675.

110. Boehr, D. D.; McElheny, D.; Dyson, H. J.; Wright, P. E., The dynamic energy landscape of dihydrofolate reductase catalysis. *Science* **2006,** 313, 1638-1642.

111. Kim, H. S.; Damo, S. M.; Lee, S.-Y.; Wemmer, D.; Klinman, J. P., Structure and hydride transfer mechanism of a moderate thermophilic dihydrofolate reductase from Bacillus stearothermophilus and comparison to its mesophilic and hyperthermophilic homologues. *Biochemistry* **2005,** 44, 11428-11439.

112. Pu, J.; Ma, S.; Gao, J.; Truhlar, D. G., Small temperature dependence of the kinetic isotope effect for the hydride transfer reaction catalyzed by *Escherichia coli* dihydrofolate reductase. *J. Phys. Chem.* **2005,** 19, 8551-8556.

113. Smith, S. L.; Burchall, J. J., Alpha-pyridine nucleotides as substrates for a plasmid-specified dihydrofolate-reductase. *Proc. Nat. Acad. Sci. USA-Biological Sciences* **1983,** 80, 4619-4623.

114. Chernyshev, A.; Fleischmann, T.; Koehn, E.; Lesley, S. A.; Kohen, A., The relationships between oxidase and synthase activities of flavin dependent thymidylate synthase (FDTS). *Chem. Commun.* **2007**, 2861-2863.

115. Basran, J.; Masgrau, L.; Sutcliffe, M. J.; Scrutton, N. S., Solution and computational studies of kinetic isotope effects in flavoprotein and quinoprotein catalyzed substrate oxidation as probeds of enzymatic hydrogen tunneling and mechanism. In *Isotope effects in chemistry and biology*, Kohen, A.; Limbach, H. H., Eds. Taylor & Francis, CRC Press.: Boca Raton, FL, 2006; Vol. Ch. 25, pp 671-690.

116. Pudney, C. R.; Hay, S.; Pang, J.; Costello, C.; Leys, D.; Sutcliffe, M. J.; Scrutton, N. S., Mutagenesis of morphinone reductase induces multiple reactive configurations and

identifies potential ambiguity in kinetic analysis of enzyme tunneling mechanisms. *J. Am. Chem. Soc.* **2007,** 129, 13949-13956.

117. Hothi, P.; Hay, S.; Roujeinikova, A.; Sutcliffe, M. J.; Lee, M.; Leys, D.; Cullis, P. M.; Scrutton, N. S., Driving force analysis of proton tunnelling across a reactivity series for an enzyme-substrate complex. *ChemBioChem* **2008,** 9, 2839-2845.

118. Klinman, J. P., An integrated model for enzyme catalysis emerges from studies of hydrogen tunneling. *Chem. Phys. Lett.* **2009,** 471, 179-193.

119. Blecher, O.; Goldman, S.; Mevarech, M., High expression in *Escherichia coli* of the gene coding for dihydrofolate reductase of the extremely halophilic archaebacterium *Haloferax volcanii*. *Eur. J. Biochem.* **1993,** 216, 199-203.

120. Meng, E. C.; Pettersen, E. F.; Couch, G. S.; Huang, C. C.; Ferrin, T. E., Tools for integrated sequence-structure analysis with UCSF Chimera. *Bmc Bioinformatics* **2006,** 7, 10.

121. Feng, Z. K.; Chen, L.; Maddula, H.; Akcan, O.; Oughtred, R.; Berman, H. M.; Westbrook, J., Ligand Depot: a data warehouse for ligands bound to macromolecules. *Bioinformatics* **2004,** 20, 2153-2155.

122. Krammer, A.; Kirchhoff, P. D.; Jiang, X.; Venkatachalam, C. M.; Waldman, M., LigScore: a novel scoring function for predicting binding affinities. *J. Mol. Graphics Modell.* **2005,** 23, 395-407.

123. Dolinsky, T. J.; Czodrowski, P.; Li, H.; Nielsen, J. E.; Jensen, J. H.; Klebe, G.; Baker, N. A., PDB2PQR: expanding and upgrading automated preparation of biomolecular structures for molecular simulations. *Nucl. Acids Res.* **2007,** 35, W522-W525.

124. Wang, J. M.; Cieplak, P.; Kollman, P. A., How well does a restrained electrostatic potential (RESP) model perform in calculating conformational energies of organic and biological molecules? *J. Comput. Chem.* **2000,** 21, 1049-1074.

125. Baker, N. A.; Sept, D.; Joseph, S.; Holst, M. J.; McCammon, J. A., Electrostatics of nanosystems: application to microtubules and the ribosome. *Proc. Nat. Acad. Sci. U.S.A.* **2001,** 98, 10037-10041.

126. Sanner, M. F., Python: a programming language for software integration and development. *J. Mol. Graphics Modell.* **1999,** 17, 57-61.

127. Ellis, K. J.; Morrison, J. F.; Daniel, L. P., Buffers of constant ionic strength for studying pH-dependent processes. *Methods. Enzymol.* **1982,** 87, 405-426.

128. Agarwal, P. K.; Webb, S. P.; Hammes-Schiffer, S., Computational studies of the mechanism for proton and hydride transfer in liver alcohol dehydrogenase. *J. Am. Chem. Soc.* **2000,** 122, 4803-4812.

129. DeLano, W. L. *The PyMOL Molecular Graphics System (http://www.pymol.org)*, DeLano Scientific: 2002.

130. Bello, A. R.; Nare, B.; Freedman, D.; Hardy, L.; Beverley, S. M., PTR1: a reductase mediating salvage of oxidized pteridines and methotrexate resistance in the

protozoan parasite *Leishmania major*. *Proc. Nat. Acad. Sci. U.S.A.* **1994,** 91, 11442-11446.

131. Fierke, C. A.; Kuchta, R. D.; Johnson, K. A.; Benkovic, S. J., Implications for enzymic catalysis from free-energy reaction coordinate profiles. *Cold Spring Harbor Symp. Quant. Biol.* 52, 631-638.

132. Rajagopalan, P. T. R.; Stefan, L.; Benkovic, S. J., Coupling interactions of distal residues enhance dihydrofolate reductase catalysis: Mutational effects on hydride transfer rates. *Biochemistry* **2002,** 41, 12618-12628.

133. Agarwal, P. K.; Billeter, S. R.; Rajagopalan, P. T. R.; Benkovic, S. J.; Hammes-Schiffer, S., Network of coupled promoting motions in enzyme catalysis. *Proc. Natl. Acad. Sci. U.S.A.* **2002,** 99, 2794-2799.

134. Myllykallio, H.; Leduc, D.; Filee, J.; Liebl, U., Life without dihydrofolate reductase FoIA. *Trends. Microbiol.* **2003,** 11, 220-223.

135. Hardy, L. W.; Matthews, W.; Nare, B.; Beverley, S. M., Biochemical and genetic tests for inhibitors of *Leishmania* pteridine pathways. *Exp. Parasitol.* **1997,** 87, 158-170.

136. Nare, B.; Hardy, L. W.; Beverley, S. M., The roles of pteridine reductase 1 and dihydrofolate reductase-thymidylate synthase in pteridine metabolism in the protozoan parasite *Leishmania major*. *J. Biol. Chem.* **1997,** 272, 13883-13891.

137. Taira, K.; Benkovic, S. J., Evaluation of the importance of hydrophobic interactions in drug-binding to dihydrofolate-reductase. *J. Med. Chem.* **1988,** 31, 129-137.

138. Howell, E. E.; Booth, C.; Farnum, M.; Kraut, J.; Warren, M. S., A second-site mutation at phenylalanine-137 that increases catalytic efficiency in the mutant aspartate-27 → serine *Escherichia coli* dihydrofolate reductase. *Biochemistry* **1990,** 29, 8561-8569.

139. Howell, E. E.; Warren, M. S.; Booth, C. L. J.; Villafranca, J. E.; Kraut, J., Construction of an altered proton donation mechanism in *Escherichia coli* dihydrofolate reductase. *Biochemistry* **1987,** 26, 8591-8598.

140. Yahashiri, A.; Jo, H.; Kohen, A., Single-step enzymatic synthesis of (*R*)-[4-^{3}H] NADPH. **in preparation**.

141. Sekhar, V. C.; Plapp, B. V., Rate constants for a mechanism including intermediates in the interconversion of ternary complexes by horse liver alcohol dehydrogenase. *Biochemistry* **1990,** 29, 4289-4295.

142. Cook, P. F.; Cleland, W. W., pH Variation of isotope effects in enzyme-catalyzed reactions. 1. Isotope- and pH-dependent steps the same. *Biochemistry* **1981,** 20, 1797-1805.

143. Pudney, C. R.; Hay, S.; Levy, C.; Pang, J.; Sutcliffe, M. J.; Leys, D.; Scrutton, N. S., Evidence to support the hypothesis that promoting vibrations enhance the rate of an enzyme catalyzed H-tunneling reaction. *J. Am. Chem. Soc.* **2009,** 131, 17072-17073.

144. Cavazzuti, A.; Paglietti, G.; Hunter, W. N.; Gamarro, F.; Piras, S.; Loriga, M.; Alleca, S.; Corona, P.; McLuskey, K.; Tulloch, L.; Gibellini, F.; Ferrari, S.; Costin, M. P.,

Discovery of potent pteridine reductase inhibitors to guide antiparasite drug development. *Proc. Nat. Acad. Sci. U.S.A.* **2008,** 105, 1448-1453.

145. Howell, E. E.; Villafranca, J. E.; Warren, M. S.; Oatley, S. J.; Kraut, J., Functional role of aspartic acid-27 in dihydrofolate reductase revealed by mutagenesis. *Science* **1986,** 231, 1123-1128.

146. Yahashiri, A. T., M.J.; Hashmi, A.; and Kohen A., Effective purification of pteridine reductase 1 from Leishmania major and comparative cross-reactive kinetic studies on pteridine reductase and dihydrofolate reductase activities **in preparation**.